Sulfate in Foraminiferal Calcium Carbonate: Investigating a Potential Proxy for Sea Water Carbonate Ion Concentration

by

Jeffrey Nicholas Berry

B. S. Chemistry (1992)
Pacific Lutheran University

Submitted in partial fulfillment of the requirements for the degree of

MASTER OF SCIENCE IN CHEMICAL OCEANOGRAPHY
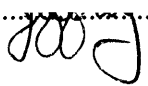
at the

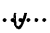MASSACHUSETTS INSTITUTE OF TECHNOLOGY
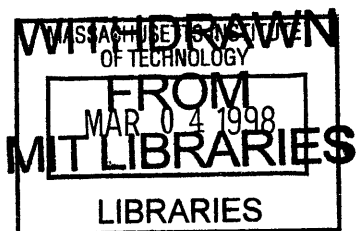
and the

WOODS HOLE OCEANOGRAPHIC INSTITUTION

June 1998

Signature of Author..
Joint Program in Chemical Oceanography
Massachusetts Institute of Technology
Woods Hole Oceanographic Institution
March 30, 1998

Certified by..
Professor Edward A. Boyle
Thesis Supervisor

Accepted by..
Professor Edward A. Boyle
Chair, Joint Committee for Chemical Oceanography
Massachusetts Institute of Technology
Woods Hole Oceanographic Institution

SULFATE IN FORAMINIFERAL CALCIUM CARBONATE: INVESTIGATING A POTENTIAL PROXY FOR SEA WATER CARBONATE ION CONCENTRATION

By

Jeffrey Nicholas Berry

Submitted to the Department of Earth, Atmospheric, and Planetary Sciences on March 30, 1998 in partial fulfillment of the requirements for the Degree of Master of Science in Chemical Oceanography

Abstract

The sulfur content of planktonic and benthic foraminifera was measured in specimens recovered from deep-sea sediment cores and individuals grown in culture. A new method for measuring sulfur in foraminiferal calcium carbonate was developed, employing a high-resolution inductively coupled plasma-mass spectrometer. The sulfur measurements, expressed as sulfur-to-calcium (S/Ca) ratios in the foraminiferal shells, ranged from 0.26 to 6.0 mmol/mol. Most analyses fell in the range of 0.7 to 2.5 mmol/mol. Culturing experiments were conducted in the planktonic foraminifer *G. sacculifer* to test the hypothesis that S/Ca ratios in the foraminifer are inversely proportional to the carbonate ion concentration in the seawater in which they grow, and hence proportional to the pH of the seawater. The slope of the relationship between cultured *G. sacculifer* S/Ca and the pH of the seawater medium was -1.92 mmol mol^{-1}/pH unit with a least squares linear correlation coefficient, $r^2=0.927$. The S/Ca ratios of planktonic and benthic foraminifera from Holocene and last glacial period sediments were measured in an effort to use the established relationship of S/Ca and pH to calculate the ocean pH gradient between Holocene and glacial time. The results indicate the pH of global ocean deepwater was 0.10 to 0.15 pH units higher during glacial time than today. Smaller pH gradients were seen for some cores which may have been caused by circulation-induced water mass changes. Surface ocean changes in pH over the Holocene-glacial interval seem to vary from region to region, with up to an 0.2 pH unit increase at the Sierra Leone Rise in glacial time. Benthic foraminifera from coretops in the thermocline of the Little Bahama Bank were analyzed for S/Ca to examine the effects of hydrographic variables on S/Ca. The relationship of S/Ca to pH and [$CO_3^=$] has a positive slope, at odds with the expected negative slope from the previous results. The S/Ca results do correlate well with salinity, suggesting that salinity or other hydrographic parameters may also influence foraminiferal S/Ca ratios.

Thesis supervisor: Dr. Edward A. Boyle
Title: Professor of Chemical Oceanography

Acknowledgments

This thesis would not have been possible without the support and encouragement of a number of people. My biggest thanks go to my advisor, Ed Boyle. I could not have hoped to work with a more brilliant scientist. Even more so, he has been an understanding human being. I thank Bill Martin, Greg Ravizza, and Roger Francois for agreeing to serve on my thesis committee, even though as it turned out I didn't give them too much work to do. Bill was also helpful early on in my tenure in the Joint Program, giving me an interesting project to work on and introducing me to the intricacies of calcium carbonate sedimentation. Dan McCorkle was also a great help during those first years and at the end for giving me access to the very recent Ontong Java Plateau cores. Roger also got me started on the ICP-MS at WHOI. I can't thank Lary Ball and Dave Schneider enough for their fantastic help in paving the way to medium-resolution glory on the ICP-MS and putting up with my strange commuting schedule from Boston. Barry Grant was indispensable as a source of laboratory knowledge, and especially for his expertise on the ICP-MS, even if barium didn't end up the way to go. Rick Kayser kept the lab running smoothly, and provided me a positive example of life after getting the degree.

Jonathan Erez originated the idea for this thesis, and gave me the incredible opportunity to culture foraminifera in Eilat. I thank him for his boundless enthusiasm for his work and his patience in teaching me how to keep those fascinating little bugs alive and happy. The folks at MBL in Eilat were invaluable in making my experiments there a success. I acknowledge the help of the core repositories at Lamont-Doherty Earth Observatory, Woods Hole Oceanographic Institution, the University of Rhode Island, and CNRS, France.

There is no way I could have made it this far without the support of my friends in the Joint Program. Jess Adkins was an incredible font of oceanographic knowledge and a good friend who not only listened to all my woes, but helped me to see what I could do about them. He was a great partner all those years in the post office, and gave me the motivation to beat the "Adkins curse." Susie Carter, Michael Horowitz, Mak Saito, Hedy Edmonds, Yu-Harn Chen, and Payal Parekh have all made life in E34 actually fun much of the time, and have also done their share to keep life fun *outside* of E34. Liz Kujawinski and Ann Pearson have been great classmates, and I wish them all the best in the completion of the quest.

I am very grateful to Alla Skorokhod, Robin Elices, and Stacy Frangos for their help in allowing me to finish this thesis with a minimum of added stress, and Alla especially for all her efforts in the "front office." Pat Judge has given me inspiration to challenge a lot of my assumptions, and his long-distance encouragement has helped me take the banner of LASAS to this far coast. My parents have been inexhaustible in their enthusiasm and support for my endeavors, and I thank them for their efforts in getting me this far. Finally, my heartfelt thanks goes to Gabriella Sanna, who has invested at least as much of her life in this thesis as I have. Without her encouragement and love, it simply would not have happened.

This thesis is dedicated to my parents.

Table of Contents

List of Figures

List of Tables

A. Introduction

Chemical and isotopic signals trapped in the shells of fossil foraminifera from deep-sea sediment cores are probably the most valuable tools available to paleoceanographers for reconstructing past oceanic conditions. There is a long history of using foraminiferal stable isotope measurements, $\delta^{18}O$ and $\delta^{13}C$, to determine parameters such as sea surface temperature and salinity, continental ice volume, terrestrial carbon inputs to the oceans, deep-water circulation and air-sea gas exchange magnitudes (Emiliani, 1955; Epstein et al., 1953; Shackleton, 1967; Shackleton, 1977; Duplessy et al., 1988; Charles and Fairbanks, 1990). Trace and minor chemical constituents of foraminifera are a more recent contribution to the paleoceanography toolbox, including Cd/Ca indicating phosphate concentrations, Ba/Ca indicating deeply regenerated components such as barium and alkalinity, and Mg/Ca probably indicating temperature (Boyle, 1988; Lea and Boyle, 1989; Bender et al., 1975; Rosenthal et al., 1997). None of these tracers are without ambiguities in their application to paleoceanographic conditions, but they have given valuable insights into the past ocean, and the investigation of these tracers and the development of new ones continues to provide valuable information. It is in this spirit that the experiments described in this thesis were undertaken.

One of the outstanding questions in paleoceanography today is the cause of the low atmospheric CO_2 pressures (pCO_2) known to exist during glacial intervals in the Quaternary. Some of the most compelling records of global change during glacial cycles are the measurements of CO_2 from trapped air bubbles in ice cores from Greenland and Antarctica (Neftel et al., 1982; Neftel et al., 1988; Barnola et al., 1987). The results from the Vostok ice core in Antarctica show that atmospheric CO_2 content was about 190 ppmv during the previous two glacial maxima, while the interglacial CO_2 value increased to 280 ppmv (Barnola et al., 1987). Because CO_2 is a

potent greenhouse gas, the changing atmospheric CO_2 content surely plays some role in the changing climate conditions of the Pleistocene glacial cycles. There is still much debate on both the phase relationship of atmospheric CO_2 with glacial cycles of climate as well as the link between ocean chemistry and glacial atmospheric CO_2. The Vostok record indicates that CO_2 increases nearly in phase with the temperature increase in the Stage 6-5 deglacial transition, but the decrease of CO_2 at the end of the Stage 5 interglacial lags the temperature decrease by several thousand years (Barnola et al., 1987; Barnola et al., 1991). There is no doubt, however, that ocean chemistry drove the observed atmospheric CO_2 changes because the ocean contains about 98% of the carbon in the combined ocean-atmosphere system. Clearly, there is a need for information on the nature and timing of changes in oceanic carbon chemistry in order to evaluate the response time of atmospheric CO_2 to such changes. A proxy for a component of the oceanic carbon system, such as pH or $[CO_3^=]$, would prove valuable for the evaluation of mechanisms for atmospheric CO_2 changes through glacial cycles. Combining such a proxy with a proxy for either dissolved inorganic carbon (TCO_2) or alkalinity ($\delta^{13}C$ and Cd/Ca were used to estimate TCO_2 and Ba/Ca to estimate alkalinity by Lea (1995) for Circumpolar Deep Water) would provide two components of the inorganic carbon system, enough to constrain the pCO_2 of the system.

A proxy for ocean pH has been developed utilizing the measurement of boron isotope ratios in foraminifera. Boron exists in seawater as the uncharged species $B(OH)_3$ and the charged species $B(OH)_4^-$. Boron isotopes fractionate between these species such that ^{11}B is enriched by about 20‰ in $B(OH)_3$. Because the ratio of charged to uncharged borate changes with pH, so too does the isotopic composition of these species. Given the assumption that only the charged borate species is incorporated in the $CaCO_3$ lattice, the $\delta^{11}B$ content of foraminifera shells is controlled by pH.

Two examples of estimating ocean pH from boron isotope fractionation in foraminifera have been published recently. Spivack and coworkers (1993) measured the $\delta^{11}B$ of foraminifera from ODP hole 803D by negative thermal ionization mass spectrometry (N-TIMS) to generate a low resolution record of surface ocean pH over the past 21 Myr. Their data indicates that surface water pH remained about 8.2 ± 0.2 between 7.5 Myr and the present, but was 7.4 ± 0.2 between 21 and 15 Myr. The lower pH results for 21 Myr are consistent with estimates from the isotopic composition of organic matter of 4.5 times the present atmospheric pCO_2 at that time.

Measurement of $\delta^{11}B$ in core-top and glacial age planktonic and benthic foraminifera by N-TIMS was done as reported by Sanyal et al. (1995). A ΔpH to $\Delta\delta^{11}B$ relationship was calibrated with coretop measurements of planktonic and benthic foraminifera from the Atlantic and Pacific oceans in waters ranging in pH from ~7.9 to 8.2. Last glacial age foraminifera were also analyzed, so that the ΔpH for both surface and deep waters between the Holocene and the last glacial was determined. The surface ocean was estimated to be 0.2 ± 0.1 pH units higher during the glacial, and the deep ocean was estimated to be 0.3 ± 0.1 pH units higher during the glacial. Translating the higher pH of the deep glacial ocean to an excess of deep ocean carbonate ion (~100 µmol/kg higher than today), suggests that the increased $[CO_3^=]$ would increase the surface ocean pH by 0.15 units compared to today, and result in pCO_2 of about 200 µatm, agreeing with the ice core results. Hence, the boron isotope method gives pH estimates consistent with the ice core pCO_2 observations.

However, there are other indications that the boron isotope method produces inconsistencies in the paleo-pH record. Gaillardet and Allègre (1995) measured $\delta^{11}B$ in modern and fossil reef corals to determine the paleo-pH record of South Pacific surface waters. The data are problematic in that the modern corals scatter over a wider than expected pH range, and the ancient corals suggest the last glacial surface water was 0.3 pH units *lower* than the present (implying higher glacial pCO_2). The

11

authors acknowledge that coral biomineralization mechanisms and diagenetic alterations may compromise the boron isotope pH proxy in corals. Sanyal and others (1996) have recently reported that measurements of $\delta^{11}B$ in equatorial Pacific planktonic foraminifera from Termination II indicate no change in pH across the glacial-interglacial transition. This result is not in accord with the atmospheric pCO_2 record or the $\delta^{11}B$ results for the last termination.

Most paleoceanographic proxies developed over the decades have shown complications in interpretation of their mechanisms and results, so inconsistencies in the behavior of the boron isotope pH proxy should not be construed as a failure of the tracer. Nevertheless, there is a strong case for the development of an independent paleo-pH indicator as a check on the boron isotope method.

The experiments described in this thesis were motivated by initial evidence for a foraminiferal sulfate-pH link based on investigations by Jonathan Erez and others. Professor Erez and students cultured the benthic foraminifer *Amphistegina lobifera* in seawater adjusted to pH between 7.9 and 8.4 and labeled with ^{35}S. The results showed a linear relationship between sulfate content and pH, with sulfate enriched at lower pH (See Fig. 1) (Erez, 1994).

This relationship is hypothesized to be due to lattice substitution of sulfate for carbonate which may be expressed as an ideal solid solution between $CaCO_3$ and $CaSO_4$ according to the following equation:

$$SO_4^{2-} + CaCO_{3\,(s)} \leftrightarrow CaSO_{4\,(s)} + CO_3^{2-} \qquad (1).$$
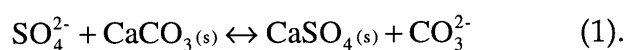
The sulfate content of the carbonate can then be expressed by the partition coefficient D, where

$$D = \frac{(aSO_4^{2-} / aCO_3^{2-})_{calcite}}{(aSO_4^{2-} / aCO_3^{2-})_{seawater}} \qquad (2).$$

Because of the conservative behavior of sulfate in seawater, it is expected that the sulfate content of biogenic carbonate is dependent upon variations in carbonate content. For any constant value of dissolved inorganic carbon in seawater, changes

SO$_4^=$ uptake in *A. lobifera* shells related to pH

$$S/Ca = -0.599 \times pH + 5.14$$
$$r^2 = 0.874$$
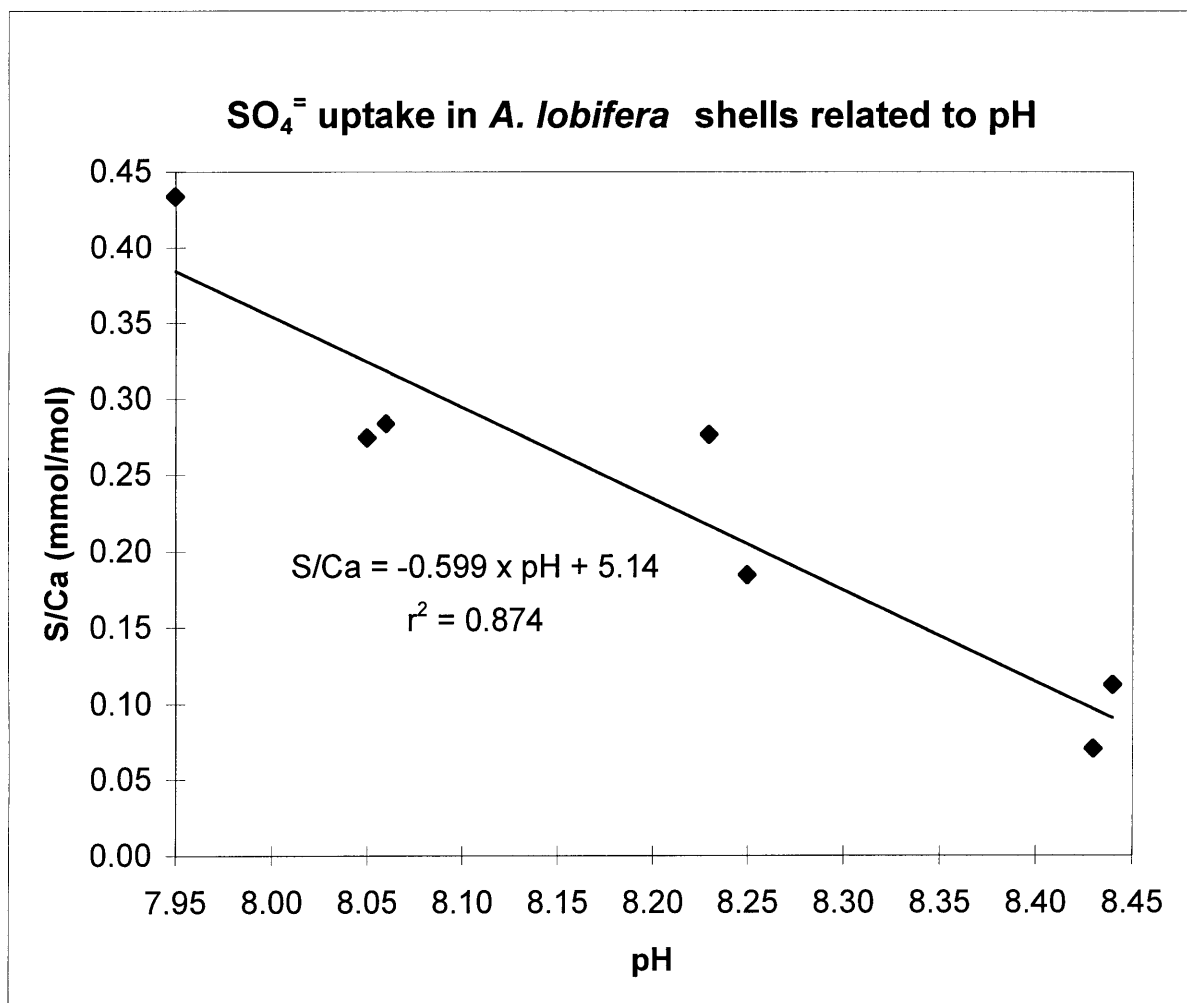
Figure 1: Data from culturing experiments on benthic foraminifer *Amphistegina lobifera* . Gulf of Eilat seawater was spiked with radioactive ^{35}S as culture medium. The cultures were adjusted to varying pH and the dissolved shells of the cultured organisms were counted in a scintillation counter to measure sulfur uptake. The sulfur data were converted to S/Ca ratio. Data courtesy of Prof. Jonathan Erez.

in pH will determine the activity of carbonate ion. Thus, the incorporation of sulfate in biogenic carbonate depends on the pH of the ambient seawater. The sulfate content of the carbonate is predicted to depend upon the inverse of the seawater carbonate concentration in the above model, which explains the negative slope of the sulfate-pH relationship found by Erez.

The validity of the above solid solution model for sulfate incorporation in calcium carbonate depends on the assumption that sulfate substitutes for carbonate ion directly into the crystal lattice. Strong evidence for such substitution has been provided by X-ray absorption studies of biogenic carbonates (Pingatore et al., 1995). Comparison of the X-ray absorption near edge structures (XANES) of sulfur in mineral standards containing S in a range of oxidation states (from sulfides to sulfates) to the XANES of modern and fossil corals definitively showed that S was present in the coral samples in the 6+ oxidation state as sulfate. Unfortunately, XANES does not give information on the nature of the atoms beyond the first shell surrounding the element of interest (i.e. past the oxygens of the sulfate anion). Nonetheless, patterns observed from the XANES analyses strongly indicate that sulfate is not incorporated as some trace phase such as $CaSO_4$, but as a substitute for carbonate in the lattice. Additionally, the geometrically and geochemically similar ion SeO_4^{2-} has been shown by the more powerful extended X-ray absorption fine structure (EXAFS) technique to coordinate with six Ca atoms in the calcite structure (Reeder et al., 1994). This coordination is that expected for the carbonate site in the calcite structure, and since SO_4^{2-} is a smaller ion than SeO_4^{2-}, it is also expected to substitute for $CO_3^=$ in the lattice.

Strictly speaking, then, $SO_4^=/CO_3^=$ ratios would be the presumed thermodynamic diagnostic for evaluating a foraminiferal $SO_4^=$ relationship with seawater carbonate ion concentration or pH. The methods described in the following section in fact involve the measurement of S/Ca ratios, but it is argued that this

ratio is in practice equivalent to the $SO_4^=/CO_3^=$ ratio. The measurement of Ca in all samples is designed to normalize for final dissolved sample size. Because foraminiferal calcite is at least 99+% pure (even minor species are present at the parts per thousand level), and the molar ratio of Ca to $CO_3^=$ in calcite is one, one can interchange $S/CO_3^=$ ratio for S/Ca ratio.

Similarly, total S measured by the ICP-MS in the dissolved foraminifera samples is almost certainly exclusively sulfate anion. Reduced forms of sulfur would probably not substitute into the calcium carbonate lattice as readily as sulfate, in addition to the fact that sulfate in oxic waters completely dominates other sulfur species. It may be possible that sulfur exists in organic material trapped within the inorganic carbonate matrix of the shell, but the fraction of glycoproteins in the bulk shell is about 0.02 to 0.04% of total mass (Robbins and Brew, 1990; Weiner and Erez, 1984), and total organic matter is no more than 0.08% (Stott, 1992). Amino acid analyses of the glycoproteins show that no more than 5% of the amino acids are sulfur-containing; these amino-acids are about 30% sulfur by weight (Robbins and Brew, 1990). Thus organic-bound sulfur is probably no more than 5% of total organic matter, or 0.001% of foraminiferal mass. The lowest measurements of sulfur concentrations in foraminifera reported here are about 0.04%, so that organic sulfur cannot be more than 3% of total sulfur measured. Thus, the contribution of sulfur associated with organic material is negligible compared to that in the carbonate matrix.

B. Methods

Hand-picked foraminifera from disaggregated sediments were used for all ocean sediment core samples. Sample weights were typically between 0.1 to 0.5 mg and consisted of several shells. Samples were crushed gently between glass plates to expose internal surfaces for cleaning. In many cases, a larger sample was crushed

and mixed before subsets in the 0.5 mg range were taken. These samples were used to determine variability of replicates in a crushed pool of foraminifera. The foraminifera fragments were transferred to acid-leached 0.5 mL polypropylene microcentrifuge tubes. The cleaning steps are modified from those published by Boyle and Keigwin (1985) and Rosenthal and Boyle (1993). All foraminifera were cleaned with ultrasonic agitation (2-5 min.) with multiple portions of distilled water and methanol to remove fine-grained clays and other surface contaminants. A test comparing the S/Ca results of sub-samples cleaned in this way with sub-samples cleaned with the addition of an oxidative cleaning step (20 μM H_2O_2 in 0.1 M NaOH at 90°C with ultrasonication) revealed no significant difference (Fig. 2). Thus, all other samples were cleaned without the oxidative step. A weak acid leach was then conducted with 0.001 N HNO_3 and ultrasonic agitation for 30 s. This step was designed to remove contaminants bound or adsorbed to the surfaces of the calcium carbonate. The weak acid leach was repeated 2-3 times unless the sample appeared very small to avoid excessive dissolution. When acid leaching was finished, the sample was rinsed with two portions of distilled water, and excess liquid was siphoned off. Samples were then dissolved in 1% HNO_3, with the volume depending upon sample size, but typically 100-130 μL. The samples were subjected to ultrasonic agitation for 10-15 min. to aid dissolution. If solid was still observed in any samples, an additional portion of 1% HNO_3 was added. Samples were checked for complete dissolution by pipeting a 5μL portion onto pH indicator paper to confirm a pH < 4. Samples were then centrifuged for 5 min. to consolidate any drops into the main solution. An aliquot of dissolved sample was then dispensed into a clean, leached 500 μL centrifuge tube; the volume was typically 100 μL, but was adjusted lower for smaller samples. The remaining sample was used for Ca analysis. An aliquot of 130 μM Na_2SO_4 solution enriched in ^{34}S ($^{32}S/^{34}S$ = 0.02, ^{34}S = 93.0%, Isotec Inc.) was then pipeted into each aliquot of sample. The spike volume was

16
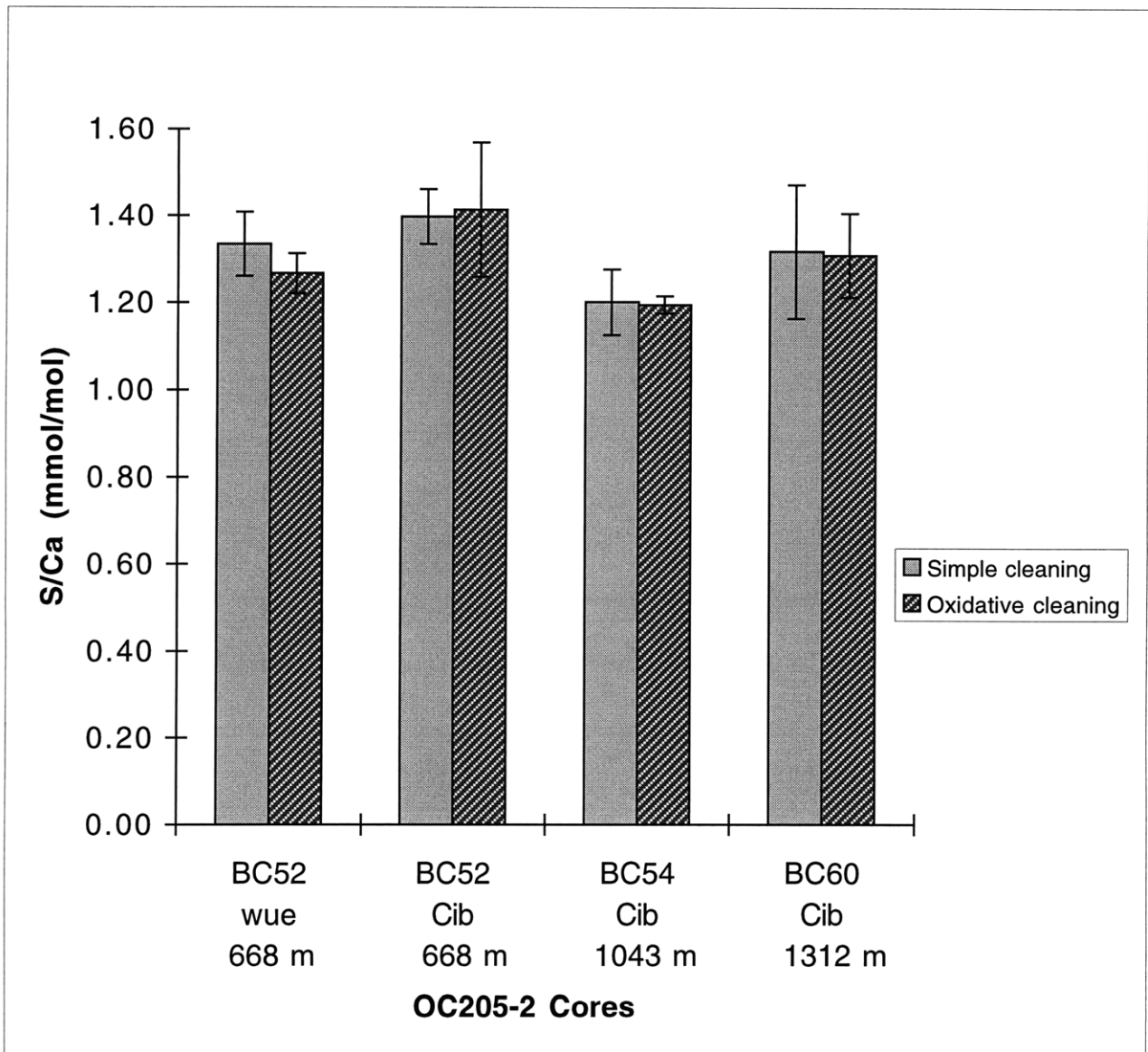
Figure 2: Comparison between S/Ca obtained in sample splits cleaned by two different procedures. Simple cleaning included ultrasonic agitation in distilled water and methanol. Oxidative cleaning added an oxidative step with hydrogen peroxide in a hot, basic solution with further ultrasonic agitation.

dependent upon sample size, but was typically 20-25 µL. The ratio of ^{32}S to ^{34}S in the spiked samples ranged from 0.1 to 4.0 but was usually in the range less than 2.0. The samples were mixed thoroughly by inverting or with a Vortex mixer to ensure equilibration of the spike and sample. The samples were again centrifuged to ensure homogeneity. Samples were then ready for analysis for sulfur.

Sulfur in dissolved foraminifera samples was analyzed by magnetic sector inductively coupled plasma-mass spectrometry (ICP-MS) using a Finnigan Element instrument. Typical operating parameters of the instrument and the acquisition method used are summarized in Table 1.

Table 1. Operating parameters and acquisition method for Finnigan Element ICP-MS

Inductively coupled plasma:

Ar cool gas flow	13-14 L/min
Ar nebulizer flow	1.00 L/min
Ar auxiliary flow	1.02 L/min
RF power	1450 W

Mass spectrometer:

lenses	tuned to S at m/z 32
extraction	-2000 V
focus	-731 V
X-deflection	6.90 V
Y-deflection	-8.63 V
shape	87.0 V
resolution	medium res. (R=3000)

Acquisition method:
S-32, S-34

mass window	200% peak width
samples per peak	20
sample time	0.005 s
detection mode	pulse counting
settling time at S-32	0.1 s
settling time at S-34	0.001 s
scanning type	E-scan
runs per acquisition	60 x 2 (120 scans, averaging every two)

The instrument was operated in medium resolution mode (nominal resolution of R=3000), which allowed sufficient separation of the ^{32}S signal from that of the isobaric interference ^{16}O-^{16}O. Dissolved samples (in a matrix of 1% HNO_3) were introduced to the plasma by a micro-concentric nebulizer, either an MCN 100 or MCN 6000 model (CETAC Technologies, Inc.) The MCN 100 delivers the nebulized sample into a quartz spray chamber which connects to the torch. The MCN 6000 incorporates a desolvating system which strips out most of the solvent through a semi-permeable membrane aided by nitrogen gas flow. The resultant dry nebulized sample stream is introduced directly to the torch. The MCN 6000 greatly reduces the size of the ^{16}O-^{16}O signal. However, the sulfur blank in clean 1% HNO_3 is a larger percentage of the signal of a 12μM SO4 standard than it is for the MCN 100. The ^{32}S blank signal in 1% HNO_3 and the accompanying ^{16}O-^{16}O interference for the two nebulizers can be compared in Figures 3 and 4(b). The MCN 6000 ^{32}S signal in Figure 3 is more than twice that for the MCN 100 (Fig. 4(b)). However, ^{16}O-^{16}O is essentially undetectable using the MCN 6000, while it is much larger than the ^{32}S signal using the MCN 100. Nonetheless, as shown in Figure 4(a), the valley between the ^{32}S peak and the ^{16}O-^{16}O peak is always wide enough to distinguish the peaks using the MCN 100, allowing the MCN 100 to be used in the analyses in order to keep the blank signal as low as possible.

Sample measurement runs were conducted with frequent analyses of acid blanks, as well as consistency standards to monitor inter-run consistency of standards with a constant S/Ca ratio. In addition, spiked gravimetric standards (SGS) with a known artificial 32S/34S ratio were measured at least twice per run to monitor instrumental mass fractionation. The intra-run precision of SGS $^{32}S/^{34}S$ ratio measurements was 1-4%. All analyses were conducted using isotope dilution in which both the ^{32}S and ^{34}S peaks were measured and the $^{32}S/^{34}S$ ratio calculated after subtracting the ^{32}S and ^{34}S signals from the blanks run nearest in sequence to

1% HNO$_3$ blank using MCN 6000 nebulizer
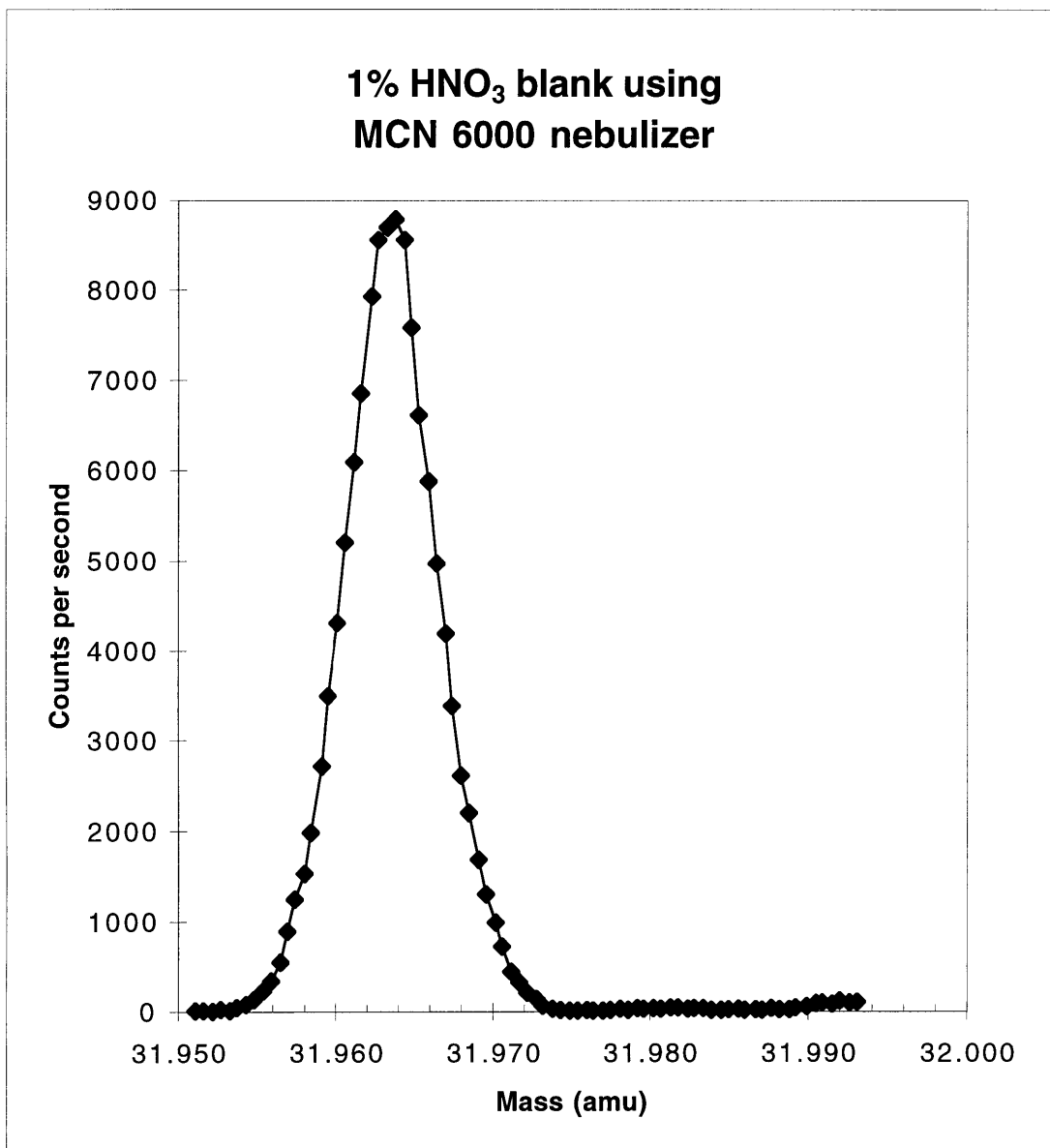
Figure 3: ICP-MS signal for ^{32}S in 1% HNO$_3$ blank using desolvating nebulizer model MCN 6000. Note the absence of a ^{16}O-^{16}O signal normally immediately adjacent to the sulfur peak.

(a)

Example of ICP-MS data file with spurious counts

Two channels in which anomalous counts were recorded

Leading edge of ^{16}O-^{16}O peak

Counts per second

Mass (amu)
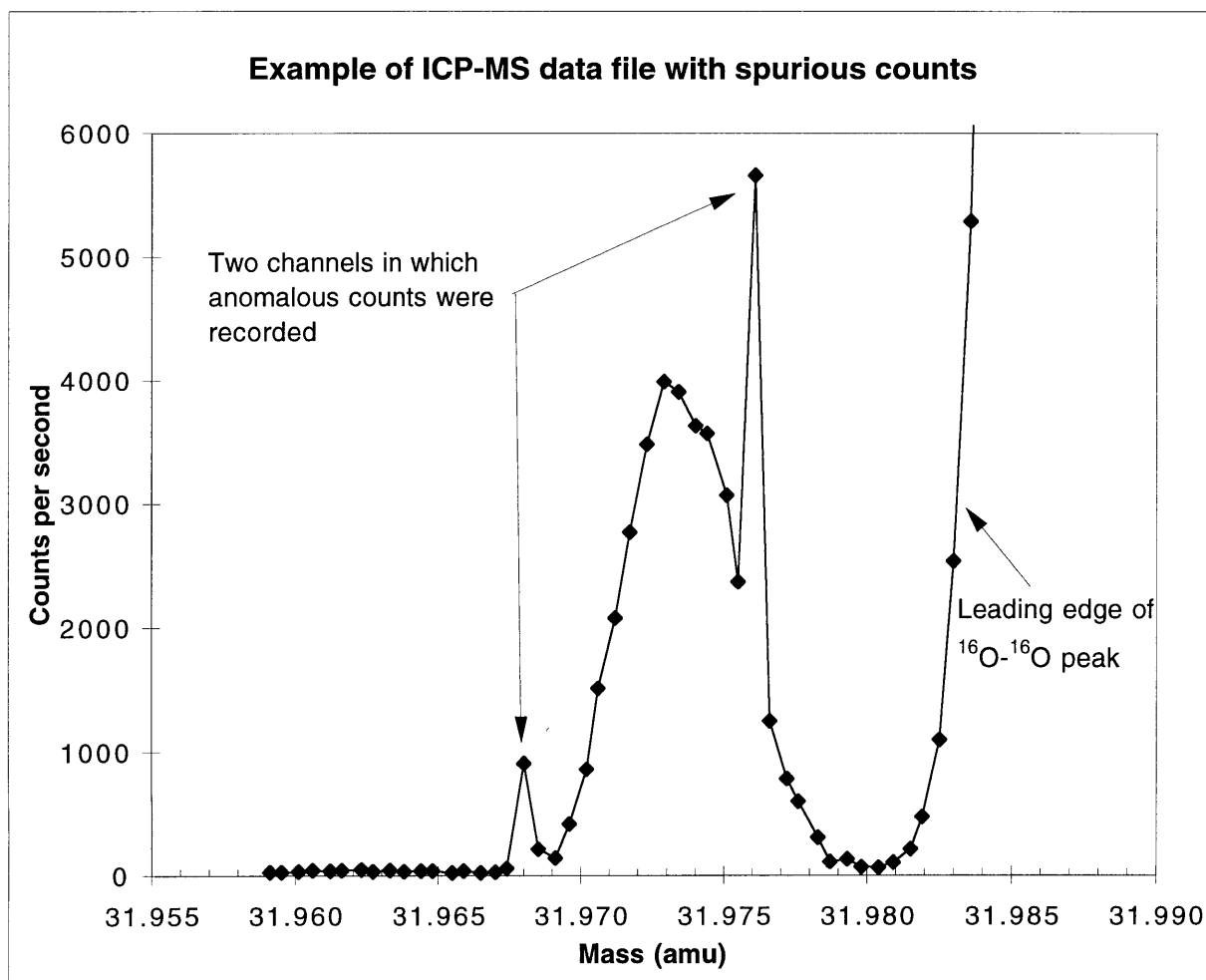
Figure 4: (a) ICP-MS signal for ^{32}S in 1% HNO_3 blank using microconentric nebulizer model MCN 100. Two channels in the peak have elevated counts due to spurious signals during acquisiton. These events are edited out during data processing. The edge of the ^{16}O-^{16}O interference is obviously resolved from the ^{32}S signal.

(b)

1% HNO₃ blank at full scale
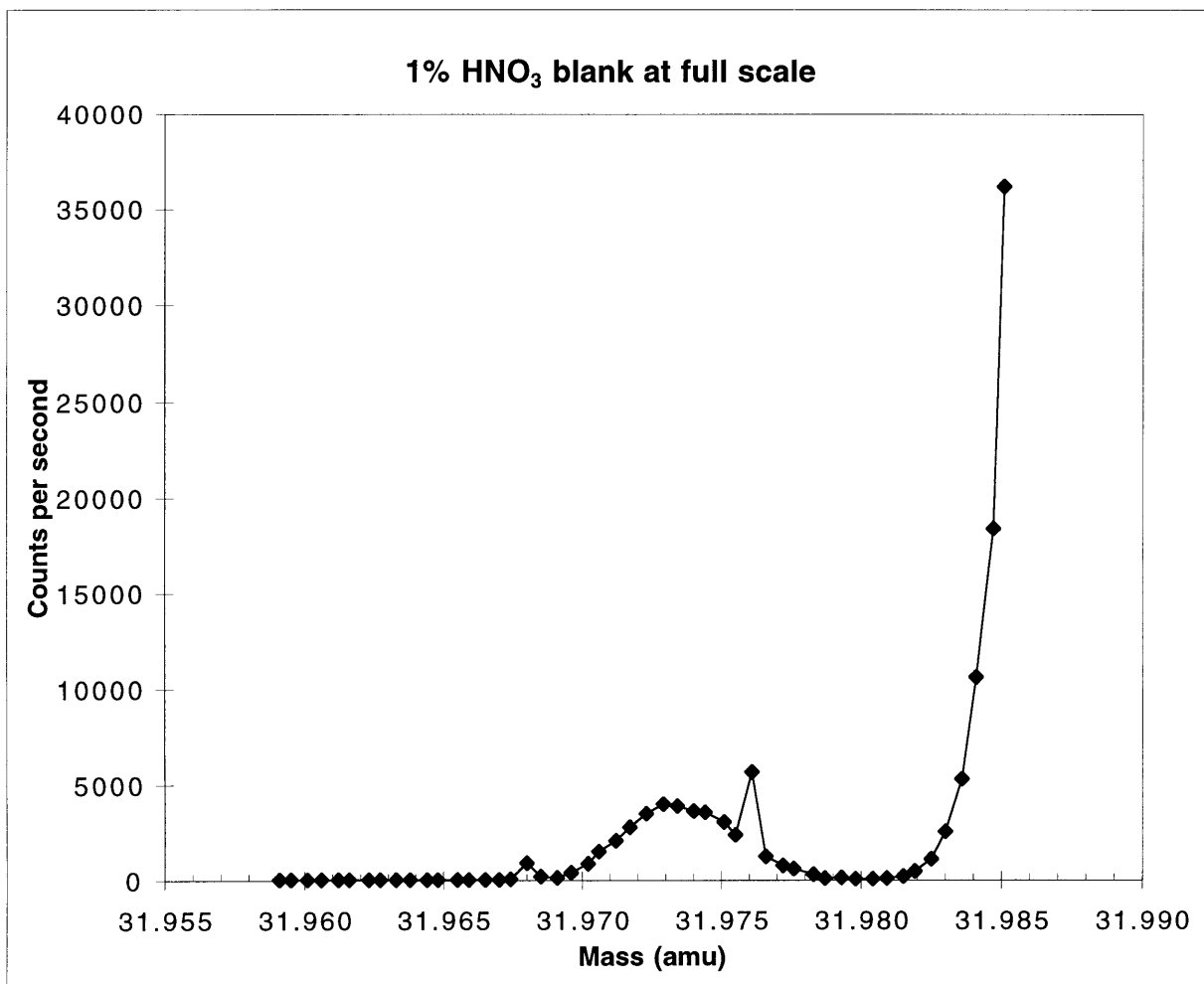
Figure 4(b): As (a) with counts per second axis at full scale to show magnitude
of oxygen signal.

the sample in question. Duplicate acid blanks were analyzed at least every seven samples in all cases. The S concentration of each sample was calculated according to the isotope dilution equation:

$$[S]_{sample} = \frac{0.930}{0.042}[S]_{spike}\left(\frac{spike}{sample}\right)_{volume}\left(\frac{R_{mix} - 0.020}{22.570 - R_{mix}}\right) \qquad (3)$$

where R_{mix} is the ratio measured for the spiked sample mixture, 0.930 is the fraction ^{34}S in the spike (Isotec value), 0.042 is the fraction ^{34}S in natural S, 0.020 is the ratio of $^{32}S/^{34}S$ in the spike (measured by ICP-MS), and 22.570 is the natural $^{32}S/^{34}S$ ratio.

The sulfur blank measured in all clean acids and clean distilled, deionized water with the ICP-MS was much higher than expected and was nearly identical despite widely varying sources and pretreatment. Attempts to reduce the blank by running a dilute HNO_3 sample numerous times through an AG1-X8 anion exchange resin column actually showed a slight increase in sulfur counts compared to untreated HNO_3. Perhaps some sulfur contained in the resin was contributing to the blank in this case. However, the ultimate source of the sulfur blank is probably not the reagents used in the processing of samples. Nitric acid and hydrochloric acid triply-distilled in a Vycor still and diluted with distilled, deionized water were aspirated through fresh polypropylene tubing and produced sulfur blanks equivalent to 20 ppb sulfur, or 0.2 μM. Nearly all samples were at least ten times this blank level, but the blank is still much higher than expected for clean acids. Non-acidified distilled, deionized water also gave the same blank level, as did nitric and hydrochloric acids of ultra-pure grade (Seastar, Inc.) provided by the instrument operators. Because the blank remains at the same level even when no liquid sample is being aspirated into the plasma, the source of contamination is likely in the instrument itself. Further steps could be taken to determine the source of the sulfur blank by systematically isolating various components of the ICP-MS and determining the effect on sulfur count rates.

Scheme for processing raw ICP-MS data into a sulfur concentration value.

Raw data is exported from the Finnigan software package as an ASCII file. Each sample acquisition is contained in a separate file. The files are easily imported into Microsoft Excel or another spreadsheet program for processing. A file consists of one column with the mass in amu of each channel collected during one scan of the method. Each succeeding column contains the counts per second detected in each mass channel for one scan. There is one such column for each scan specified in the method, subject to any averaging included in the method. For example, a method of 50 x 2 scans acquires 100 scans, automatically averages each pair, and only writes the fifty averaged scans to the data file.

A Microsoft Excel Visual Basic macro was written to parse the ASCII files into spreadsheets and calculate the average and relative standard deviation of all the scans for each mass channel for each sample. The peak shapes for each sulfur isotope were then plotted from the averaged data. Each data file was screened for channels in which spurious counts were recorded both by inspecting the peak shape plots for anomalously high counts that distorted peak shape in some channels, and by checking the relative standard deviations of each channel for significantly large deviations. Instances of large deviations from the mean were relatively common; an example of spurious counts in a HNO_3 blank analysis is shown in Figure 4.

Spurious counts usually occurred in the same way throughout the analyses made for this thesis. One channel in a particular scan would have greatly exaggerated count rates, say 2×10^5 to 4×10^5 counts per second. This value could be from two to one thousand times the median count rate for that channel, depending on the concentration of the sample. In most cases, the initial channel with anomalous counts would be followed by one to five succeeding channels also with high counts, although not as high as the initial one. Then, the next five to twenty

channels would often have reduced counts, as if the anomalously high counts recorded earlier had saturated the detector or other components of the data acquisition system, causing further response to be below normal for some time as the mass spectrometer continued to scan through the specified mass range. The abnormal responses would not continue to the next isotope measured in the scan, however. It is unclear whether the spurious readings are actual burst of ions entering the detector or some sort of error produced by the electronics. The spurious data were easily edited out by excluding the affected data from the calculation of the average signal for that channel.

When the editing was completed, the total counts for each sulfur isotope were calculated by summing the average count rates for the channels under the peak and multiplying by the factor 0.005. The factor represents the time in seconds each isotope was scanned as specified in the method. The number of channels per peak was set at twenty in the method. This number was used to determine the number of channels to be summed in the spreadsheet. The channels were chosen by inspection to be as close to symmetrical about the maximum of the peak as possible. This criterion was necessary because the mass calibration of the ICP-MS was susceptible to drift over time or even in discrete steps between two sample analyses. The drift of the calibration made it impossible to use a fixed mass range (for instance, 31.9680 to 31.9804 amu for ^{32}S) for each sample peak. If calibration drift was observed in the course of analyzing samples, two strategies were used to deal with it. If the sulfur isotope peak was moving near the edge of the mass window, the method was modified to increase the width of the window in order to maintain the peak within the mass window. Increasing the width of the mass window also increased the time required to scan the window, which was a drawback when low volume samples were measured. Another problem with increasing the mass window is that the nearby ^{16}O-^{16}O peak, which can reach count rates in excess of 10^7

counts per second, may no longer be cut off at the edge of the window; this leads to excessive bombardment of the detector with ^{16}O-^{16}O ions. (See Figure 4(b) for an example of how the ^{16}O-^{16}O peak is cut off at the edge of the mass window.). In this case, and also when the calibration continued to drift, the sample runs were interrupted to perform a new mass calibration. This procedure usually took about one-half hour, after which sample analyses were resumed, with the mass window again set to its minimum value of 200% peak width.

Ca measurements were conducted by flame atomic absorption spectrometry. A known aliquot of 20 to 25 μL of the unspiked, dissolved sample was diluted with 5 mL of a lanthanum/HCl modifier in order to suppress the signal from phosphine in the acetylene flame. Ca concentrations were calculated from the absorbance of a 100 μM Ca standard measured every 4-7 samples. Linearity of the absorbance signal was confirmed for [Ca] in the concentration range of all samples measured.

C. Preliminary survey of planktonic foraminifera S/Ca ratios

Sulfur/calcium ratios were determined in planktonic and benthic foraminifera shells picked from marine sediment cores. Core locations for these and subsequent samples are listed in Table 2 and plotted in Figure 5. These analyses were designed to evaluate variability in foraminiferal sulfur content due to a number of variables and to determine whether foraminiferal sulfur can be used as a proxy measurement for the pH of the seawater in which the organism grew.

Six species of planktonic foraminifera from different locations in the Atlantic Ocean that calcify at different depths (Fairbanks et al., 1979; Hemleben et al., 1989) were measured in the initial analyses (run AA) to establish the ability of the ICP-MS method to measure foraminiferal sulfur consistent with levels expected for biogenic carbonates. Table 3 shows the results from these analyses on 0.18 to 0.77 mg of foraminiferal carbonate, yielding S/Ca ratios of 0.10 to 1.36 mmol/mol. Four
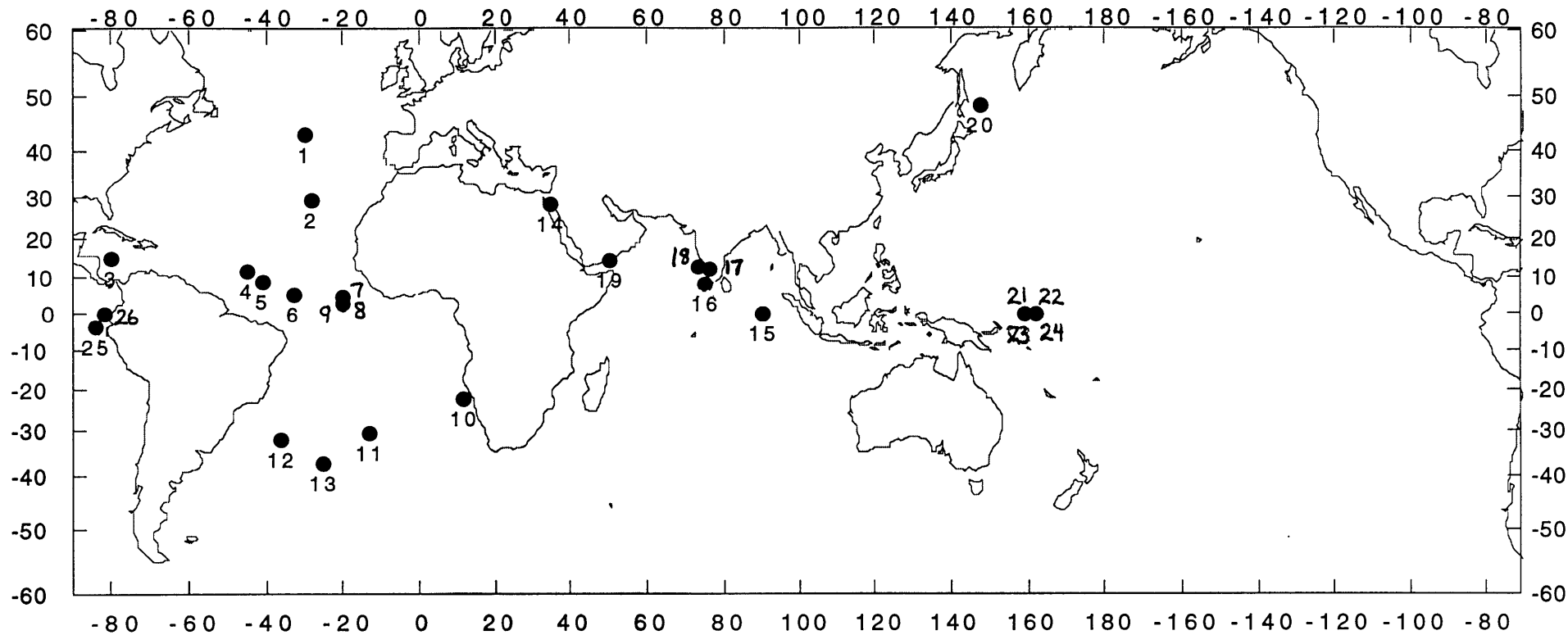
Figure 5: Locations of cores studied. Numbers refer to cores as listed in Table 2.

Table 2. List of sediment cores with samples analyzed
in this thesis.

#	Core	Lat	Long	Depth
	Atlantic			
1	CHN82 20PC	43.50	-29.87	3070
2	V23-91	29.58	-28.57	2758
3	V18-357	15.03	-80.23	1818
4	V25-44	11.51	-45.16	4049
5	V22-26	8.72	-41.25	3720
6	V20-234	5.32	-33.03	3133
7	EN66-38GGC	4.92	-20.50	2931
8	EN66-26GGC	3.08	-20.02	4745
9	V22-186	3.38	-20.12	4471
	South Atlantic/Southern Ocean			
10	RC13-228	-22.33	11.20	3204
11	V19-240	-30.58	-13.28	3103
12	AII107-65GGC	-32.03	-36.19	2795
13	RC12-294	-37.16	-25.47	4144
	Red Sea			
14	AII93-74PG	28.30	34.52	884
	Indian Ocean			
15	RC14-36	-0.47	90.00	3706
16	MD76-125	8.35	75.20	1878
17	MD76-127	12.08	75.90	1610
18	MD76-128	13.08	73.18	1712
19	MD76-135	14.27	50.32	1895
	Pacific Ocean			
20	V32-159	48.67	147.40	1235
21	MW91-9 BC36	0.00	158.91	2314
22	MW91-9 BC58	0.00	162.22	4341
23	MW97-20 MC18	-0.01	158.92	2293
24	MW97-20 MC28	0.00	162.22	4325
25	TR163-31p	-3.62	-83.97	3210
26	V19-27	0.47	-82.07	1373

Note: # references location on map in Figure 5. Positive
coordinates are north and east.

samples had [Ca] less than 5 mM in the primary dissolved solution, indicating

substantial loss of sample during the cleaning process. The anomalously low result

of 0.10 mmol/mol comes from one of these low recovery samples; it is likely that

the result is an artifact of sample loss. The other samples exhibit a sulfur content

that is consistent with expectation for biogenic carbonates (Busenberg and Plummer,

1985; Staudt et al., 1993).

It may be inadvisable to try to determine trends in S/Ca with calcification

depth from this preliminary data set, but the *Globorotalia tumida* and *Globorotalia*

truncatulinoides samples have S/Ca ratios of 0.45 mmol/mol and 0.69 mmol/mol,

Table 3. Initial test of ICP-MS measurement of sulfur in foraminifera.

ID	Species	Core	Location	Weight (mg)	S (µM)	Ca (mM)	S/Ca (mmol/mol)	Comments
AA3	*G. menardii*	V18-357	Carib.	0.45	38.21	34.94	1.09	
AA4	*G. menardii*	V18-357	"	0.18	25.39	18.72	1.36	
AA5	*G. sacculifer*	V25-44	tr. W. Atl.	0.37	12.70	17.05	0.74	
AA6	*G. sacculifer*	V25-44	"	0.57	2.59	3.00	0.86	low Ca
AA7	*G. sacculifer*	V25-44	"	0.44	5.66	5.93	0.96	
AA8	*G. sacculifer*	V20-234	tr. MAR	0.77	2.88	4.40	0.65	low Ca
AA9	*G. sacculifer*	V20-234	"	0.60	0.51	4.93	0.10	low Ca
AA10	*G. sacculifer*	V20-234	"	0.38	1.19	1.24	0.96	low Ca
AA11	*G. ruber (pink)*	V22-26	tr. MAR	0.55	11.87	16.64	0.71	
AA12	*O. universa*	V22-26	"	0.42	13.22	19.19	0.69	
AA13	*G. menardii*	RC14-36		0.57	33.80	42.23	0.80	
AA14	*G. tumida*	V22-186	tr. E. Atl.	0.61	19.99	44.22	0.45	
AA15	*G. truncat.*	V23-91	E. Atl.	0.60	23.64	34.24	0.69	
TW22	*C. wue.*	TR163-31p	E. Eq. Pac.		4.73	12.96	0.36	benthic
UB29	*Hoeglundina*	Chn 82-20pc	N. Atl.		1.50	17.06	0.09	benthic aragonite

respectively. These are the lowest values in the data set (aside from the 0.10

mmol/mol result discussed above) and also represent deeper calcifying species, as

compared with *Globigerinoides sacculifer, Globigerinoides ruber,* and *Orbulina*

universa which calcify very near the surface. However, *Globorotalia menardii* also

calcifies deeper than the surface waters, and it has the highest S/Ca ratios measured.

Varying core locations may make these trends impossible to decipher as purely

depth dependent, especially because replicates of these samples were not analyzed.

Another complication in this data set is that it is the only one included here that

was not measured by isotope dilution. The measurements were made before

obtaining [34]S enriched Na_2SO_4 for spiking, so that the results were calculated by a

standard curve. Considerable drift in the ICP-MS response occurred during the run,

so that corrections for response ratio (mass counts per second per sulfur

29

concentration) were assumed to be linear between repeated measurements of sulfate standards.

D. Analytical and sample variability of S/Ca ratios in Gulf of Aqaba planktonic foraminifera

The next run of foraminifera samples (run AB) was conducted with material from 0-2 cm of gravity core AII93-74PG raised from the Gulf of Aqaba in the Red Sea (core location listed in Table 2). The coarse fraction was sieved and planktonic foraminifera species *G. sacculifer*, *G. ruber*, *Globigerinella siphonifera*, *Globigerinella calida*, and *O. universa* were picked from the 300-425 μm and 425-600 μm size fractions for sulfur analysis. The results of these analyses are shown in Table 4. This run was intended to provide a comparison with living planktonic

Table 4. ICP-MS (run AB) results for core AII93-74PG (Gulf of Aqaba) samples.

sample	species		size	# indiv	wt. (mg)	[S] (μM)	[Ca] (mM)	S/Ca (mmol/mol)	Avg.	SE	CV
AB17	G. siph		425-	9	0.37	37.56	25.38	1.48			
AB18	G. ruber		425-	4	0.02	(2.77)	(2.55)	(1.09)			
AB19	O. univ		425-	5	0.26	15.46	6.18	2.50			
AB20	O. univ		425-	0.5	0.01	(0.85)	(1.04)	(0.82)			
AB21	G. calida		425-	3	0.08	(10.17)	(4.31)	(2.36)			
AB25	G. sac	w/sac	300-	2	0.01	(4.84)	(3.39)	(1.43)			
AB26	G. sac	w/sac	300-	1	0.03	(4.37)	(2.72)	(1.61)			
AB27	G. sac	w/o sac	300-	22	0.80	24.23	13.06	1.86			
AB28	"	"	"			12.78	7.72	1.65	1.78	0.07	6.34%
AB29	"	"	"			21.40	11.61	1.84			
AB30	G. sac	w/o sac	300-	1	0.02	(4.14)	(2.04)	(2.03)			
AB31	G. sac	w/sac	300-	24	0.90	28.60	14.66	1.95			
AB32	"	"	"			42.21	21.19	1.99	2.07	0.10	8.16%
AB33	"	"	"			40.70	18.00	2.26			
AB34	G. sac	w/sac	425-	13	1.17	(-0.07)	(0.21)	(-0.35)			
AB35	"	"	"			(-0.07)	(1.93)	(-0.04)			
AB36	"	"	"			26.36	14.07	1.87			
AB37	G. sac	w/sac	425-	2	0.14	8.74	5.34	1.64			
AB38	G. siph		425-	4	0.31	16.73	9.10	1.84			
AB39	G. sac	w/sac	425-	5	0.30	17.00	9.26	1.84	1.92	0.08	5.90%
AB40	"	"	"			15.94	7.99	2.00			

Notes: SE is standard error of the mean (s.d./√n) for replicate samples, and CV is the coefficient of variation. Parentheses enclose values below the 5mM [Ca] threshold.

foraminifera collected from the Gulf of Aqaba and cultured in seawater with pH adjusted in a range from 7.7 to 8.6. Ultimately, the only species analyzed for the sulfate-pH calibration was *G. sacculifer,* in the size range of 460-730 μm.

The variables examined in run AB were total sample size (few vs. many individuals) as indicated by [Ca] of the sample, different species of the same size fraction, the single species *G. sacculifer* in both 300-425 μm and 425-600 μm size fractions, *G. sacculifer* samples with and without the terminal sac-like chamber (300-425 μm), and large samples of *G. sacculifer* crushed and split into two or three replicate samples compared to crushed samples not split into replicates. Too few samples of species other than *G. sacculifer* were run to make meaningful comparisons. The data are included in the table for reference.

The S/Ca ratio vs. Ca concentration is plotted for Gulf of Aqaba samples in Figure 6. The Ca concentration indicates the size of the dissolved sample. Two *G. sacculifer* samples (AB34 and AB35) with negative S/Ca ratios calculated by isotope dilution are artifacts of sample loss during cleaning. Little or no foraminifera fragments remained in those samples, so that the analysis provides no meaningful results. These samples are not included in the discussion of the results of this run.

Examining those samples below a threshold of 5 mM [Ca], indicates a probable bias in S/Ca ratios for small sample sizes. Figure 6 shows that the three lowest S/Ca ratios occur below the 5 mM [Ca] threshold, although the second highest S/Ca ratio also occurs below this threshold. In Table 5, the results in run AB are organized according to different variables in the data set in order to evaluate the effect of these variables on the measured S/Ca ratios. Including all species analyzed, the average S/Ca ratio for six samples with [Ca] less than 5 μM is 1.55 mmol/mol, while thirteen samples with [Ca] greater than 5 μM have an average S/Ca ratio of 1.90 mmol/mol. The inclusion of different species may contribute to this sample size effect; restricting the examination to G. sacculifer samples may be more useful. Three

31

Gulf of Aqaba planktonic foraminifera
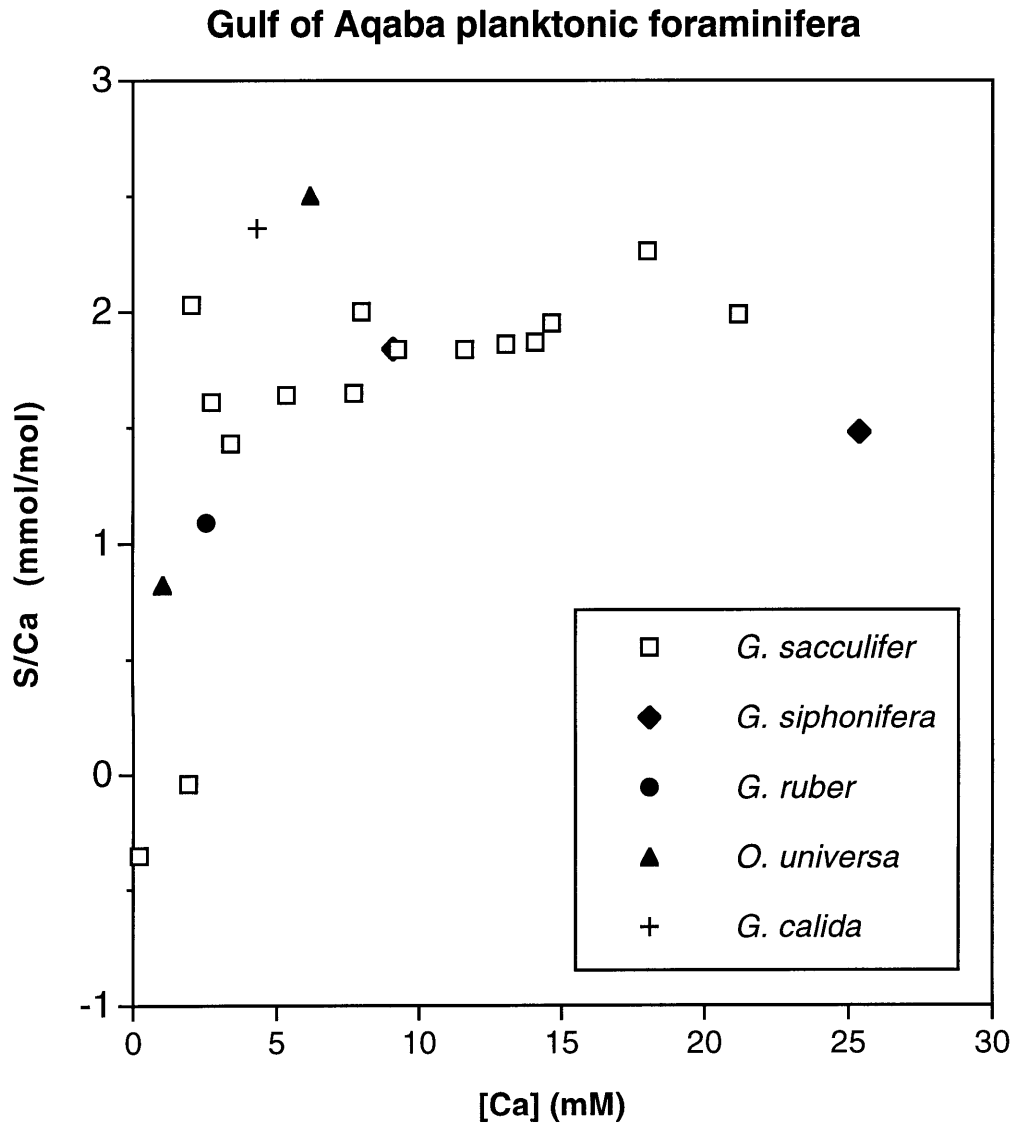
Figure 6: S/Ca ratios measured in planktonic foraminifera from the Gulf of Aqaba plotted against the Ca concentration measured in the sample. Bias in the S/Ca measurement due to [Ca] effects can be evaluated.

G. sacculifer samples with [Ca] less than 5 μM have an average S/Ca of 1.69 mmol/mol, while the average for ten G. sacculifer samples with [Ca] greater than 5 μM is 1.89 mmol/mol.

Table 5. Run AB: examining effect of sample size ([Ca]), foram size (length), species, and presence of sac-like chamber variables on S/Ca ratio.

row	Species	sac ?	[Ca]	size (μm)	Avg. S/Ca	SE	CV	n
1	all		< 5 μM	300-600	1.55	0.24	37.10%	6
2	all		> 5 μM	300-600	1.90	0.07	13.87%	13
3	G. siph.		> 5 μM	425-600	1.66	0.18	15.29%	2
4	O. univ.		both	425-600	1.66	0.84	71.93%	2
5	G. sacc.		both	300-600	1.84	0.06	11.88%	13
6	G. sacc.	both	< 5 μM	300-425	1.69	0.18	18.34%	3
7	G. sacc.	both	> 5 μM	300-600	1.89	0.05	9.04%	10
8	G. sacc.	both	> 5 μM	300-425	1.93	0.15	10.46%	6
9	G. sacc.	yes	both	300-425	1.85	0.09	17.89%	5
10	"	"	< 5 μM	"	1.52	0.10	8.45%	2
11	"	"	> 5 μM	"	2.07	0.08	8.16%	3
12	G. sacc.	no	both	300-425	1.85	-	8.33%	4
13	"	"	< 5 μM	"	2.03	0.07	-	1
14	"	"	> 5 μM	"	1.78	0.07	6.34%	3
15	G. sacc.	yes	> 5 μM	425-600	1.84	0.08	8.15%	4

Notes: sac ? column indicates presence of terminal sac-like chamber in *G. sacculifer* samples; [Ca] column indicates whether samples are less than or greater than 5 μM [Ca]. The entry 'both' indicates entry includes samples of both types of that category. SE is the standard error of the mean (s.d./√n), and CV is the coefficient of variation. S/Ca units are (mmol/mol).

Comparing rows 6 and 8, and rows 10 and 11 shows that in *G. sacculifer* samples restricted to 300-425 μm, and those restricted to 300-425 μm *and* possessing a terminal sac-like chamber, respectively, the samples below 5 μM [Ca] have a lower average S/Ca ratio than those above 5 μM [Ca]. Comparing rows 13 and 14, however, shows that for *G. sacculifer* in the size range 300-425 μm without the sac-like chamber, the sample less than 5 μM [Ca] has a higher S/Ca ratio than the average for those greater than 5 μM [Ca]. In this case, row 13 consists of only a single sample. It appears that in most cases, samples of less than 5 μM [Ca] have lower S/Ca ratios than those samples greater than 5 μM [Ca], so to avoid possible artifacts due to

sample size, the remaining data in this thesis is screened for samples with [Ca] less than 5 μM, which are disregarded.

Comparing rows 11 and 15 of Table 5 shows that with other variables held constant, three *G. sacculifer* samples between 300-425 μm have an average S/Ca ratio of 2.07 mmol/mol, and four samples between 425-600 μm have an average S/Ca ratio of 1.84 mmol/mol. Again, this difference is not significant within error bounds of ± 2 SE (SE = s.d./√n). *G. sacculifer* samples that differ only in the presence or absence of a sac-like chamber (rows 11 and 14) show that three samples with a sac-like chamber have an average S/Ca ratio of 2.07 mmol/mol, while three samples without a sac-like chamber have an average S/Ca ratio of 1.78 mmol/mol. Once again, these values are equal within an error of ± 2 SE.

Table 4 shows the average and standard deviation for three sets of *G. sacculifer* samples that were crushed and pooled before they were split into separate samples, thus representing replicates in which only analytical errors should apply. The coefficients of variation of the S/Ca ratio for these replicate sets range from 5.9% to 8.2%. The grand average S/Ca ratio and coefficient of variation for all thirteen *G. sacculifer* samples analyzed in this run (row 5 of Table 5) is 1.84 mmol/mol ± 11.9%. The pooled replicates may indicate a slight statistical improvement in precision over the entire data set. The grand average *G. sacculifer* S/Ca ratio may also be useful for comparison to the cultured foraminifera calibration of S/Ca ratio vs. pH (described in section F). According to the calibration generated using cultured *G. sacculifer* from the Gulf of Aqaba, an S/Ca ratio of 1.84 ± 0.22 mmol/mol corresponds to a pH of 8.40 ± 0.13. The pH of the modern surface waters of the Gulf of Aqaba is usually about 8.2 (Reiss and Hottinger, 1984), so this estimate appears too high.

E. Little Bahama Banks depth transect study

The analysis of foraminiferal sulfate was extended to benthic foraminifera from a suite of box cores collected in a depth transect from the southwestern slope of the Little Bahama Bank (LBB). Figure 7 indicates the locations of the cores. This setting is ideally suited for the assessment of foraminiferal paleoceanographic proxies in the thermocline due to its hydrography and the abundance of benthic foraminifera in the sediments.

The Providence Channels connect the western North Atlantic with the Straits of Florida and provide a conduit for waters overlying the LBB. Hydrographic data (primarily temperature-salinity relationships) has established that the thermocline and deeper waters of the channels and overlying the LBB originate in the Sargasso Sea and North Atlantic Deep Water, rather than the shelf waters off Florida (Slowey and Curry, 1995). Thus, this location allows the comparison of benthic foraminifera S/Ca ratios to hydrographic parameters varying in the thermocline representative of the Sargasso Sea, emphasizing pH and $[CO_3^=]$, and including temperature and salinity. The box cores sampled range in depth from 301 m to 1585 m (Table 6). Three genera or species were analyzed for sulfur content from these cores: *Uvigerina* species, *Cibicidoides wuellerstorfi*, and other mixed *Cibicidoides* species consisting predominantly of *C. pachyderma*. Not all species were abundant throughout the depth range, but *Cibicidoides* species were most consistently available throughout the depth range sampled. *Uvigerina* were measured in the interval 301 m to 668 m, *C. wuellerstorfi* were measured from 301 m to 1312 m, and *Cibicidoides* from 301 m to 1585 m (Figure 8). Not only were *Cibicidoides* species more abundant, but the S/Ca data for these samples are more reproducible than for *Uvigerina* and *C. wuellerstorfi* (Table 7). Hence, the following discussion refers only to the *Cibicidoides* data. The detailed analytical data for these samples is given in Table A1 in the Appendix.

35
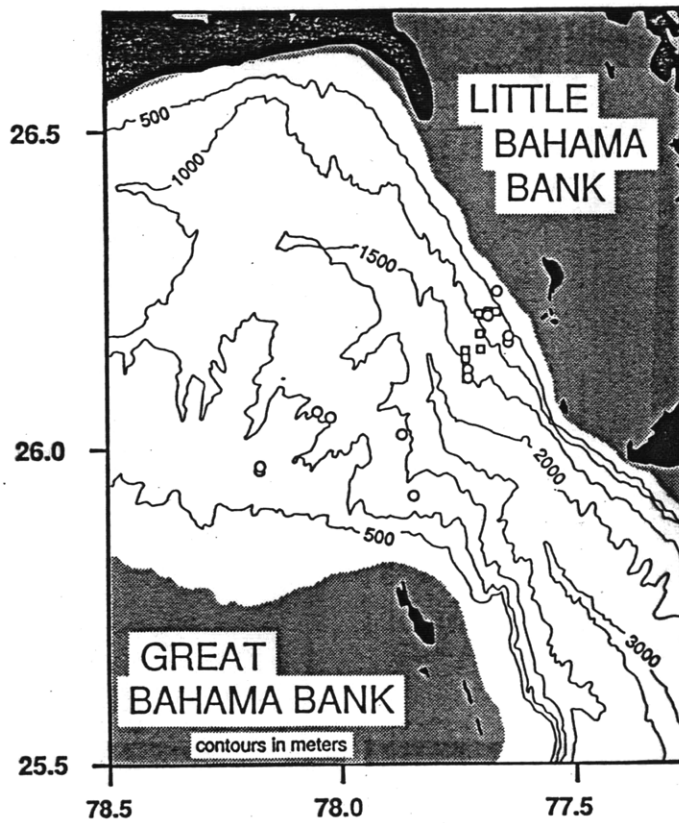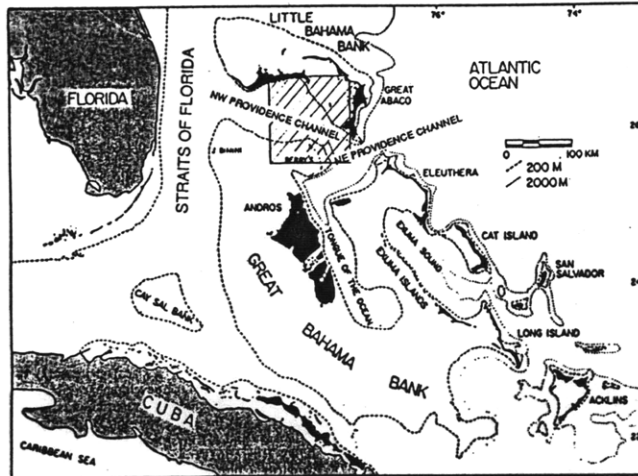
Figure 7: Locations of Little Bahama Banks box core samples. Lower figure is enlargment of hatched area in upper figure. Boxes indicate box core locations.

Table 6. Box cores from Little Bahama Banks.

Core	Latitude °N	Longitude °W	Depth m	Temp °C	Salinity psu	$[CO_3^=]$ µmol/kg	pH
OC205-2 BC79	26.23	77.65	301	18.38	36.53	220.6	8.13
OC205-2 BC77	26.23	77.66	433	16.55	36.27	203.9	8.13
OC205-2 BC48	26.24	77.68	580	13.31	35.76	150.9	8.04
OC205-2 BC52	26.24	77.69	668	11.49	35.50	136.4	8.03
OC205-2 BC51	26.23	77.70	830	8.20	35.17	103.6	7.97
OC205-2 BC54	26.19	77.71	1043	5.34	35.04	107.9	8.06
OC205-2 BC60	26.14	77.74	1312	4.35	34.99	104.1	8.08
OC205-2 BC61	26.12	77.75	1585	4.05	34.98	103.5	8.10

Note: Carbonate concentration and pH were estimated from hydrographic and TCO2/Alk data from GEOSECS Stn. 31.

Table 7. Benthic foraminifera S/Ca ratios from Little Bahama Banks.

	S/Ca (mmol/mol)											
Depth	Cibicidoides			C. wuellerstorfi			Uvigerina			All species		
(m)	Average	SE	n	Average	SE	n	Average	SE	n	Average	SE	n
301	1.99	0.06	6	3.92	1.07	3	1.21	0.20	3	2.28	0.38	12
433	1.94	0.24	6				0.79	0.01	2	1.65	0.26	8
580	1.39	0.04	3	1.70	0.18	2	1.90	0.31	3	1.66	0.14	8
668	1.41	0.04	6	1.30	0.02	6	1.12	0.14	3	1.31	0.04	15
830	1.38	0.11	6							1.38	0.11	6
1043	1.20	0.02	6							1.20	0.02	6
1312	1.31	0.04	6	1.80	0.23	3				1.47	0.11	9
1585	1.57	0.03	6							1.57	0.03	6

Notes: SE is the standard error of the mean (s.d./$\sqrt{n}$).

In order to calibrate S/Ca data with environmental parameters, hydrographic data from GEOSECS station 31 were chosen as representative of Sargasso Sea water (Bainbridge, 1981). The pH and carbonate data were linearly interpolated in order to obtain values corresponding to the temperatures (from OC205-89) at the depths of the box cores (Table 6). This was done by temperature rather than depth in order to account for the likelihood that properties remain the same between the open Sargasso Sea and the LBB along constant density surfaces rather than by depth. Density was not calculated for the OC205-89 data, so temperature was assumed to be a close indicator of density. Because the pH and carbonate data were not measured at OC205-89, there may be slight differences between the actual pH and carbonate values bathing the box core sites and those taken from GEOSECS 31. Depth profiles

OCE205-2 Little Bahama Banks benthic foraminifera

Figure 8: Benthic foraminiferal S/Ca ratios from box cores taken at the Little
Bahama Banks. Abbreviations are Uvi for   Uvigerina , wue for Cibicidoides
wuellerstorfi , and Cib for Cibicidoides spp. One sample is off the scale of
the plot at S/Ca = 6.03 mmol/mol.
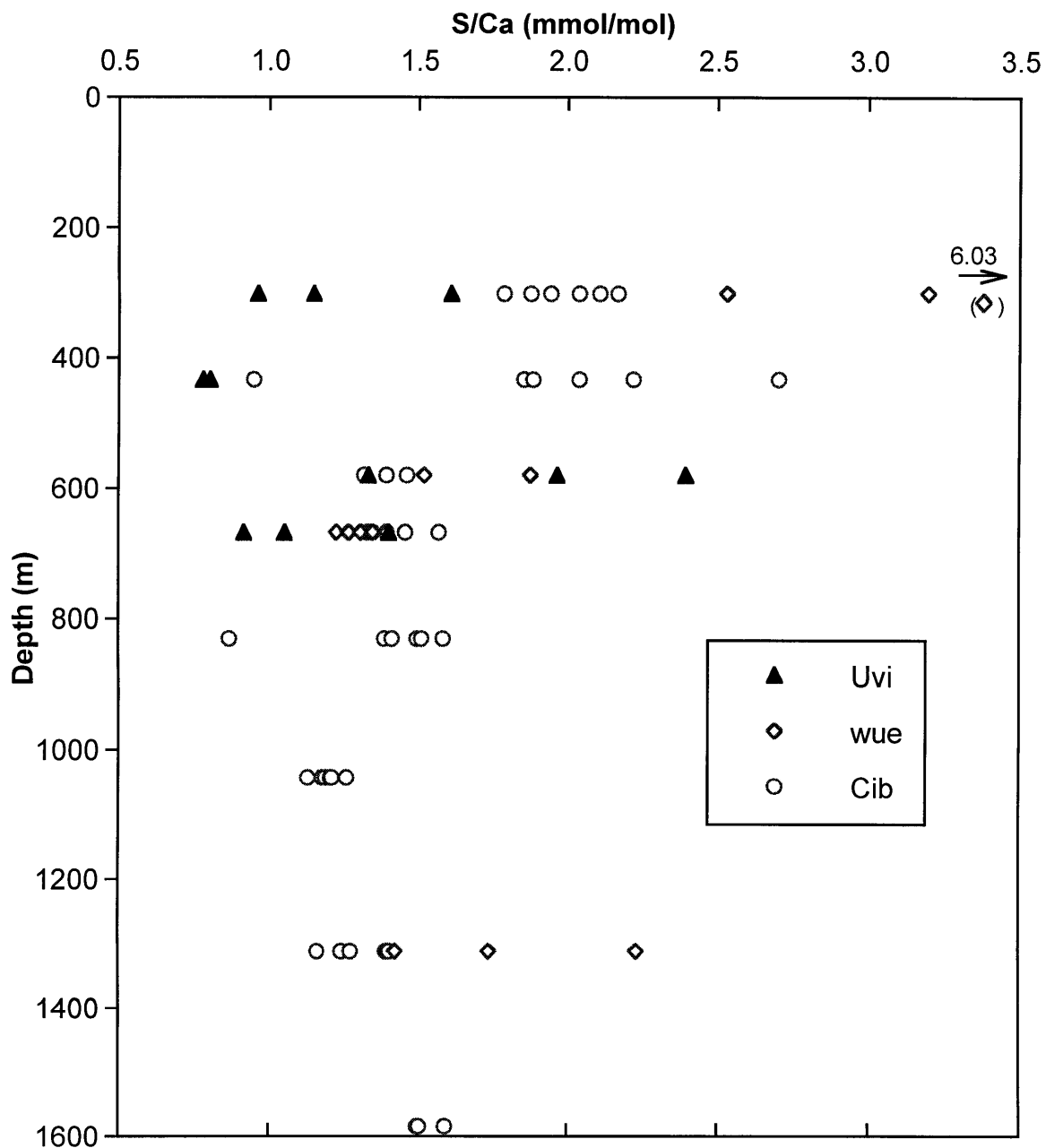
of *Cibicidoides* S/Ca ratios and the average S/Ca ratios of all species matched with four parameters: temperature (T), salinity (S), pH, and [$CO_3^=$] are shown in Figures 9-16. Scatter plots of *Cibicidoides* S/Ca ratios against temperature and salinity measured at station OC205-89 (Rosenthal et al., 1997) and [$CO_3^=$] and pH calculated from GEOSECS 31 data are shown in Figures 17 and 18.

The *Cibicidoides* S/Ca data were fit to the four parameters T, S, pH, and [$CO_3^=$] by least-squares linear regression. The T, S, pH, and [$CO_3^=$] data were also fit against each other to determine correlations in the hydrographic data. Table 8 summarizes the correlation coefficients (r^2) for each pair of variables. The S/Ca data correlate

Table 8. Linear correlation coefficients for variables at Little Bahama Banks.

r^2	S/Ca	T	S	[$CO_3^=$]	pH
S/Ca		0.587	0.720	0.772	0.475
T	0.587		0.961	0.903	0.101
S	0.720	0.961		0.983	0.234
[$CO_3^=$]	0.772	0.903	0.983		0.374
pH	0.475	0.101	0.234	0.374	

relatively well with [$CO_3^=$] and salinity, but less well with temperature and pH; in each case the slope of the linear fit is positive. The relationship of S/Ca to pH and [$CO_3^=$] does not fit the solid solution model proposed in the introduction or the Erez *A. lobifera* culture data because the predicted slope is negative. However, the S/Ca data are somewhat well correlated with salinity, and a positive slope for these two variables is supported by the solid solution model. In this case, if a constant carbonate ion activity is assumed during calcification, the S/Ca ratio will then only depend on variations in seawater [$SO_4^=$] which reflects salinity. The predicted relationship has a positive slope. Since [$CO_3^=$] is strongly correlated with salinity at the LBB, a strong salinity control on S/Ca may create the apparent *positive* correlation with [$CO_3^=$].
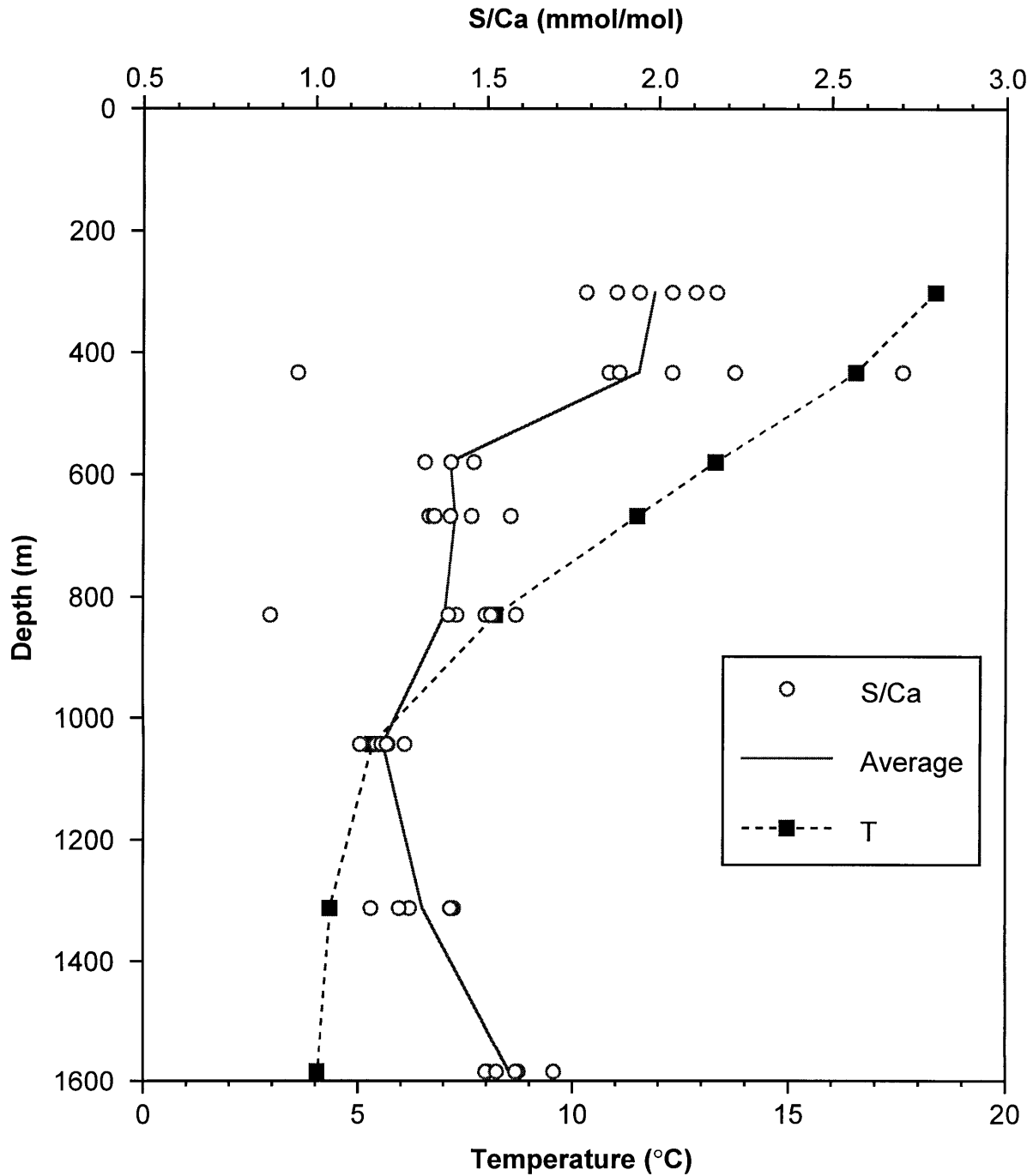
Figure 9: S/Ca data for Cibicidoides at Little Bahama Banks versus depth. Circles are individual measurements. Solid line connects averages of S/Ca at each depth sampled. Temperature versus depth measured at hydrographic station OC205-89.
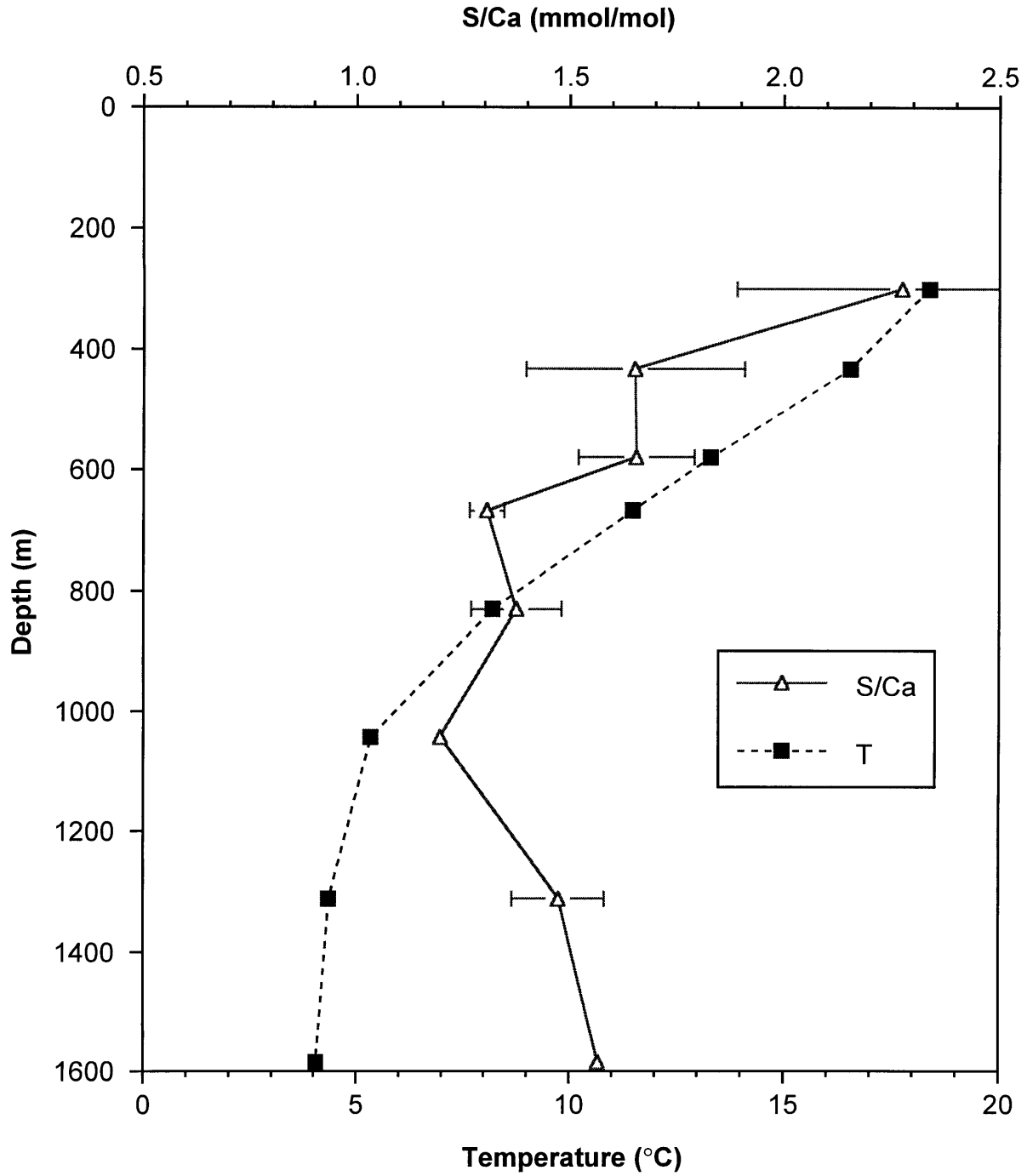
Figure 10: S/Ca data for all benthic foraminifera at Little Bahama Banks versus
depth. Solid line connects averages of S/Ca at each depth sampled. Error
bars represent one standard error of the mean. Temperature versus depth
measured at hydrographic station OC205-89.

41
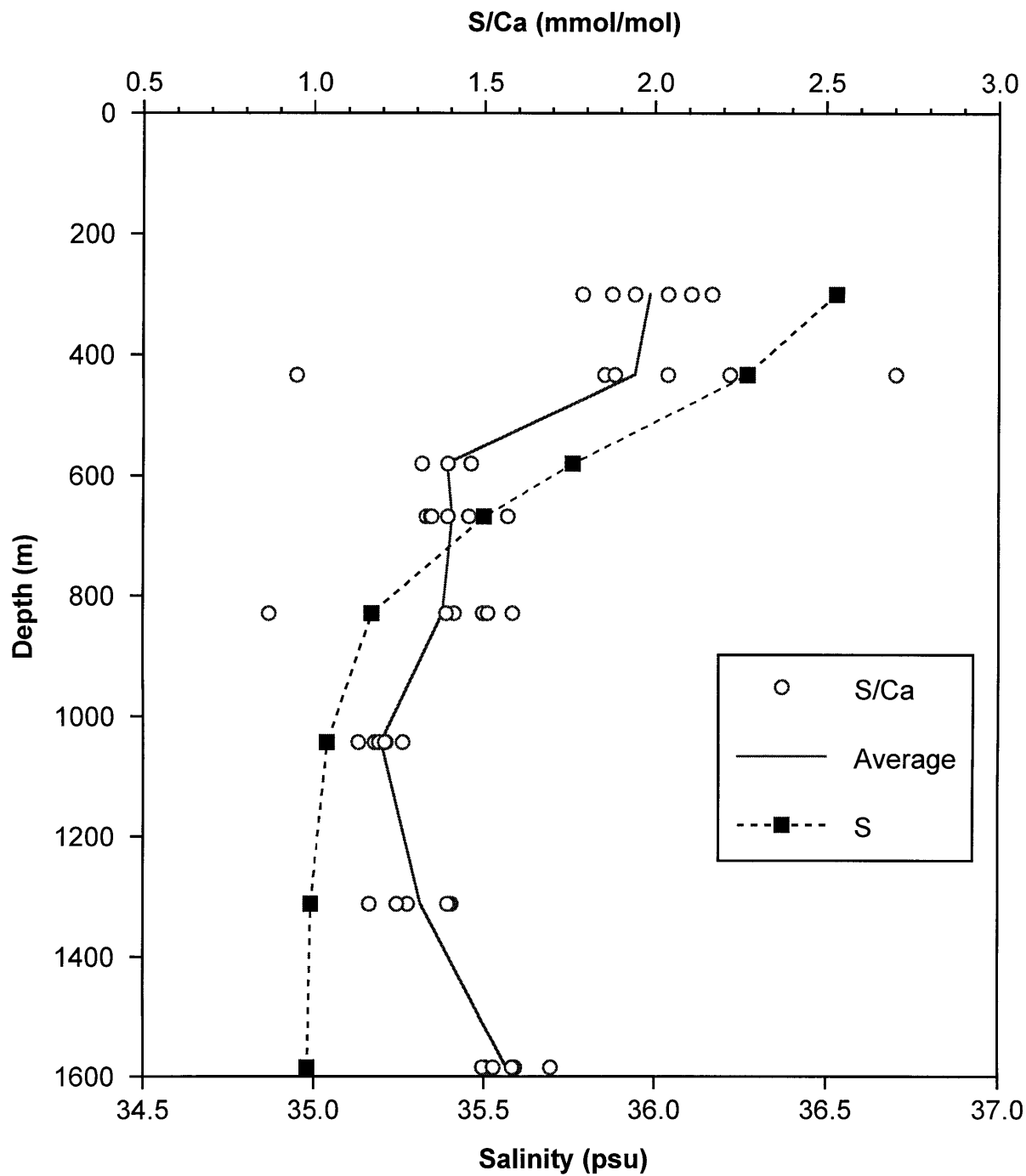
Figure 11: S/Ca data for Cibicidoides at Little Bahama Banks versus depth. Circles are individual measurements. Solid line connects averages of S/Ca at each depth sampled. Salinity versus depth measured at hydrographic station OC205-89.
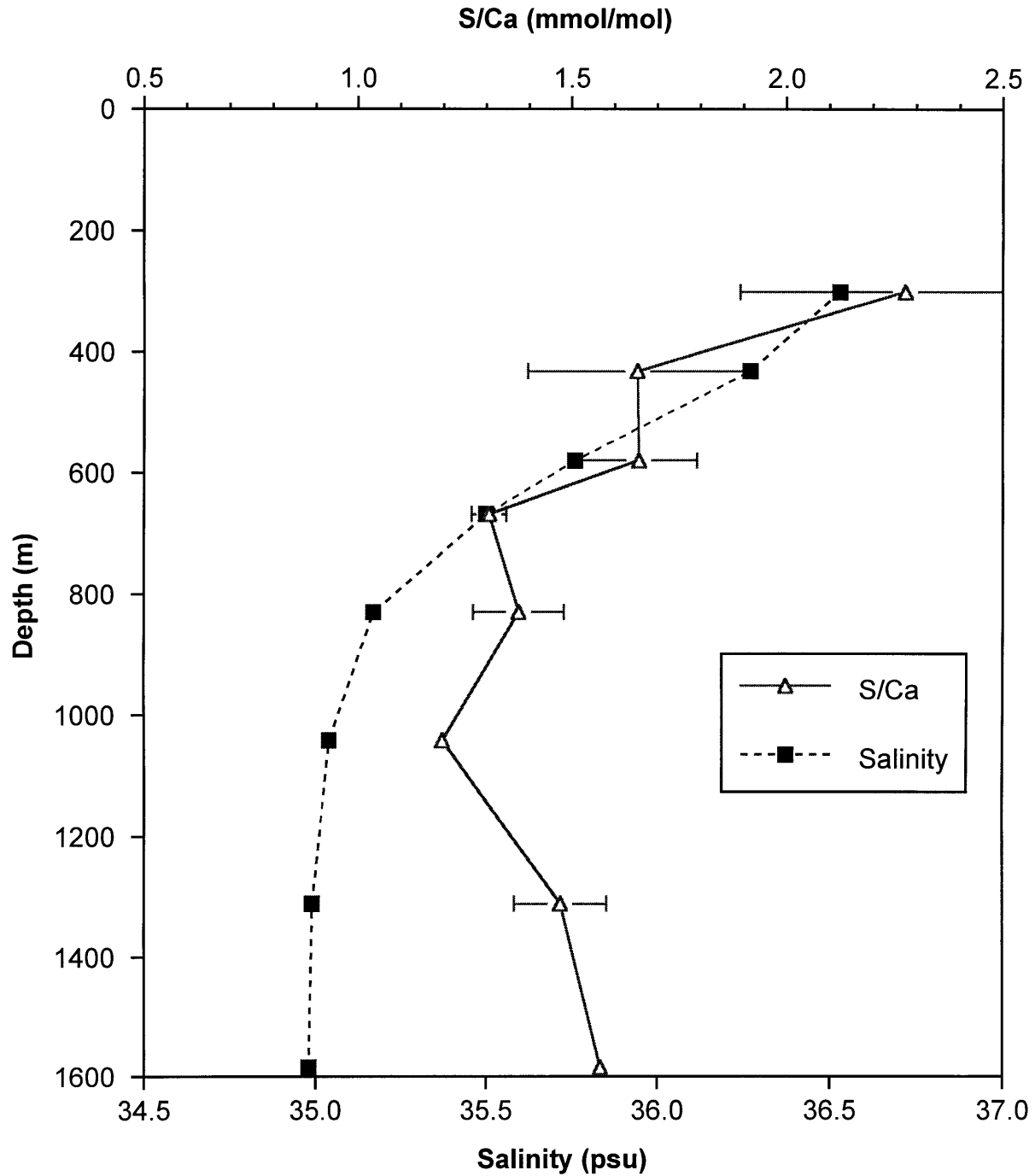
Figure 12: S/Ca data for all benthic foraminifera at Little Bahama Banks versus depth. Solid line connects averages of S/Ca at each depth sampled. Error bars represent one standard error of the mean. Salinity versus depth measured at hydrographic station OC205-89.
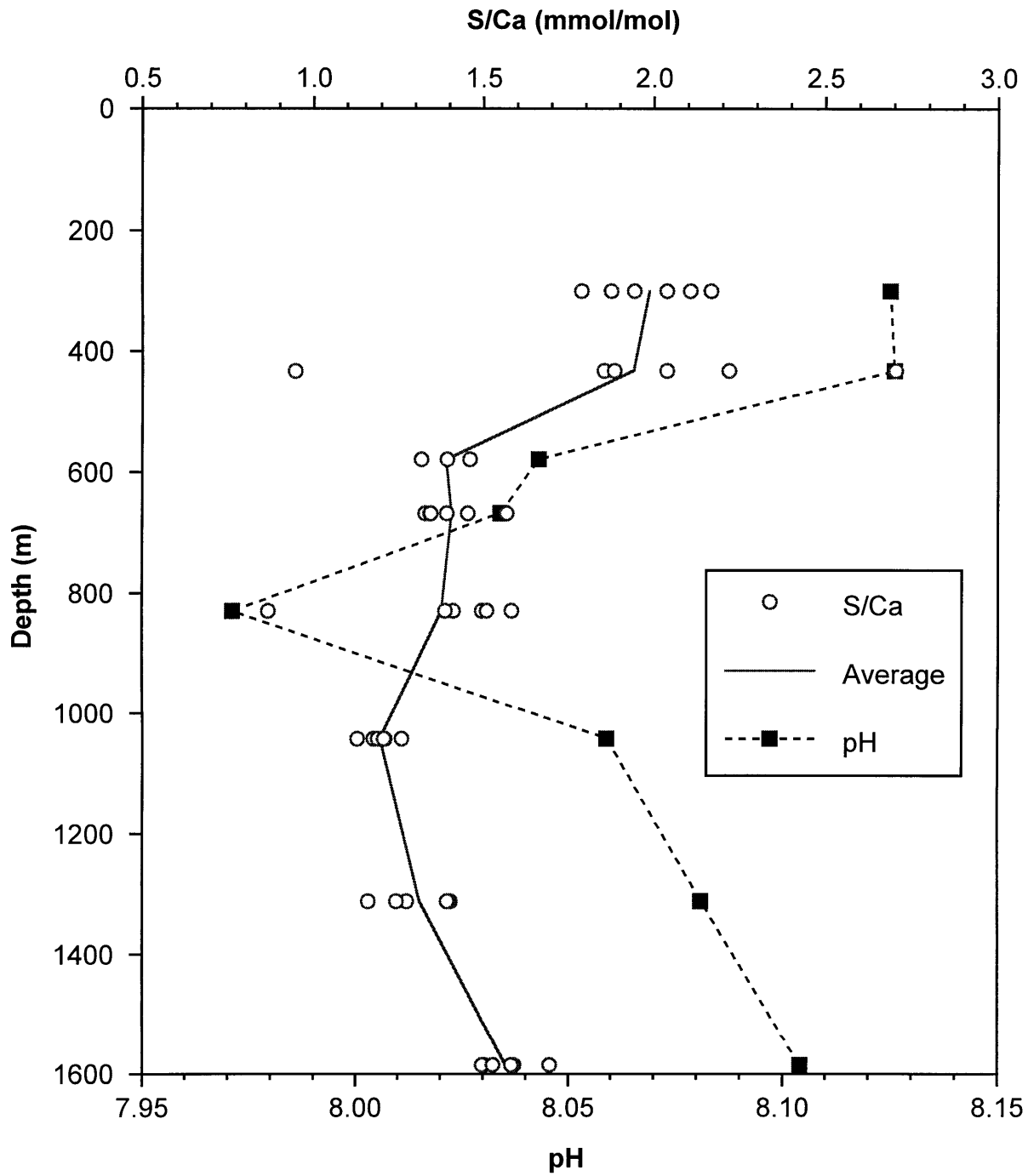
Figure 13: S/Ca data for <u>Cibicidoides</u> at Little Bahama Banks versus depth. Circles
are individual measurements. Solid line connects averages of S/Ca at
each depth sampled. pH versus depth extrapolated from GEOSECS station
31 data by correlating with temperatures at the depths of the core sites.
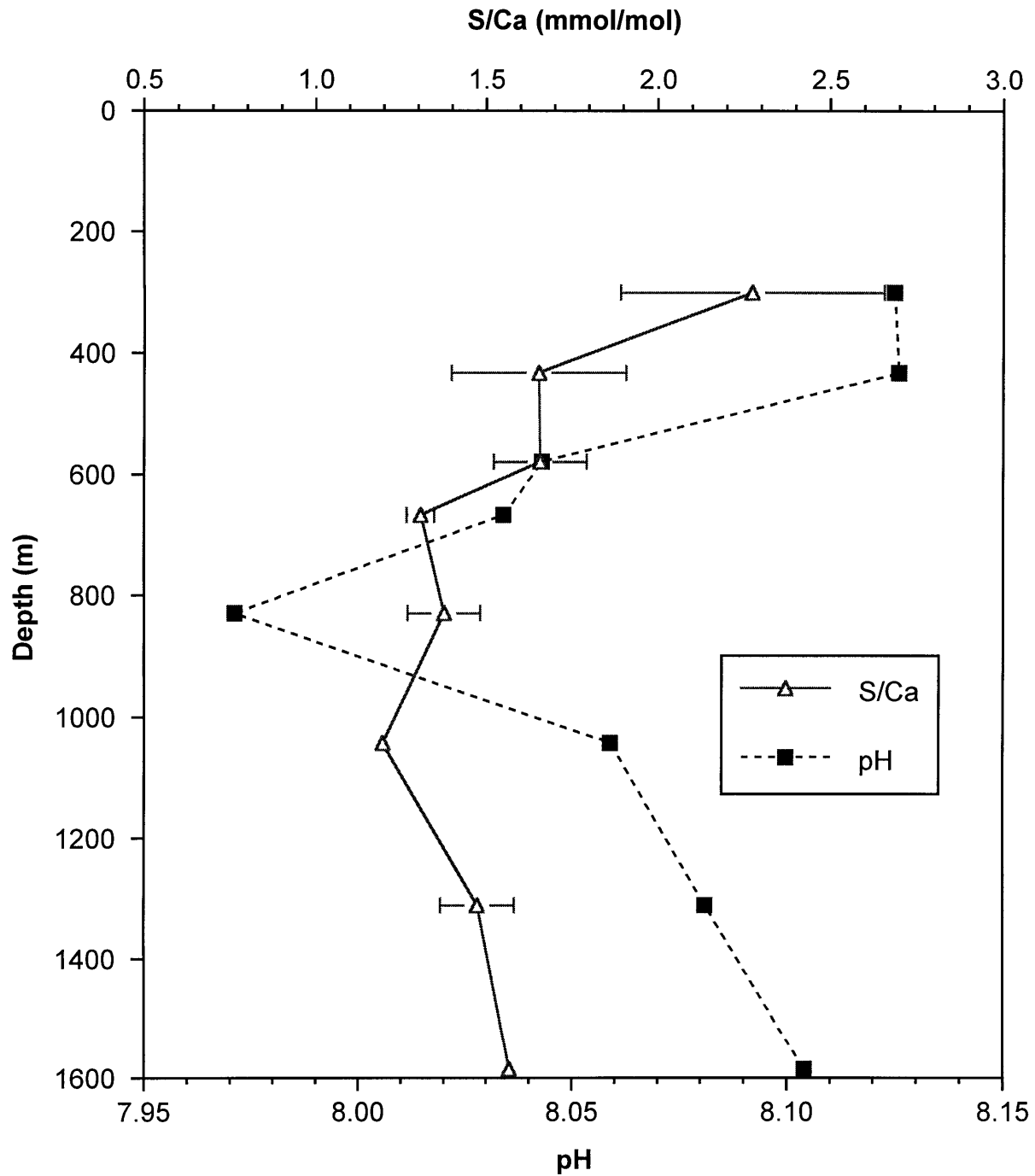
Figure 14: S/Ca data for all benthic foraminifera at Little Bahama Banks versus depth. Solid line connects averages of S/Ca at each depth sampled. Error bars represent one standard error of the mean. pH versus depth extrapolated from GEOSECS station 31 data by correlating with temperatures at the depths of the core sites.
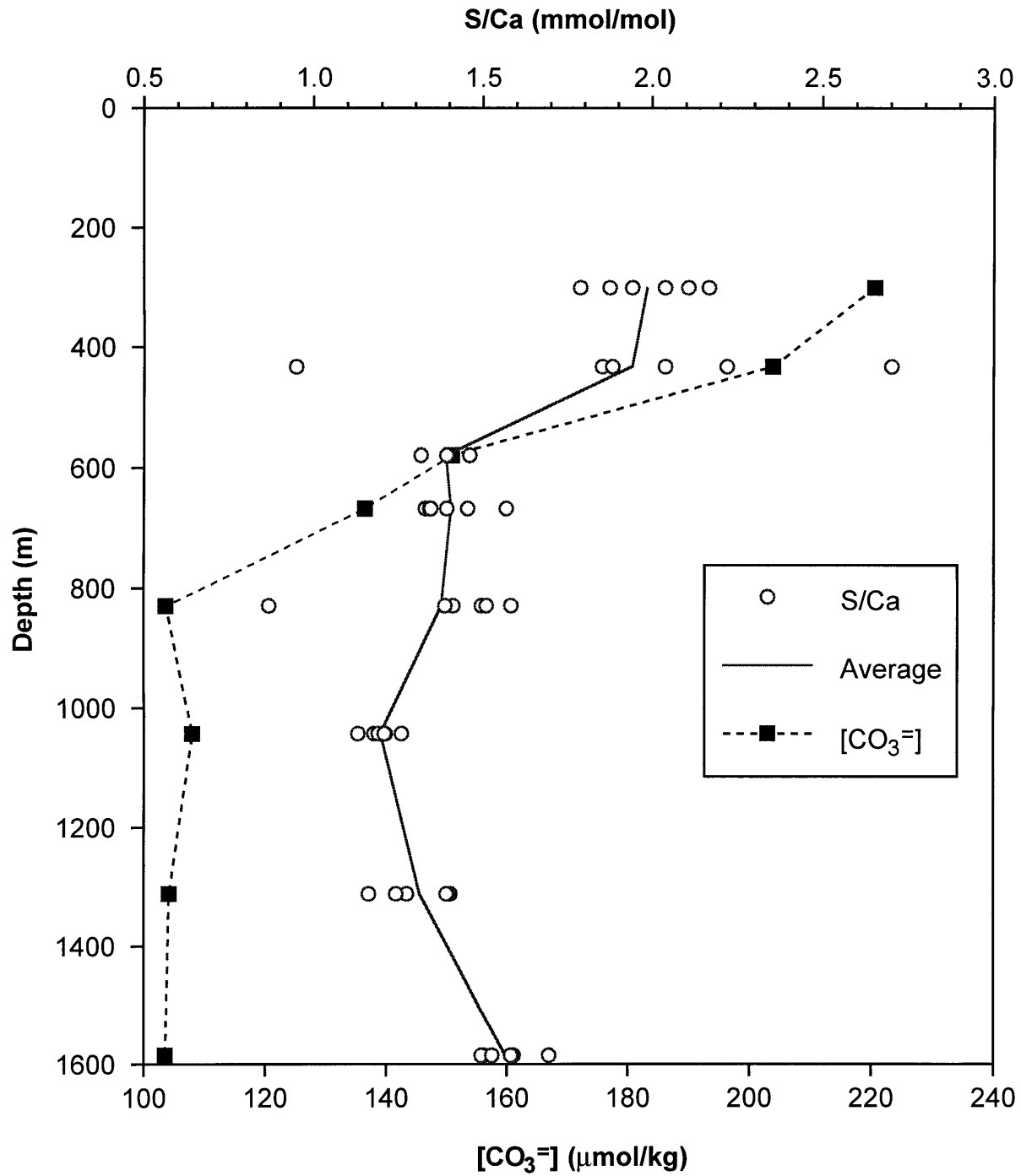
Figure 15: S/Ca data for Cibicidoides at Little Bahama Banks versus depth. Circles are individual measurements. Solid line connects averages of S/Ca at each depth sampled. [CO$_3^=$] versus depth extrapolated from GEOSECS station 31 data by correlating with temperatures at the depths of the core sites.
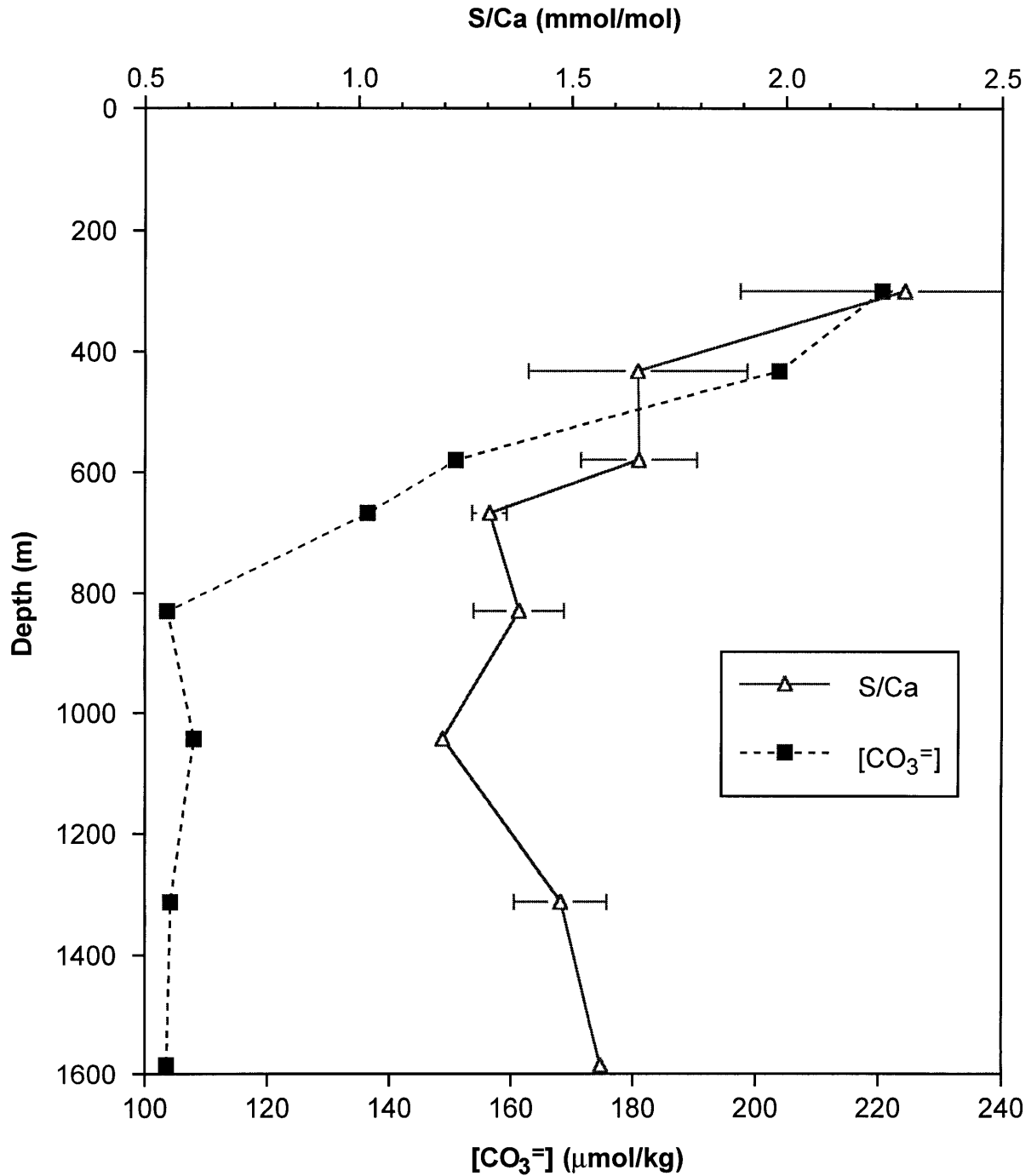
Figure 16: S/Ca data for all benthic foraminifera at Little Bahama Banks versus depth. Solid line connects averages of S/Ca at each depth sampled. Error bars represent one standard error of the mean. $[CO_3^=]$ versus depth extrapolated from GEOSECS station 31 data by correlating with temperatures at the depths of the core sites.
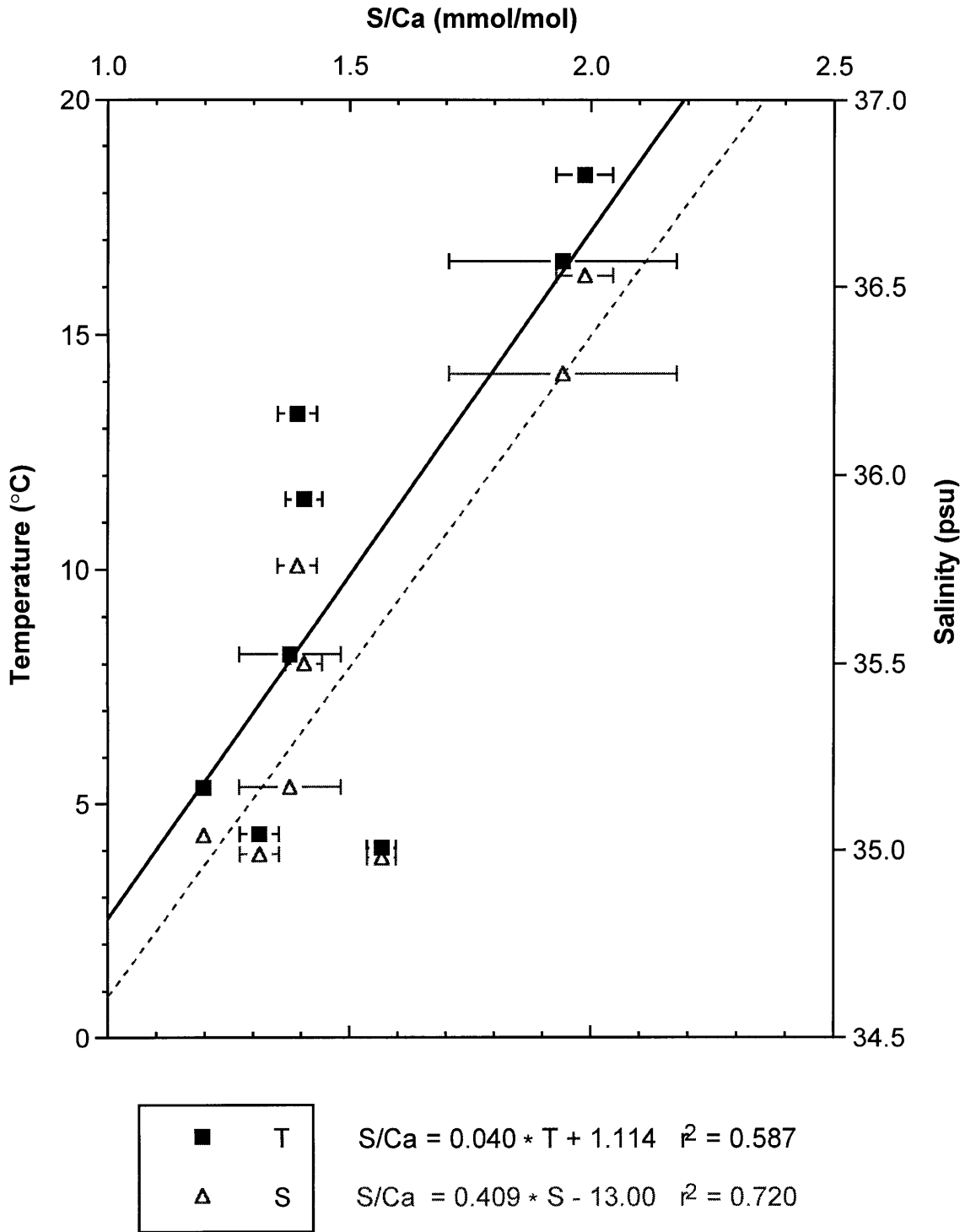
Figure 17: Scatter plot of Little Bahama Banks average Cibicidoides S/Ca ratios versus temperature and salinity. Error bars are one standard error of the mean. Lines are least squares linear regressions. Solid line is versus temperature and dashed line is versus salinity. The respective equations are given.
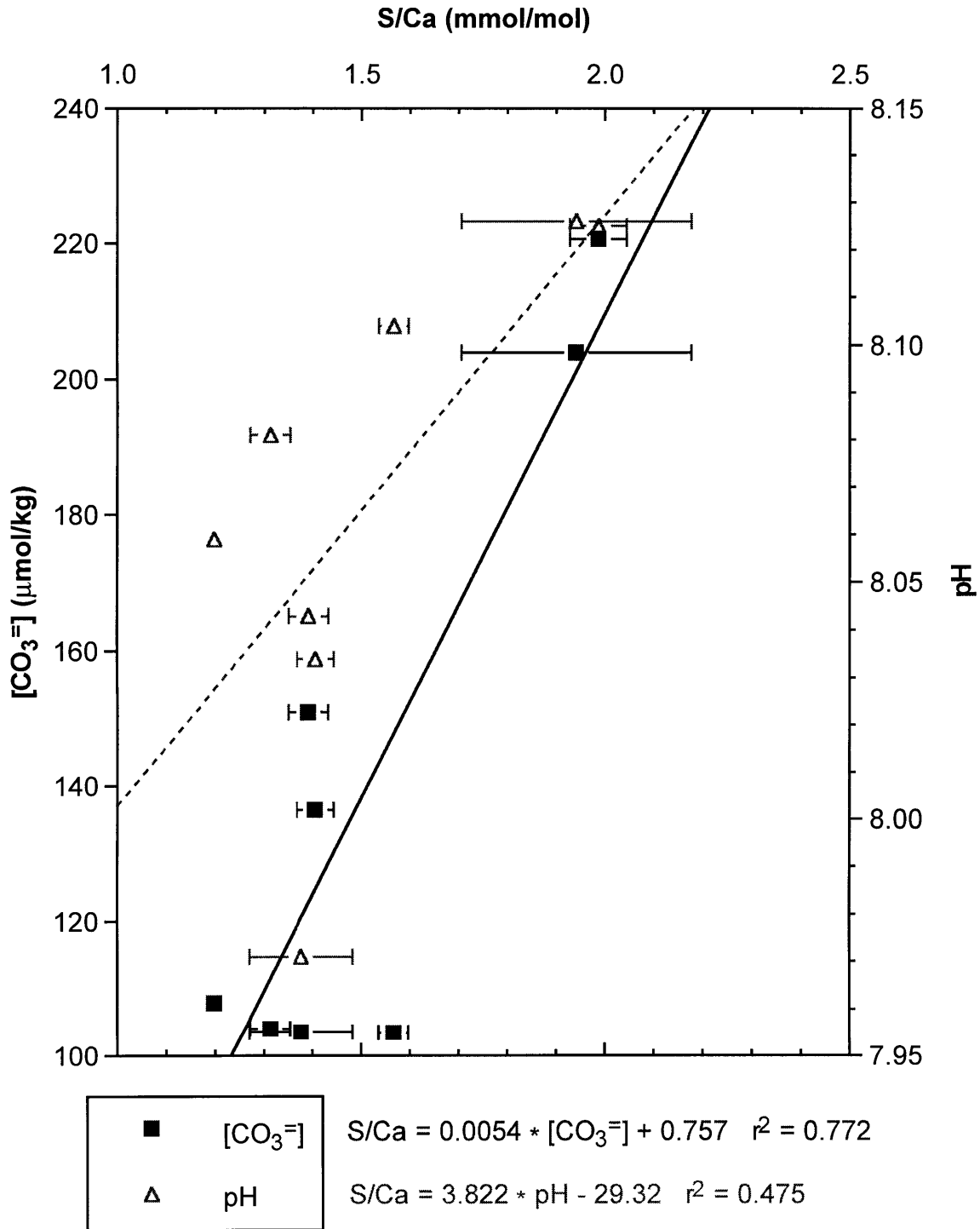
Figure 18: Scatter plot of Little Bahama Banks average <u>Cibicidoides</u> S/Ca ratios versus [CO$_3$=] and pH. Error bars are one standard error of the mean. Lines are least squares linear regressions. Solid line is versus carbonate and dashed line is versus pH. The respective equations are given.

The S/Ca-salinity relationship for *Cibicidoides* at LBB is not extremely strong, but provides some indication that salinity may have a role to play in controlling foraminiferal sulfur content. The Erez culture experiments were probably carried out with constant salinity, so if salinity has a large effect on foraminiferal sulfur incorporation, that data would not reveal it. Also, it is quite possible that biological factors have an influence on minor element uptake in foraminifera, so that interspecies differences could cause *Cibicidoides* to incorporate sulfur differently than *A. lobifera*.

Given the correlations between $[CO_3^=]$ and temperature and salinity, it is difficult to conclude whether there is an independent relationship of S/Ca with carbonate. In fact, the slope of the relationship of S/Ca with the carbonate variables is positive, contrary to the expectation of a negative slope given the results of culture experiments discussed below and the assumption that the S/Ca ratio (see earlier argument for equivalence of S/Ca and $SO_4^=/CO_3^=$ ratios) in calcite is directly proportional to the $SO_4^=/CO_3^=$ ratio in seawater. Due to this unexpected reversal of correlation of sulfur with pH and $[CO_3^=]$, it appears that other hydrographic parameters such as temperature and salinity may be driving the S/Ca contents of the foraminifera analyzed. Based on this data, any causal relationship between foraminiferal sulfate content and pH or $[CO_3^=]$ is inconclusive. However, other data exists which supports the expected inverse relationship of foraminiferal S/Ca ratio with pH, for both benthic and planktonic species. The planktonic data is discussed in the following section.

F. Calibration of cultured *G. sacculifer* S/Ca ratio with pH and $[CO_3^=]$.

Planktonic foraminifera culturing experiments were conducted in spring 1997 at the Marine Biological Laboratory in Eilat, Israel. The aim of the research was to culture planktonic foraminifera under conditions of varying pH to monitor the effects of pH on incorporation of sulfate in foraminiferal calcite.

The experiments at Eilat were conducted in the following manner. Plankton tows were conducted 1-3 km offshore from the H. Steinitz Marine Biological Laboratory using a 65 μm net for ten minute tows at 5-10 m depth. Living plankton samples were returned to the laboratory immediately and examined under a dissecting microscope. Foraminifera were picked out individually using a Pasteur pipette and transferred to culture dishes filled with filtered seawater. The picked species were *G. sacculifer*, *G. ruber*, *O. universa*, *G. calida*, and *G. siphonifera*. The picked individuals were monitored for recovery from the collection operation, indicated by the regrowth of long spines within 1-2 days. These healthy foraminifera were transferred to individual Petri dishes with seawater, measured with an ocular micrometer and fed one recently hatched *Artemia* nauplius before transferring to the culture medium. Those foraminifera which did not recover were saved to conduct size-weight calibrations.

Surface seawater was collected during plankton tows and filtered through 0.45 μm polycarbonate filters. A glass carboy was filled with ten to fifteen liters of filtered seawater, and the pH adjusted by the addition of NaOH or HCl. The reservoir was well mixed and equilibrated with the atmosphere before sealing. The pH was measured potentiometrically, as was alkalinity by Gran titration. Fifty or 100 mL glass Erlenmeyer flasks with ground glass stoppers were then filled from the reservoir. Newly fed foraminifera were transferred to these culture flasks, with one or two individuals per flask. Foraminifera in shared flasks were chosen from different species to eliminate confusion in identifying individuals. Flasks were sealed with the stoppers to eliminate air bubbles, and placed in a constant temperature (22.5 °C) circulating water bath under strong light. The light was on a twelve hour on/off cycle.

Foraminifera were removed from the culture flasks and transferred to small Petri dishes every one to two days to feed and monitor their condition. Each

foraminifer was measured by micrometer and offered an *Artemia* nauplius. If an individual refused to feed, an attempt was made the following day. While the foraminifera were out of their flasks, the pH of each flask as well as the reservoir was measured in order to monitor the constancy of pH. Occasionally the pH varied by a few hundredths of a unit up to a tenth of a unit, possibly due to trapped air, respiration within the flask, or inorganic precipitation of carbonate at higher pH. Samples were also collected for alkalinity titrations at the end of the experiment in order to check for changes in alkalinity.

When a foraminifer had been observed to have undergone gametogenesis (shell empty and white with no spines), the foraminifer was measured and set aside for collection. These foraminifera were placed in a 65 μm mesh sieve and washed with many portions of distilled water. They were then transferred to micropaleontological slides to await weighing and chemical analysis.

Gametogenic foraminifera in the early experiments were allowed to sit in seawater for a few weeks before washing and collection. Some of these foraminifera were observed to have a mineral crust on parts of the outside surface, which was identified as inorganically precipitated aragonite by electron probe measurements of elements enriched in aragonite (J. Erez, personal communication). This crust affects about 28 out of 110 total foraminifera. None of these crusted foraminifera were used for calibration. Culturing experiments were conducted at five different pH values, one at the ambient seawater pH of 8.2, and the others at 7.8, 7.9, 8.4, and 8.6. At least twenty individuals were successfully cultured to gametogenesis in each experiment.

Analysis of cultured foraminifera by ICP-MS for sulfur content was restricted to *G. sacculifer* because this was the only single species with sufficient material for analysis throughout the pH range. An additional sample of *G. siphonifera* was analyzed at pH 8.6 for comparison. The sample weights ranged from <0.1 mg to 0.27 mg, and required from four to eleven individuals depending on size. The sample at

pH 8.2 was made up of "dead controls" not fed in culture because of an accidental loss of the cultured foraminifera at this ambient seawater pH. Foraminifera were not crushed before cleaning because they were free of sedimentary contamination. This also prevented accidental loss of very small samples. The foraminifera were cleaned with distilled water and methanol portions during ultrasonication. The volume of weak HNO_3 used to dissolved these samples was adjusted downward due to the small samples in order to obtain calcium concentrations ranging between about 10 and 20 mM. Samples consisting of an aliquot of 50 or 75 µL plus a 10 µL aliquot of [34]S spike solution were analyzed by ICP-MS for S and flame atomic absorption for Ca.

The resulting S/Ca ratios (Table 9) are plotted against culture pH to determine a calibration relationship (Figure 19(a)). The culture pH for each foraminifer was

Table 9. S/Ca and pH data for cultured planktonic foraminifera experiments. Linear regression and statistical parameters included.

pH	[CO$_3$=] µmol/kg	1/[CO$_3$=] (µmol/kg)$^{-1}$	S/Ca mmol/mol	S/Ca vs. pH linear regression		S/Ca vs. [CO$_3$=] exponential regression	
7.81	123.50	0.0081	2.91	r^2	0.927	r^2	0.932
8.20	279.30	0.0036	2.52	m	-1.919		
8.41	414.60	0.0024	1.66	b	17.985		
8.60	573.50	0.0017	1.42	F	38.079		
8.62	592.30	0.0017	1.52	(G. siphonifera)			

Notes: [CO$_3$=] calculated from pH and alkalinity data. Regression equations are found on plots in Figure 19. [S] and [Ca] measurements and sample sizes are listed in Table A2 in the Appendix.

calculated as an average of the pH measured in its culture flask over the duration of its calcification within that flask. Because each sample analyzed in the experiment is made up of multiple individuals, the average pH for each sample is calculated by weighting the contribution of each individual by its proportion of the total mass of the sample. The *G. siphonifera* sample was included in the regression because its S/Ca ratios in both this calibration experiment and the Gulf of Aqaba sediment core analyses do not seem offset from those of *G. sacculifer* under the same conditions.

(a)

Cultured *G. sacculifer* calibration vs. pH

S/Ca = -1.919 x pH + 18.0

$r^2 = 0.927$

Y-axis: S/Ca (mmol/mol)

X-axis: pH
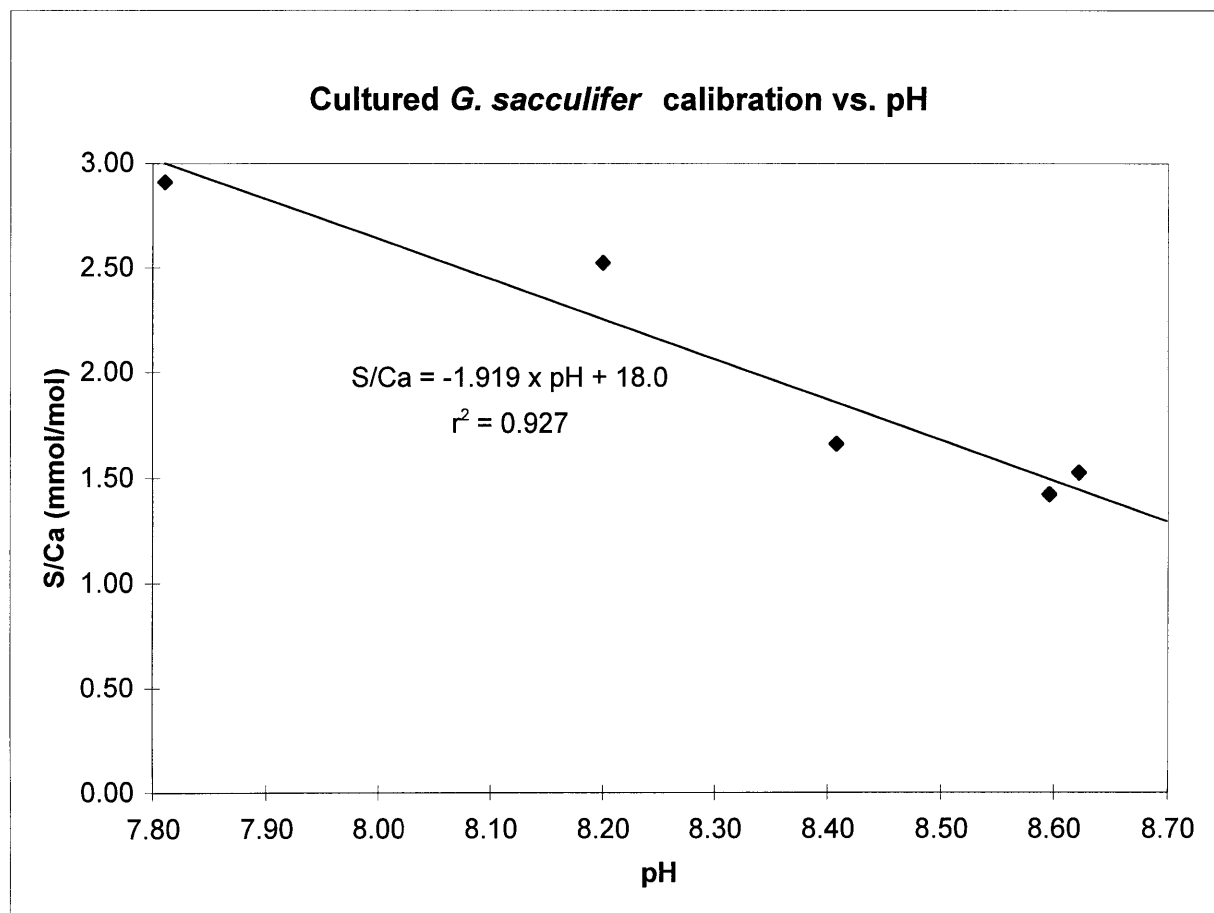
Figure 19: (a) Data from culturing experiments on planktonic foraminifer *Globigerinoides sacculifer* . Foraminifera were cultured in Gulf of Eilat seawater adjusted to varying pH with acid or base. The cleaned shells of cultured, gametogenic foraminifera were analyzed for S/Ca. Least squares linear regression of S/Ca versus pH and resulting equation are displayed.

(b)

G. sacculifer S/Ca vs. [CO$_3^=$]

$$S/Ca = 3.57e^{-0.0016[CO3]}$$

$$r^2 = 0.932$$

Y-axis: **S/Ca (mmol/mol)** (3.00, 2.50, 2.00, 1.50, 1.00, 0.50, 0.00)

X-axis: **[CO$_3^-$] (μmol kg^{-1})** (0, 100, 200, 300, 400, 500, 600)
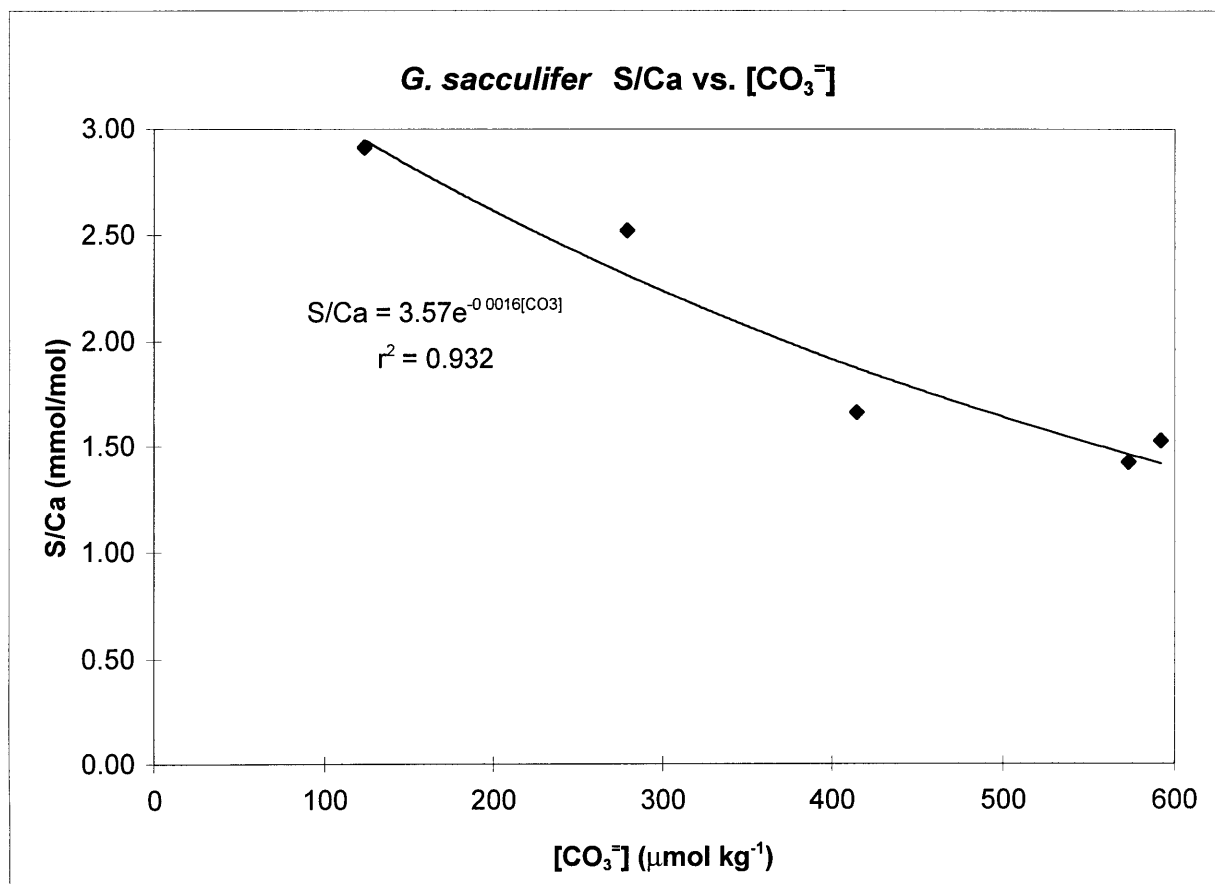
Figure 19: (b) pH data for *G. sacculifer* culture experiments converted to carbonate ion concentrations using alkalinity measurements. S/Ca plotted versus [CO$_3^-$] and fit to an exponential function.

(c)

Cultured *G. sacculifer* calibration vs. $(1/[CO_3^=])_{sw}$

S/Ca (mmol/mol)

$(1/[CO_3^=])_{sw}$ (kg µmol^{-1})

$S/Ca = 462.41x \, (1/[CO_3^=])$
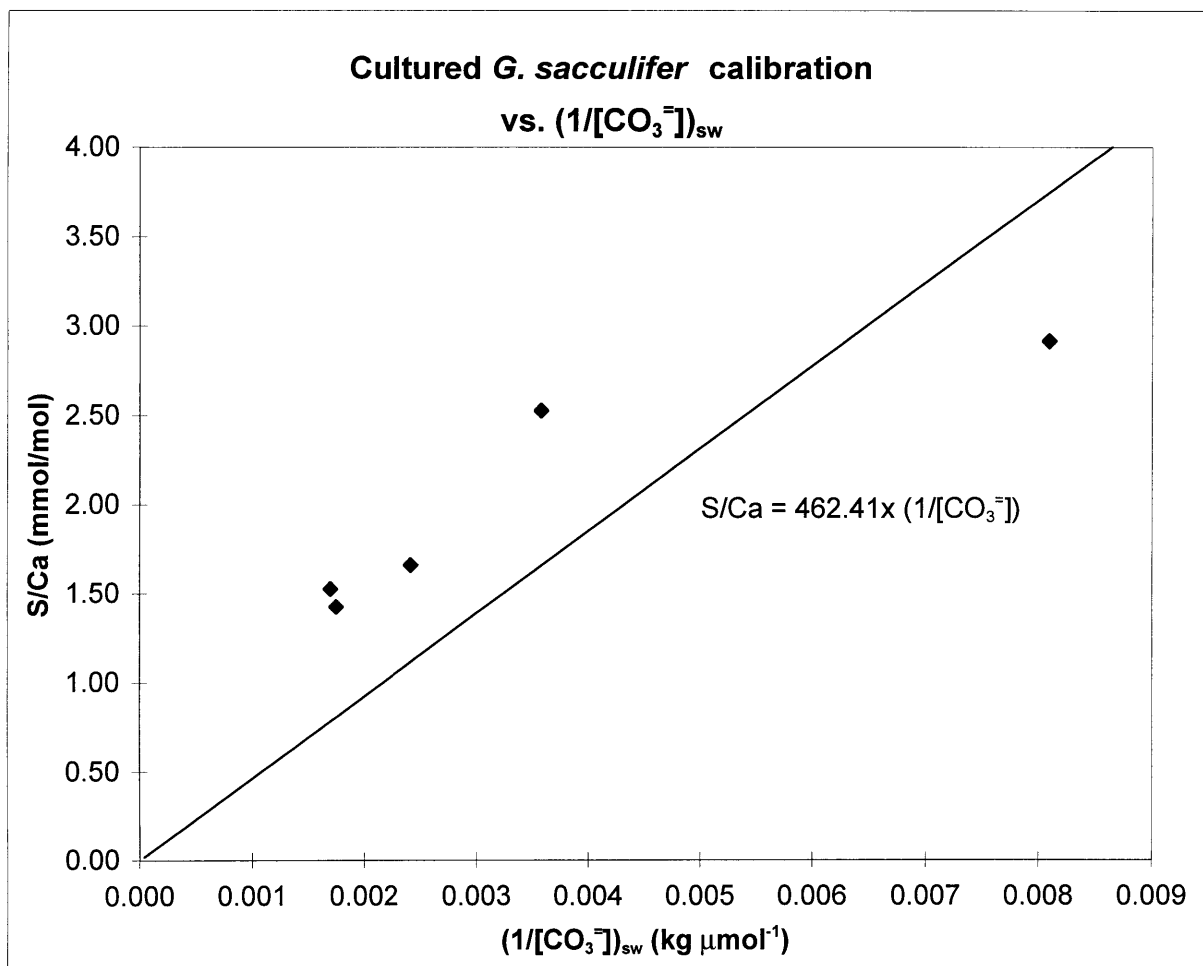
Figure 19: (c) Cultured *G. sacculifer* S/Ca plotted versus $1/[CO_3^=]$ and fit to a linear function constrained to pass through the origin.

The scatter diagram shows the expected inverse relationship between pH and S/Ca. The correlation coefficient, $r^2 = 0.927$ is high, and statistical tests can be used to evaluate the probability that the linear relationship indicated by the regression could arise by chance (see Table 9). The probability distribution for the linear correlation coefficient r indicates that there is about a 3% probability that the r-value observed could result from an uncorrelated set of variables. In addition, the F-statistic test applied to the data also indicates less than a 3% probability that an uncorrelated set of variables could produce the linear correlation observed. Thus, the linear calibration between S/Ca and pH in the cultured foraminifera can be accepted with a high degree of confidence. Nevertheless, uncertainty in the calibration relationship is contributed from S/Ca analytical uncertainty on the order of 10%, as well as uncontrolled factors such as biological effects during calcification.

The S/Ca data were also fit to the carbonate ion concentration and its reciprocal, because the solid-solution model described earlier predicts that sulfur incorporation is directly proportional to the inverse of the carbonate ion concentration in solution. Although $[CO_3^=]$ is a calculated parameter rather than measured in the culture experiments, the fact that the model for sulfur incorporation is an explicit function of $[CO_3^=]$ makes it a better parameter for calibration. Values for $[CO_3^=]$ and $1/[CO_3^=]$ in the seawater used in the Eilat *G. sacculifer* culture experiments were calculated using measured pH and alkalinity data. A spreadsheet incorporating the current literature values for the constants of the dissolved inorganic carbon system in seawater was used to calculate $[CO_3^=]$ (spreadsheet programmed by E. Boyle). A least-squares exponential fit was made to the plot of S/Ca vs. $[CO_3^=]$ to reflect the condition that S/Ca approaches zero and cannot be negative as $[CO_3^=]$ approaches very large values (Figure 19(b)). Based on the ideal thermodynamic situation in which foraminiferal S/Ca is linearly proportional to $1/[CO_3^=]$, S/Ca was plotted against $1/[CO_3^=]$ and a linear least-squares

fit was applied (Figure 19(c)). The line was constrained to pass through the origin, in order to obey the condition that S/Ca must approach zero at very high $[CO_3^=]$. The least-squares fits show a good correlation between the variables plotted as given by the r^2 values on the plots. The correlation coefficient was not calculated for the fit to $1/[CO_3^=]$ due to the forcing of the line through the origin. The fit does not appear to be as good as for those in Figure 19(a,b).

G. Comparison of glacial and interglacial foraminifera from global ocean sediment cores

With data for the calibration of S/Ca in foraminifera with seawater $[CO_3^=]$ and pH in hand, samples were taken from sediment cores distributed around the world to evaluate differences in S/Ca ratios between foraminifera living in glacial and interglacial periods. Two sources of samples were used: archived dissolved benthic foraminifera previously analyzed for other elements, and picked foraminifera that were crushed and cleaned before dissolution and immediate analysis in the usual way. The archived samples had experienced evaporation in clean polypropylene vials during years of storage. Because most of these samples had completely evaporated, the selection of samples was limited to those with at least 25 μL of liquid remaining in order to perform a quick check of Ca concentration followed by subsequent dilution to an appropriate concentration. A 5 μL aliquot was removed for Ca analysis (diluted with 5 mL of La/HCl matrix modifier) to determine the necessary dilution for S and Ca analysis. An aliquot of the original sample was dispensed into a new clean polypropylene vial and 1% HNO3 was added to make up to approximately 10 mM [Ca]. This solution was spiked and analyzed by ICP-MS for S and AA for Ca. The results of the archived samples are shown in Table 10. The number of each sample is keyed to the core site map in Figure 5. The limitation on samples with sufficient volume resulted in a rather non-systematic distribution of

geographic locations, ages and species in the data set. The samples were from either
Holocene or last glacial maximum intervals, as indicated in the table.

Table 10. S/Ca data for archived dissolved benthic foraminifera.

#	Core	Water depth (m)	Core depth (cm)	Species	Age	[S] (μM)	[Ca] (mM)	S/Ca (mmol/mol)
7	EN66-038	2931	3.5	Hoe	Holocene	18.52	6.81	2.72
11	V19-240	3103	60.5	kul	LGM	39.62	10.26	3.86
13	RC12-294	3308	6.5	kul	Holocene	12.36	16.39	0.75
13	RC12-294	3308	44.5	wue	LGM	49.10	9.33	5.26
16	MD76-125	1878	114.0	Uvi	LGM	101.13	12.34	8.19
17	MD76-127	1610	43.0	Hoe	LGM	34.50	7.53	4.58
17	MD76-127	1610	43.0	Uvi	LGM	38.36	14.97	2.56
17	MD76-127	1610	55.0	Uvi	Stage 2	18.55	12.43	1.49
17	MD76-127	1610	55.0	Uvi	Stage 2	53.93	9.73	5.54
18	MD76-128	1712	5.0	Hoe	Holocene	3.10	12.38	0.25
19	MD76-135	1895	232.3	Hoe	LGM	31.92	13.16	2.43
19	MD76-135	1895	232.3	Hoe	LGM	44.39	10.96	4.05
20	V32-159	1235	16.0	Uvi	Holocene	7.75	5.57	1.39
20	V32-159	1235	16.0	Uvi	Holocene	1.42	7.66	0.19
26	V19-027	1373	127.5	wue	Stage 2	43.41	11.30	3.84

Notes: Age determined from oxygen isotope documentation of cores as described in Boyle
(1992). LGM designates the last glacial maximum Stage 2 designates oxygen isotope stage 2, slightly
later than the LGM. Species abbreviated are *Uvigerina* spp. (Uvi), *Cibicidoides kullenburgi* or
Cibicidoides pachyderma (kul), and *Cibicidoides wuellerstorfi* (wue).

The S/Ca ratios from these samples are problematic. Many of the values are
disturbingly high; S/Ca values above 3.00 mmol/mol were not measured in any
other foraminifera samples in this work, except for two *C. wuellerstorfi* samples
from the shallowest depth of the Little Bahama Bank. The highest values are
confined to the glacial samples, but both Holocene and glacial samples exhibit a large
scatter. The mean S/Ca ratio for Holocene foraminifera is 1.06 ± 0.47 mmol/mol,
and the mean S/Ca ratio for glacial foraminifera is 4.18 ± 0.60 mmol/mol; the error
quoted is the standard error of the mean (SE = s.d./$\sqrt{n}$).

The apparent non-systematic variations in this data set rule out an
interpretation of the difference between the means for Holocene and glacial
foraminifera as a consequence of seawater pH differences, or of other oceanic
environment differences. The calcium concentrations of all the samples are not
below the threshold of 5 mM, and fall in a narrow range between 5.5 and 16.5 mM,

ruling out a possible bias in the data based on [Ca]. The factors that may have caused the large variance in the data set are difficult to isolate, but it is likely that circumstances arising from the storage of the samples have a role to play. The evaporation of the archived samples during storage may have altered the original sulfur concentration of the dissolved foraminifera solutions, but could not have altered the S/Ca ratio unless a mineral phase precipitated. It is unlikely that a solid phase such as $CaSO_4$ has precipitated out of the solutions, since the solubility product for $CaSO_4$ (7.10×10^{-5} L^2 mol^{-2}) was not exceeded in the solutions as calculated from the [S] and [Ca] data. Calcium sulfate precipitation would only be able to explain low S/Ca ratios, leaving the unprecedented high ratios unaccounted for. A very unlikely hypothesis is that the foraminifera had harbored calcium sulfate precipitates prior to dissolution that had not been adequately removed when cleaned, since evidence for such precipitates was never seen in the foraminifera cleaned for this study. A more stringent cleaning protocol was used for these samples (Boyle and Keigwin, 1985) than for the present study, but contamination from the oxidizing and reducing reagents used is unlikely because any sulfur containing impurities would be decreased to a negligible contribution after rinsing and dissolution. Absorption of sulfur contained in the plastic walls of the centrifuge tubes or from sulfur oxides in the air over years of storage is the most likely explanation for contamination. Because of the severe contamination problems, this group of data was not used to derive any information on environmental controls on foraminiferal sulfate, but prompted the conclusion that foraminifera from freshly taken cores, or foraminifera sampled soon after coring could avoid any effects due to storage.

A test of whether core storage can cause artifacts in foraminiferal S/Ca ratios was conducted on a set of cores from the Ontong Java Plateau (OJP). Samples were available from box cores collected in September 1997 at essentially the same sites as

box cores collected in 1991. Planktonic foraminifera were sampled at 2-3 cm core depth from two pairs of "old" and "new" cores, at about 2300 m (MW91-9 BC36 and MW97-20 MC18) and 4330 m (MW91-9 BC58 and MW97-20 MC28). The exact locations and depths of these cores are included in Table 2. Both core sites are undersaturated for calcite, as indicated by carbonate system calculations based on data from the GEOSECS 241 station (Ed Boyle, personal communication). The value for omega ($\Omega = [Ca^{++}][CO_3^=]/K_{sp}$) at 2300 m is about 0.95, and omega at 4330 m is about 0.72. Clearly the extent of calcite dissolution at the deeper site is greater, and a comparison between the two depths may give information about any dissolution effects on S/Ca ratios in planktonic foraminifera. *Globorotalia menardii* and *G. sacculifer* were sampled from the shallower cores, while only *G. menardii* were sampled from the deeper cores due to excessive dissolution of other species. The results of the S/Ca analysis of duplicates or triplicates of crushed and pooled samples of planktonic foraminifera from these cores is shown in Table 11 and Figure 20.

Table 11. S/Ca data for planktonic foraminifera from the Ontong Java Plateau.

Core	Year	Depth m	S/Ca, mmol/mol G. menardii			G. sacculifer			Average mmol/mol	SE (s.d./√n)
MW97-20 MC18	1997	2314	0.846	1.006	0.892				0.915	0.048
						1.120	1.121	1.122	1.121	0.000
MW91-9 BC36	1991	2293	0.984	0.880	1.308				1.057	0.129
						1.187	1.134	1.273	1.198	0.041
MW97-20 MC28	1997	4325	0.624	0.637					0.631	0.007
MW91-9 BC58	1991	4341	0.540	0.595					0.567	0.027

Notes: Core locations are listed in Table 2. [S] and [Ca] measurements and sample sizes are listed in **Table E4**.

Addressing first the difference between archived and fresh core material, there are no significant intraspecies differences in S/Ca ratios at either depth within two standard errors of the mean. For *G. menardii*, the S/Ca data of MW91-9 BC36 have a high scatter, but without the high value of 1.308 mmol/mol, the difference with its fresher counterpart core is practically negligible. The S/Ca ratios of *G. menardii* from both cores at about 4330 m are also equal within error. The

61
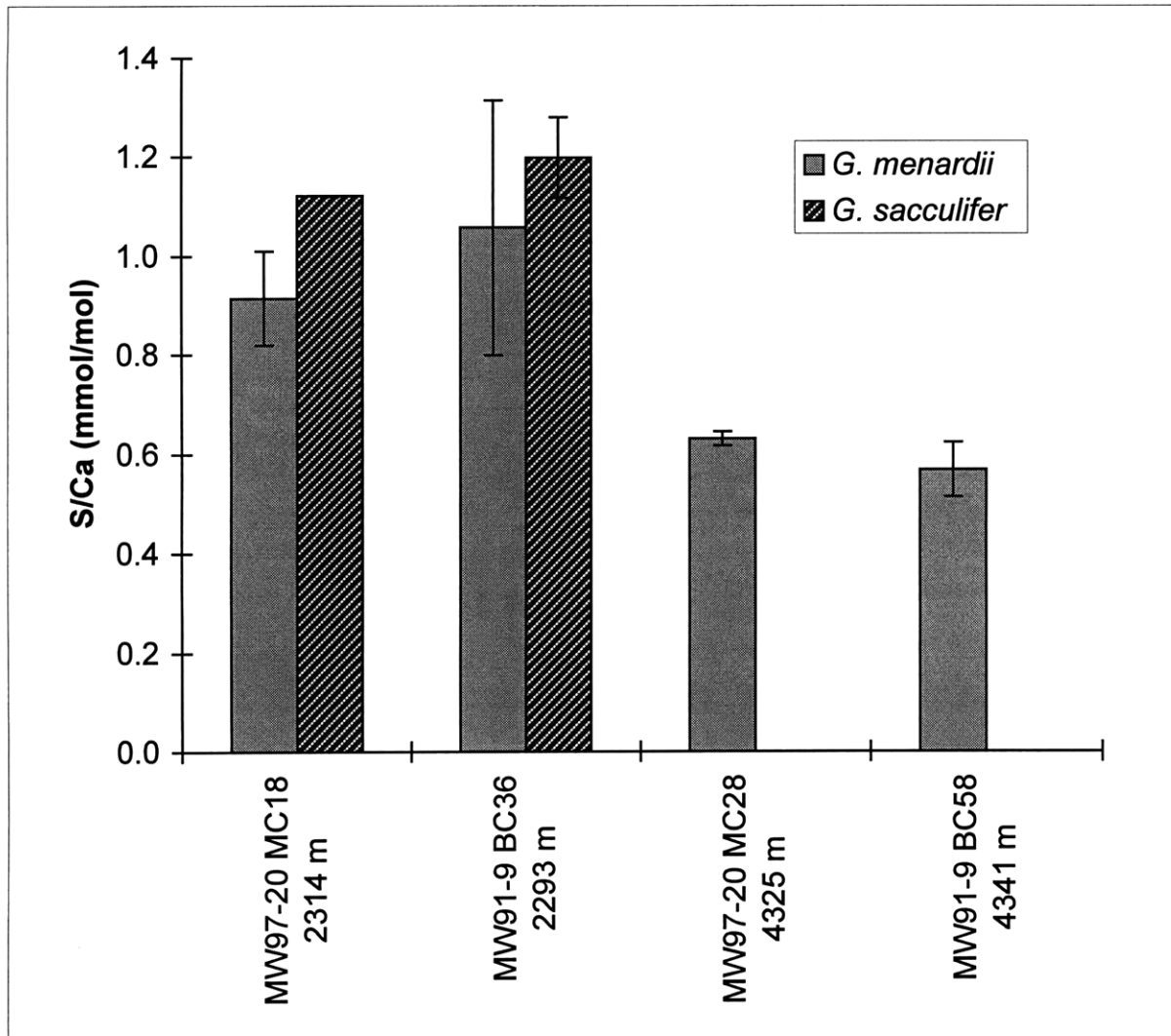
Figure 20: S/Ca results of crushed and pooled replicates of planktonic foraminifera *G. menardii* and *G. sacculifer* from four cores at the Ontong Java Plateau. Cores of MW91 designation were retrieved in 1991, while MW97 cores are "fresh" cores from 1997. Unfragmented *G. sacculifer* shells were not present in the cores from below 4300 meters. Error bars represent two standard errors of the mean.

G. sacculifer S/Ca data of MW97-20 MC18 have practically no scatter, which may just be a random occurrence, and agree within error with *G. sacculifer* S/Ca ratios from the archived core MW91-9 BC36. This test of possible artifacts in foraminiferal S/Ca ratios due to unknown processes occurring in stored sediment cores is negative for the planktonic species studied. Benthic species could not be analyzed for a more direct comparison to the archived benthic samples that gave anomalous results because of low abundance in the OJP cores. Nonetheless, the results are encouraging because they suggest that the large resource of archived sediment cores can be sampled for foraminiferal S/Ca ratios without a strong concern for bias. Limiting the use of S/Ca data to freshly collected sediment cores would severely restrict the number of measurements that could be made to evaluate its usefulness.

Secondly, the mean S/Ca ratios of *G. sacculifer* are higher than for *G. menardii* in the 2300 m cores, which, because *G. sacculifer* tends to calcify nearer the sea surface than *G. menardii* (Fairbanks et al., 1982; Hemleben et al., 1989), suggests a response of foraminiferal S/Ca to changing environmental parameters from the mixed layer to the top of the thermocline. Data from the nearest GEOSECS station (241) indicates a salinity decrease of 0.4‰ from the surface to the top of the thermocline, and an accompanying 0.3 unit decrease in pH. The sense of the S/Ca difference between *G. menardii* and *G. sacculifer* is opposite to that expected for pH control, but is consistent with a salinity correlation as observed for the Little Bahama Banks benthic foraminifera. A strong caveat to this observation is that when the S/Ca data for each species are pooled from both cores at the nominal water depth of 2300 m, there is no difference between *G. menardii* and *G. sacculifer* within the bounds of two standard errors of the mean. Without a larger data set to test the statistical significance of a difference in S/Ca ratios in *G. sacculifer* and *G. menardii*, a conclusion cannot be drawn on interspecies differences at this site. The S/Ca data

from planktonic foraminifera from the Gulf of Aqaba tend to confirm that significant differences between species cannot be isolated from analytical variability.

Finally, a significant difference with depth is apparent in the *G. menardii* S/Ca ratios. The mean S/Ca ratio at 4330 m nominal depth is 0.599 ± 0.022 mmol/mol, while at 2300 m nominal depth it is 0.986 ± 0.069 mmol/mol (errors are ±2 SE). It appears that dissolution on the seafloor may be altering the sulfur content of the assemblages of the planktonic foraminifer *G. menardii*. Surface water properties are not expected to differ in the small area of surface ocean overlying the core sites, so that variations in surface pH, temperature, or salinity are not factors causing the observed differences in S/Ca with core depth. A dissolution mechanism for altering S/Ca ratios could operate through selective dissolution of particular shells or parts of shells that are enriched in sulfur. This explanation requires either that sulfur is heterogeneously distributed in individual shells and its distribution coincides with dissolution-susceptible portions of the shell, or that individual shells with higher sulfur content are more susceptible to dissolution than lower sulfur content shells. This kind of selective dissolution mechanism has been suggested to affect the isotopic composition (Berger and Killingley, 1977) and F/Ca and Mg/Ca ratios (Rosenthal and Boyle, 1993) of planktonic foraminifera. Samples from depths intermediate to those reported here from the Ontong Java Plateau, including data for other species, are needed to definitively interpret the depth-dependent S/Ca signal as a dissolution artifact. As an aside, the *G. menardii* individuals chosen for analysis from the 4330 m cores were those least visibly affected by dissolution, so that the observed difference in planktonic foraminifera S/Ca ratios between these cores and the 2300 m cores may be less than the full range including increasingly fragmented foraminifera.

In order to test for possible cleaning artifacts in foraminiferal S/Ca measurements due to absorption or enrichment of sulfur on the surfaces of the

foraminiferal calcite, a sequential dissolution experiment was performed on a 14.8 mg sample of *Cibicidoides* from core OC205-2 BC48 (580 m) on the Little Bahama Banks. The sample was cleaned in the normal way with ultrasonic agitation in distilled water and methanol. The sample was transferred to a clean 500 µL centrifuge tube and a 100 µL aliquot of 1N HNO_3 was added. The sample was subjected to ultrasonic agitation until the cessation of visible bubbling suggested partial dissolution was completed. The overlying acidic solution was siphoned off, and a new aliquot of 1N HNO_3 was added and the dissolution repeated. In total three aliquots were required to complete dissolution of the sample. S/Ca measurements were made on the aliquots, and the data are presented in Figure 21. The initial portion of calcite dissolved, presumably the outermost surfaces of the crystals, is actually lower in sulfur content than the later portions, ruling out the idea that the outer surfaces may not be sufficiently cleaned for S/Ca analysis. Of course, other sedimentary environments may have particular conditions that would affect the ability to clean the foraminifera adequately for S/Ca analysis that these samples did not experience. The results do not indicate a substantial difference in the sulfur content of the foraminifera based on susceptibility to dissolution. Interspecific differences in S/Ca ratios based on dissolution susceptibility are not ruled out, however.

Sequential dissolution experiment
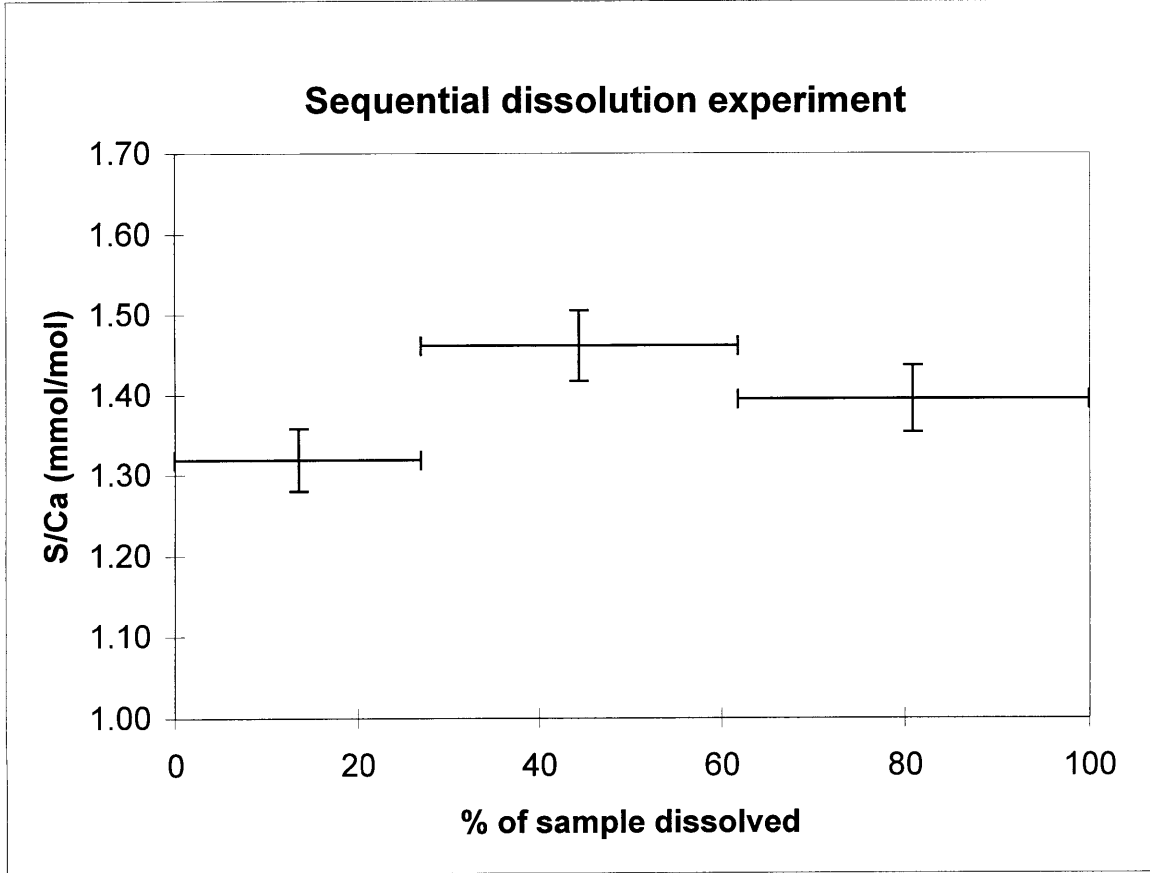
Figure 21: A 14.8 mg crushed sample of *Cibicidoides* from core OC205-2 BC48 at 580 m on the Little Bahama Banks was dissolved in three sequential steps with 1N HNO_3. After each dissolution step, the overlying solution was removed for S/Ca analysis. The S/Ca ratio for each aliquot is plotted over the range of the percentage of dissolved sample it represents.

The final set of data presented is S/Ca ratios in planktonic and benthic foraminifera picked from both Holocene and marine oxygen isotope Stage 2 core depths in four sediment cores from the Atlantic and Pacific oceans. These samples were intact, handpicked foraminifera rather than previously dissolved solutions, so that possible solution storage artifacts previously discussed do not apply to this data set. The locations and depths of the four cores are listed in Table 2. Foraminifera were chosen from previously picked samples, so that the species analyzed depended upon availability. The S/Ca data from these samples is presented in Table 12, and the detailed analytical measurements in Table A2 in the Appendix.

Table 12. S/Ca data for picked benthic and planktonic foraminifera from Holocene and glacial horizons.

ID	Core #	Core	Core depth (cm)	Age	Sp.	S/Ca (mmol/mol)			Average	SE (s.d./√n)
AF19-20	25	TR163-31p	10-13.3	Holocene	Uvi	0.515	0.498		0.506	0.008
AF21-22			90-96.6	Stage 2	Uvi	0.301	0.264		0.283	0.018
AF13-15			10-13.3	Holocene	dut	0.428	0.472	0.517	0.472	0.026
AF16-18			93.3-96.6	Stage 2	dut	0.621	0.589	0.601	0.604	0.009
AF23	8	EN66-26GGC	7-8	Holocene	umb	0.421			0.421	
AF24			20-28	Stage 2	umb	0.434			0.434	
AF29-31			0-1	Holocene	dut	1.226	1.133	1.227	1.195	0.031
AF32-34			33-34	Stage 2	dut	0.857	0.776	1.689	1.107	0.292
AF35-36	12	AII107-65GGC	14-17.5	Holocene	Uvi	0.468	0.446		0.457	0.011
AF37-38			38-39	Stage 2	Uvi	0.474	0.438		0.456	0.018
AF39-40			14-15	Holocene	Cib	0.875	0.921		0.898	0.023
AF41-42			38-39	Stage 2	Cib	0.976	0.924		0.950	0.026
AF25	10	RC13-228	16-27	Holocene	wue	0.693			0.693	
AF26-28			121-127	Stage 2	wue	0.492	0.529	0.504	0.508	0.011

Notes: Holocene and Stage 2 assignments are from age models from Boyle (1992) for TR163-31p and EN66-26GGC, Jones et al. (1984) for AII107-65GGC, and Rosenthal et al. (1997) for RC13-228. Species abbreviations are as for Table 10, except for *N. dutertrei* (dut), *N. umbonifera* (umb), and *Cibicidoides* spp. (Cib). ID refers to the analytical sample ID cross-referenced to Appendix xx in which the [S] and [Ca] are tabulated. The column (#) cross-references the core data listed in Table A2 in the Appendix.

In each core, the same species was analyzed from both Holocene and Stage 2 sediments, although sample constraints prevented consistency in species analyzed

from core to core. At least one benthic species was analyzed in each core, and the planktonic species *N. dutertrei* was analyzed in TR163-31p and EN66-26GGC. The data are plotted in Figure 22 to point out differences between Holocene and glacial S/Ca values with error bars corresponding to twice the standard error. The data for glacial *N. dutertrei* in core EN66-26GGC have a very large scatter due primarily to one high measurement of 1.689 mmol/mol. This high value may result from contamination and will be rejected for the purpose of further calculations. The mean of the two remaining measurements is 0.817 ± 0.41 mmol/mol ($\pm$ 1 SE).

A consistent pattern of either enrichment or diminishment of foraminiferal S/Ca is not seen between glacial and Holocene samples in these cores. A pattern may be seen in the data based on the apparent accumulation rates of the cores. The separation between the Holocene and glacial intervals sampled in cores TR163-31p and RC13-228 is at least 80 cm, making it unlikely that glacial age foraminifera have been mixed into the younger horizon through bioturbation. In fact, these two cores show significant differences in S/Ca ratios between Holocene and glacial foraminifera. In contrast, the Holocene and glacial samples in EN66-26GGC and AII107-65GGC are only separated by 15-30 cm; it is quite possible that glacial foraminifera have been mixed into the Holocene sediments. In these two cores, the differences in foraminiferal S/Ca ratios from the glacial to the Holocene is nearly insignificant, perhaps as a result of mixing. Another explanation for the patterns may be made based on the conversion of the S/Ca data to $[CO_3^=]$ and pH estimates as described in the following discussion.

Data discussed earlier suggests that interspecies S/Ca variations may exist, so that absolute S/Ca ratios cannot be directly compared between species. However, the difference between S/Ca (denoted Δ(S/Ca)) ratios for each glacial-Holocene pair and the fractional change in S/Ca from glacial to Holocene might be used to evaluate possible changes in seawater pH or carbonate ion concentration. The first
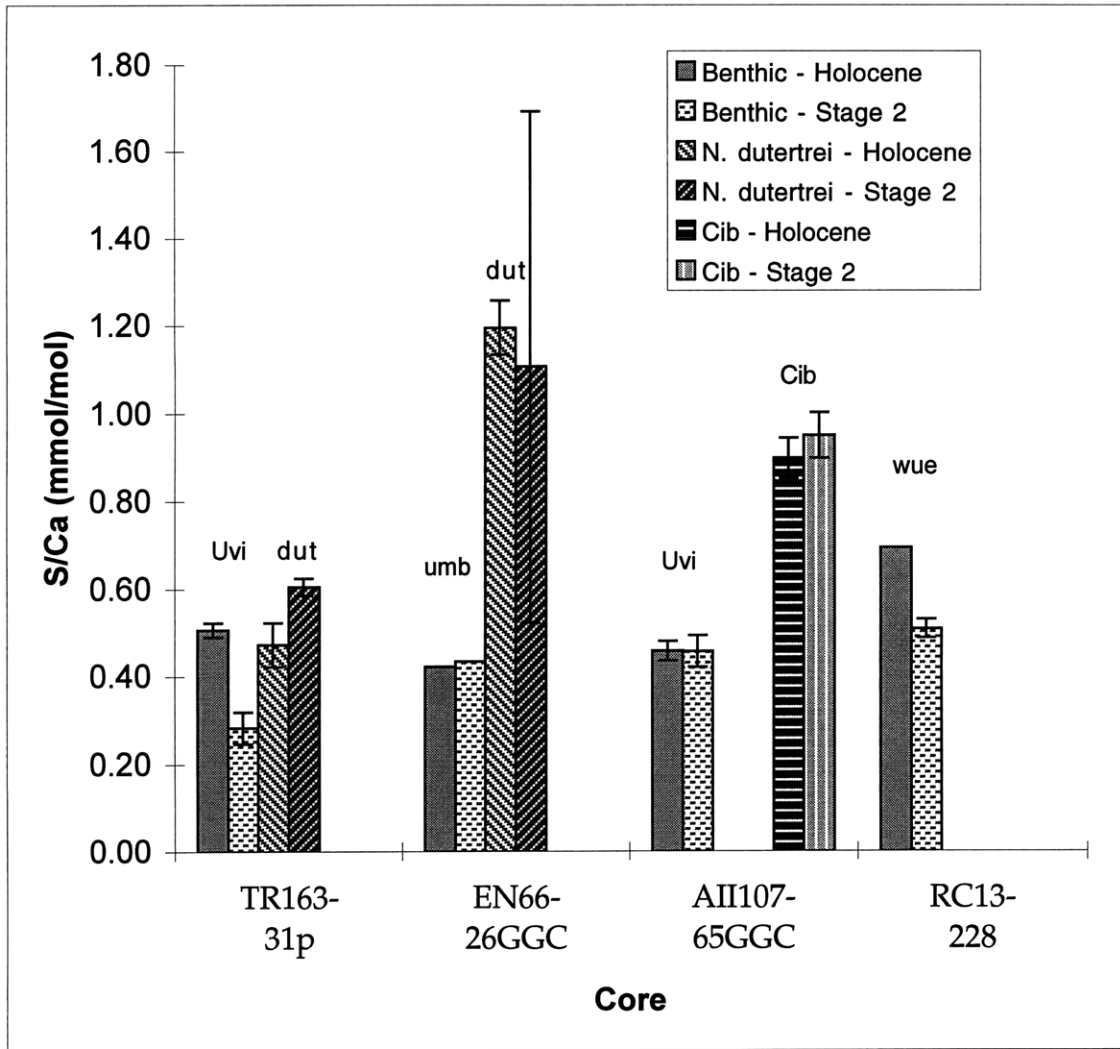
Figure 22: S/Ca data from planktonic and benthic foraminfera of Holocene and glacial age. Abbreviations above the bars indicate taxa analyzed as follows: Uvi is *Uvigerina* , dut is *N. dutertrei* , umb is *N. umbonifera* , Cib is *Cibicidoides* , and wue is *C. wuellerstorfi* . The first bar in each pair is the Holocene age sample, and the second bar is the glacial age sample. Error bars represent two standard errors of the mean.

scheme, using $\Delta(S/Ca)$, relies upon a calibration of foraminiferal S/Ca with pH or $[CO_3^=]$ to calculate a change in pH. The second scheme does not rely upon a calibration, and assumes that the fractional change in S/Ca is caused by the same fractional change in the reciprocal of the carbonate ion concentration $(1/[CO_3^=])$.

Unpublished data from Prof. J. Erez for sulfate concentrations of the benthic foraminifer *A. lobifera* cultured in seawater of different pH measured by the uptake of ^{35}S-labeled sulfate is shown in Figure 1 (J. Erez, personal communication, 1996). The concentration of carbonate ion in the culture solutions was estimated from the pH data and assuming the TCO_2 of the solutions was 2.06 mmol/L, which is the average value for surface waters in the Gulf of Aqaba near Eilat, Israel (Reiss and Hottinger, 1984). A spreadsheet was used to calculate $[CO_3^=]$ as previously described for the *G. sacculifer* calibration dataset. The S/Ca data were also plotted against $[CO_3^=]$, and $1/[CO_3^=]$, and least squares fits were made to the data (Figure 23). Linear fits were made to pH and $1/[CO_3^=]$, and an exponential fit to $[CO_3^=]$, as explained for the *G. sacculifer* calibration. The equations and correlation coefficients are indicated in the figures. Because these data are the only available calibration of S/Ca with pH and $[CO_3^=]$ for a benthic foraminifer species, they were used for the ensuing calculations of pH from the benthic foraminifera data of Table 12. The planktonic foraminifer *G. sacculifer* calibration was used to evaluate the *N. dutertrei* data from Table 12.

The results of two schemes for estimating a change in pH for waters overlying the four cores studied are shown in Table 13. The Holocene $[CO_3^=]$ is calculated from hydrographic, alkalinity and TCO_2 data from the closest GEOSECS station, which is identified in the table (Bainbridge, 1981; Broecker et al., 1982). For core TR163-31p, the nearest GEOSECS station is nearly 1500 km to the west, but comparing dissolved O_2 values from hydrographic stations located near the core site with GEOSECS Stn. 331 indicates no significant difference in properties at the depth of the core. For this

(a)

SO$_4^=$ uptake in *A. lobifera* as function of estimated [CO$_3^=$]

S/Ca = 0.988e$^{-0.005[CO3]}$

r^2 = 0.876

[CO$_3^=$] (μmol kg^{-1})

S/Ca (mmol/mol)

(b)

SO$_4^=$ uptake in *A. lobifera* as a function of (1/[CO$_3^=$])$_{sw}$

S/Ca = 68.68 x (1/[CO$_3^=$])

r^2 = 0.826

(1/[CO$_3^=$])$_{sw}$ (kg μmol^{-1})

S/Ca (mmol/mol)
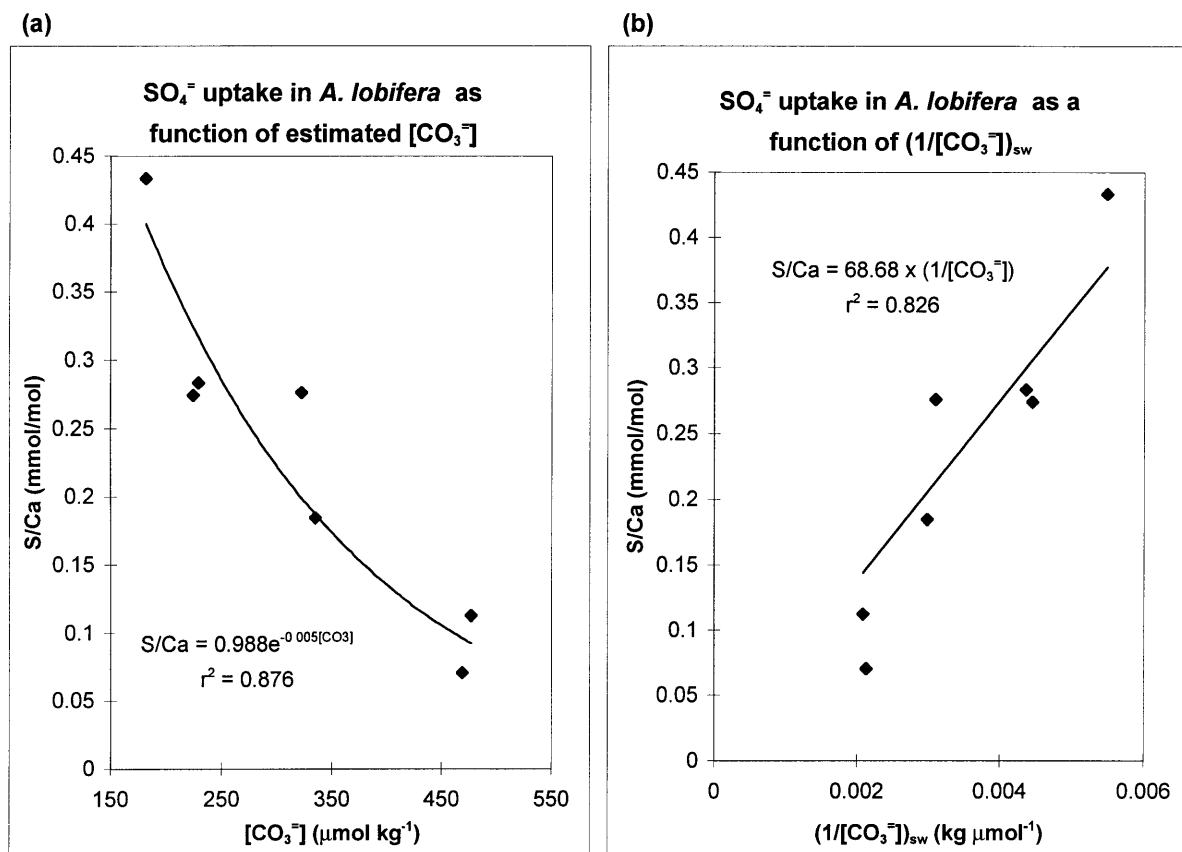
Figure 23: Data from cultured *A. lobifera* experiments shown in Figure 1. pH data were converted to carbonate ion concentration. (a) S/Ca plotted versus [CO$_3^=$] and fit to an exponential function. (b) S/Ca plotted versus 1/[CO$_3^=$] and fit to a linear function constrained to pass through the origin.

71

Table 13. Calculations of glacial pH based on foraminiferal S/Ca ratios.

| Location/type | Core/species | Holocene S/Ca (mmol/mol) | Glacial (S/Ca) | Δ(S/Ca) G-H | Using fractional change in S/Ca to estimate change in [CO₃] | | | | | | | Using calibrations | | |
					frac. change S/Ca	Holocene [CO₃]	Holocene 1/[CO₃]	Holocene pH	Glacial 1/[CO₃]	Glacial [CO₃]	Glacial pH	Glacial 1/[CO₃]	Glacial [CO₃]	Glacial pH
Trop. Atlantic	EN66 26GGC													
planktonic	dut	1.195	0.817	-0.378	1.463	237.1[a]	4.22E-03	8.05	2.88E-03	346.8	8.22	3.40E-03	294.1[g]	8.15
benthic	umb	0.421	0.434	0.013	0.970	79.1[b]	1.26E-02	8.25	1.30E-02	76.7	8.21	1.28E-02	77.9[h]	8.21
S. Atl/ S. Ocean	RC13-228													
benthic	wue	0.693	0.508	-0.185	1.363	84.9[c]	1.18E-02	8.15	8.64E-03	115.7	8.27	9.09E-03	110.0[h]	8.25
	AII107 65GGC													
benthic	Uvi	0.457	0.456	-0.001	1.003	95.7[d]	1.04E-02	8.19	1.04E-02	96.0	8.16	1.04E-02	95.9[h]	8.16
benthic	Cib	0.898	0.950	0.052	0.945	95.7[d]	1.04E-02	8.19	1.11E-02	90.5	8.14	1.12E-02	89.2[h]	8.13
trop. E. Pacific	TR163-31p													
planktonic	dut	0.472	0.604	0.131	0.782	236.3[e]	4.23E-03	8.04	5.41E-03	184.9	7.97	4.52E-03	221.4[g]	8.04
benthic	Uvi	0.506	0.283	-0.224	1.792	76.0[f]	1.32E-02	8.11	7.34E-03	136.2	8.32	9.90E-03	101.0[h]	8.20

Species abbreviations as in Table 12. S/Ca units are mmol/mol. [CO₃⁻] units are μmol/kg

[a] Calculated from measurements at GEOSECS Stn. 111, 2°N, 14°W, 52 m

[b] Calculated from measurements at GEOSECS Stn. 111, 2°N, 14°W, 4698 m

[c] Calculated from measurements at GEOSECS Stn. 103, 24°S, 8.5°W, 3204 m

[d] Calculated from measurements at GEOSECS Stn. 60, 33°S, 42.5°W, 2870 m

[e] Calculated from measurements at GEOSECS Stn. 331, 4.6°S, 125.1°W, 59 m

[f] Calculated from measurements at GEOSECS Stn. 331, 4.6°S, 125.1°W, 3324 m

[g] Slope of G. sacculifer S/Ca vs. $1/[CO_3^=]$, $\Delta(S/Ca) \div \Delta(1/[CO_3^=]) = 462.4$ (mmol mol^{-1})/(μmol^{-1} kg)

[h] Slope of A. lobifera S/Ca vs. $1/[CO_3^=]$, $\Delta(S/Ca) \div \Delta(1/[CO_3^=]) = 68.7$ (mmol mol^{-1})/(μmol^{-1} kg)

reason, the carbonate parameters from GEOSECS Stn. 331 are used for the site of TR163-31p.

In the first scheme, the ratio of the Holocene S/Ca value to the glacial S/Ca value is taken. This is labeled as the fractional change in S/Ca. Foraminiferal S/Ca is assumed to be proportional to the reciprocal of the seawater $[CO_3^=]$ according to thermodynamic considerations of solid-solution. Hence, the value of $1/[CO_3^=]$ is then multiplied by the fractional change in S/Ca to give the glacial $1/[CO_3^=]$. The reciprocal is again taken to give the estimate for glacial $[CO_3^=]$. Glacial pH is estimated from the $[CO_3^=]$ value using a scheme similar to that of Sanyal et al. (1995) (Sanyal et al., 1995). The GEOSECS station salinity, alkalinity, and TCO_2 are increased by 3% to account for the growth of ice sheets. The estimated glacial $[CO_3^=]$ is then assumed to result from either calcite dissolution or precipitation, so that alkalinity and TCO_2 are changed in a 2:1 ratio. Alkalinity and TCO_2 are modified in a 2:1 ratio so that the carbonate system equations produce the estimated glacial $[CO_3^=]$. The resulting pH is taken as the glacial pH.

The second scheme uses the difference between glacial and Holocene foraminiferal S/Ca ratios (Δ(S/Ca)) to estimate glacial pH. The calibration of *A. lobifera* S/Ca ratios versus $1/[CO_3^=]$ is used to calculate deep ocean $[CO_3^=]$ from benthic foraminifera Δ(S/Ca), and the equivalent calibration of *G. sacculifer* is used to calculate surface ocean $[CO_3^=]$ from planktonic foraminifera Δ(S/Ca). The parameter Δ(S/Ca) is divided by the slope of the appropriate calibration, Δ(S/Ca)÷Δ(1/$[CO_3^=]$), and the result added to the Holocene value of $1/[CO_3^=]$ determined previously to give the glacial value of $1/[CO_3^=]$. The resulting glacial $[CO_3^=]$ is then converted to glacial pH in the same way as for the first scheme.

Two schemes were employed primarily to allow a calculation not based on a specific calibration, since the foraminifera species for which calibrations are available may not have a similar response in their S/Ca ratios to seawater pH as for

those species actually measured. Comparing the glacial pH values obtained from both schemes shows that substantial differences between the two schemes occur when the value of Δ(S/Ca) is larger than about 0.2 mmol/mol. The largest discrepancies occur in TR163-31p (up to 0.12 pH units) and in the planktonic data of EN66-26GGC (0.07 pH units). In these cases, the scheme using calibration data gives a lower difference between glacial and Holocene pH. This is because the first scheme is in essence the same as the second scheme assuming a calibration with a slope of 1000 mmol mol^{-1}/kg µmol^{-1}, which is larger than either of the slopes applied in the second scheme. In the interest of allowing a visual comparison of the data, the glacial pH values from the two schemes were averaged and the pH data from Table 13 are shown in Figure 24. Because of uncertainty in the results due to analytical error, interspecies differences, and uncertainty in the method used to calculate the pH data, a subjective error bound on the accuracy of the pH estimates of at least $\pm$ 0.10 pH units should be considered to apply to the reported results. However, analytical reproducibility is better than that, so that *differences* between S/Ca ratios and, by calculation, pH estimates should have smaller error bounds. These differences are the focus of the following discussion.

At first, the pH estimates appear contradictory. An increase of 0.15 pH units is shown for TR163-31p in the glacial deep eastern tropical Pacific, but a small decrease of 0.03 pH units is estimated for the glacial surface ocean there. A decrease in surface ocean pH suggests a net source of CO_2 to the atmosphere, which is inconsistent with the knowledge that the glacial atmosphere had a lower pCO_2. Similar ΔpH estimates, however, have been reported by Sanyal et al. (1996) using foraminiferal boron isotope measurements, but for the Stage 5-6 transition. Here they found a 0.30 pH unit increase in the Stage 6 deep eastern equatorial Pacific over modern pH, but no significant pH difference in the surface waters. They surmised that stronger

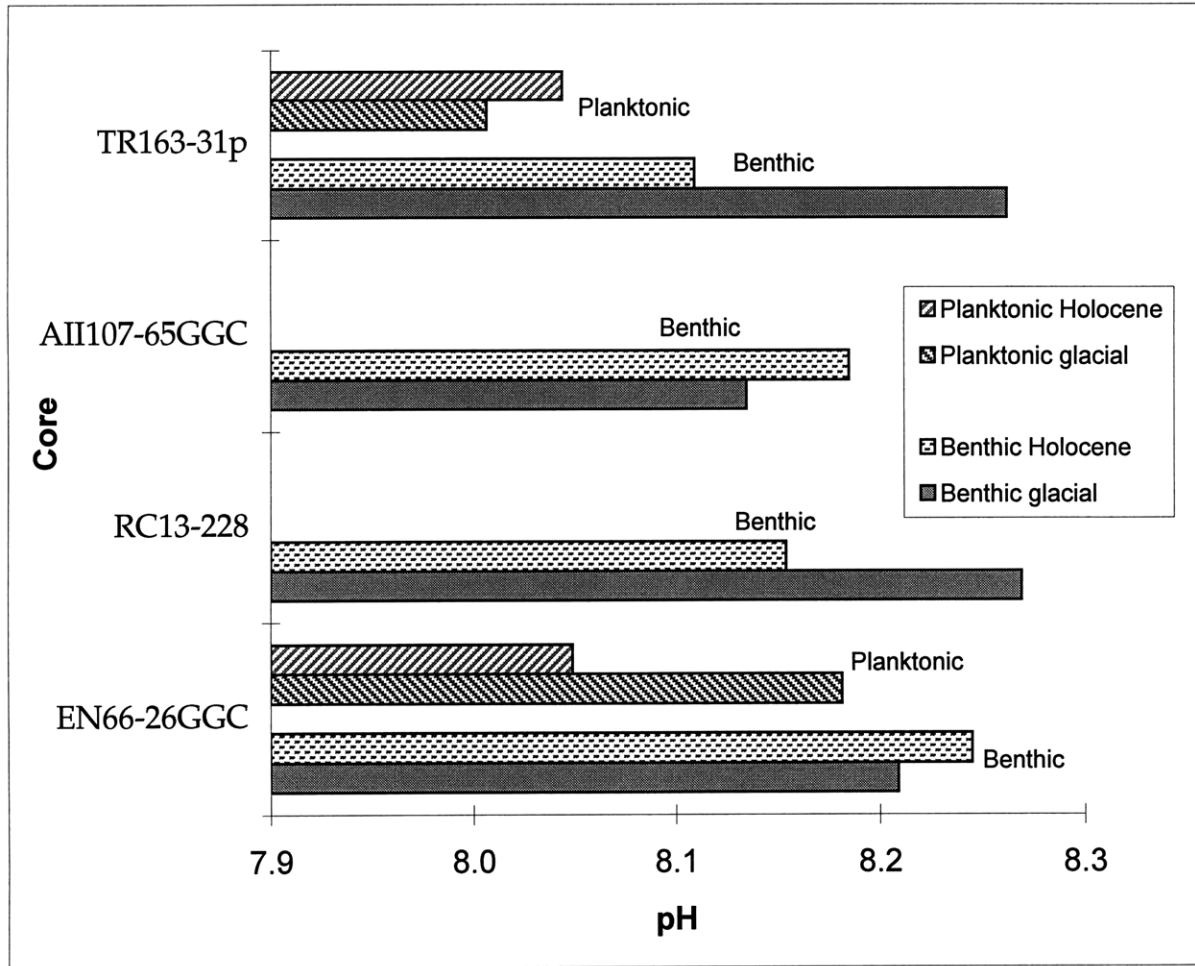Figure 24: pH estimates made from S/Ca data from Figure 22. Each pair of horizontal bars is a Holocene-glacial pair for the same taxon of foraminifer. Planktonic and benthic taxa are labeled, representing surface and deep water pH, respectively. The accuracy of each estimate may be subject to uncertainty on the order of 0.1 pH units, but inferences made from Holocene-glacial pH differences may be more reliable than that.

upwelling in the region during glacial periods could reduce nutrient utilization in the surface waters and lead to increased pCO_2.

On the other hand, planktonic S/Ca data from the eastern tropical Atlantic ocean (EN66-26GGC) indicates a 0.13 pH unit increase in surface water pH in the glacial compared to the Holocene, while the glacial deep waters were estimated to be lower in pH by about 0.04 pH units. The surface pH estimate from EN66-26GGC is corroborated by foraminiferal boron isotope derived paleo-pH data (Sanyal et al., 1997). They report a 0.2 ± 0.07 pH unit increase in the surface ocean off northwest Africa during glacial periods; this was calculated to lead to a lower glacial ocean-atmosphere pCO_2 gradient in this upwelling region, although not a negative gradient. S/Ca data from RC13-228 on the Walvis Ridge in the south Atlantic, today influenced primarily by NADW, suggests the deep water glacial pH was 0.12 pH units higher than today. Finally, S/Ca data from AII107-65GGC on the Rio Grande Rise in the western South Atlantic suggest a deep water glacial pH lower by 0.05 pH units.

The data suggest that some areas experienced lower glacial pH (contradicting the expected change based on lower atmospheric pCO_2 levels), and others experienced higher glacial pH. While some spatial heterogeneity in pH may not be unexpected, perhaps one would expect a more homogeneous pattern for deep waters, especially in one ocean basin, as for the three cores in the Atlantic studied here. The predictions of lower glacial deepwater pH at the sites of AII107-65GGC and EN66-26GGC may not be at odds, however, with the expectation of higher glacial global ocean pH. The proportions of water masses that form the water bathing core sites can change over glacial cycles, so that regional differences may occur despite a global trend toward increasing ocean carbonate ion concentration. For example, neglecting for a moment the postulated global ocean [$CO_3^=$] increase, if the sites of AII107-65GGC and EN66-26GGC had a higher proportion of southern source water

during the last glacial period than today, the water mass would have a lower $[CO_3^=]$ than today, because southern source waters have a higher remineralized TCO_2 content than northern source waters. Now, even if the global ocean had a higher $[CO_3^=]$ in the glacial period than in the present day, a significant increase in southern source waters bathing a specific site could compensate for the global $[CO_3^=]$ increase and reduce glacial $[CO_3^=]$ at that site.

A calculation was made to test the validity of this scenario. There is abundant evidence that northern source nutrient-depleted deepwater in the Atlantic Ocean (North Atlantic Deep Water - NADW) was shallower in the last glacial period than today and that deepwater below 2500 m had a much higher nutrient content in the last glacial period, signifying a greater proportion of southern source water (Antarctic Bottom Water - AABW) at these depths (Boyle, 1988; Boyle, 1992). Based on GEOSECS measurements, AABW is lower in $[CO_3^=]$ than NADW by about 25 $\mu mol/kg$, pH is 0.18 units lower, $\delta^{13}C$ is 0.7‰ lower, and [Cd] (calculated from foraminiferal Cd/Ca as described in Boyle, 1992) is 0.27 nmol/kg higher. If carbon isotope and Cd/Ca data from coretop and glacial age foraminifera in AII107-65GGC and EN66-26GGC are assumed to reveal the change in proportion of NADW and AABW at their locations during the glacial period, the modern gradient in $\delta^{13}C$ and [Cd] in those waters masses can be used to predict the change in glacial pH due to water mass effects alone. The $\delta^{13}C$ gradient at EN66-26GGC is -0.72‰ (Curry and Lohmann, 1983), after correcting by +0.3‰ for the global average $\delta^{13}C$ shift. The [Cd] gradient at AII107-65GGC (calculated from Cd/Ca data) is +0.22 nmol/kg (Boyle, 1984). Thus, both core sites shifted to a much higher proportion of AABW in the glacial period. The calculated water mass effect indicates a 0.15 unit decrease in pH at AII107-65GGC, and a 0.18 unit increase in pH at EN66-26GGC. If water mass effects are considered negligible at TR163-31p and RC13-228, as will be argued below, those sites can be considered indicative of the global pH change(+0.12 to +0.15 pH units).

Hence, water mass effects and a global ocean pH increase combine to account for the pH changes calculated in Table 13 for AII107-65GGC (-0.05 pH units) and EN66-26GGC (-0.04 pH units).

Cadmium data of Boyle and Rosenthal (1996) for RC13-228 indicate no discernible glacial-Holocene nutrient gradient, $i.e.$ no water mass change. Carbon isotope data, however, suggest a shift to higher nutrient waters in the glacial period, but the accuracy of the $\delta^{13}C$ data set may be questioned due to productivity effects on foraminiferal $\delta^{13}C$ at the site (Mackensen et al., 1993; Bickert and Wefer, 1996). Cadmium data for TR163-31p (Boyle, 1992) suggest a small decrease in nutrient concentrations during the glacial period that probably reflects the balancing of increased deepwater nutrient concentrations in the North Atlantic rather than a regional water mass effect. This evidence supports the use of these sites as a representation of the global deepwater change in pH during the last glacial period.

H. Summary and implications

The benthic records at TR163-31p and RC13-228 and the planktonic record at EN66-26GGC suggest a higher pH at glacial time, on the order of 0.15 pH units. The rest of the foraminiferal data indicate rather small pH changes; however, water mass effects from changing circulation patterns in the glacial ocean can explain small decreases in deepwater pH, if real, postulated at AII107-65GGC and EN66-26GGC. The contrasting surface pH estimates for TR163-31p (lower glacial pH) and EN66-26GGC (higher glacial pH) agree with boron isotope pH estimates for the same regions. Contrasts in surface productivity and upwelling intensities at the two sites during glacial periods may explain the differences.

The patterns seen in the glacial-interglacial comparison S/Ca dataset can be explained by the foregoing discussion of water mass shifts and a whole ocean carbonate ion accumulation. (A mechanism for carbonate ion accumulation cannot

be defined from the data, although the pore-water carbonate dissolution mechanism driven by excess organic carbon flux to the sediments of Archer and Maier-Reimer (1994) is one possible scenario.) The validity of the explanation described, however, depends on many factors that have not been definitively proven. The central hypothesis that S/Ca is a proxy for seawater carbonate ion concentration is strongly supported by the culture experiment data, but the Little Bahama Banks thermocline benthic foraminifera data do not agree with the hypothesis that $[CO_3^=]$ is the only control on foraminiferal S/Ca. Yet, because the LBB data seem to correlate well with salinity, it may turn out that salinity provides a primary control on S/Ca ratios. But, when foraminifera grow in constant salinity, they incorporate sulfur under carbonate ion, or pH, control. In fact, this "dual control" situation fits with the original hypothesis, if foraminiferal S/Ca is more sensitive to $[SO_4^=]$ changes due to changes in salinity than to $[CO_3^=]$ changes. This could be tested by culturing foraminifera in changing salinity conditions while holding $[CO_3^=]$ constant. It is important to try to differentiate between salinity and pH controls on S/Ca so that data can be interpreted appropriately. The utility of foraminiferal S/Ca as a paleoceanographic tracer is uncertain until the factors controlling it are better defined.

Because there appears to be regional differences in the glacial-interglacial gradient of S/Ca in benthic foraminifera, further work should explore a more detailed downcore record of S/Ca in a Pacific Ocean site such as TR163-31p where regional water mass changes are unlikely to disturb a global deepwater $[CO_3^=]$ signal. This core also has the advantage of a rather high sedimentation rate so that the time resolution of the data can be maximized. Comparison of the data to boron isotope pH estimates would serve to confirm the validity of both tracers. The advantage of S/Ca measurements is that they can be done on a much smaller sample size than for

boron isotopes, so that they can serve as a rapid screening tool which can be followed up by boron isotope measurements where the data warrants.

On the topic of interspecies S/Ca differences, the LBB data are somewhat inconclusive. The scatter in the data for *Uvigerina* and *Cibicidoides* species as a whole is large, so it is difficult to tell whether the results for different taxa are the same within the scatter. *Uvigerina* S/Ca tends to be lower than *Cibicidoides* at 301 and 433 meters, but is similar to or higher than *Cibicidoides* at 580 and 668 meters. S/Ca data for *Uvigerina* and *Cibicidoides* also coexist for core AII107-65GGC. Here, *Uvigerina* is clearly lower in S/Ca than *Cibicidoides*. Because of different growth environments for these genera within the sediments, and variations in food supply, it is reasonable to expect interspecies differences. In fact, growth environment within the sediments may have a significant effect on S/Ca if the pH gradient in the porewaters of the sediment mixed layer is steep. This may be another factor complicating the determination of deepwater pH from benthic foraminifera. A more detailed downcore study of multiple species would be a good test for benthic foraminiferal S/Ca interspecies differences. As for planktonic foraminifera, the small amount of multiple species data presented here suggests little difference in S/Ca in the species studied. The Gulf of Aqaba samples (Fig. 6) were predominantly *G. sacculifer*, but the *G. siphonifera*, *O. universa*, and *G. calida* measurements were similar within the scatter. These species likely grew at the same depth, so that environmental factors should not cause interspecies S/Ca differences. The single Eilat culture datum of *G. siphonifera* was nearly the same as the *G. sacculifer* datum for the same pH (Table 9). The comparison of *G. menardii* and *G. sacculifer* data from 2300 meters on the Ontong Java Plateau shows higher S/Ca for *G. menardii*, but the scatter of the data is too large to say this definitely. In this case, calcification environment may make a difference, since *G. menardii* is known to calcify deeper than *G. sacculifer*.

The cumulative dataset of foraminiferal S/Ca presented in this thesis is not large enough to evaluate the full accuracy and precision of S/Ca measurements. Further work on building the dataset as well as further investigation of blanks and sample handling are important for definitively evaluating the prospects of foraminiferal S/Ca as a paleoceanographic carbonate (or salinity) tracer.

References

Archer D. and Maier-Reimer E. (1994) Effect of deep-sea sedimentary calcite preservation on atmospheric CO_2 concentration. *Nature* **367**, 260-263.

Bainbridge A. E. (1981) *GEOSECS Atlantic Expedition Vol. 1 Hydrographic Data 1972-1973*. National Science Foundation.

Barnola J. M., Pimienta P., Raynaud D., and Korotkevich Y. S. (1991) CO_2-climate relationship as deduced from the Vostok ice core: a re-examination based on new measurements and on a re-evaluation of the air dating. *Tellus* **43B**, 83-90.

Barnola J. M., Raynaud D., Korotkevich Y. S., and Lorius C. (1987) Vostok ice core provides 160,000-year record of atmospheric CO_2. *Nature* **329**, 408-414.

Bender M. L., Lorens R. B., and Williams F. D. (1975) Sodium, magnesium, and strontium in the tests of planktonic foraminifera. *Micropaleontology* **21**, 448-459.

Berger W. H. and Killingley J. S. (1977) Glacial-Holocene transition in deep-sea carbonates: Selective dissolution and the stable isotope signal. *Science* **269**, 563-566.

Bickert T. and Wefer G. (1996) Late Quaternary deepwater circulation in the South Atlantic: Reconstruction from carbonate dissolution and benthic stable isotopes. In *The South Atlantic: Present and Past Circulation* (ed. G. Wefer, W. H. Berger, G. Siedler, and D. J. Webb). Springer-Verlag.

Boyle E. A. (1984) Sampling statistic limitations on benthic foraminifera chemical and isotopic data. *Mar. Geol.* **58**, 213-224.

Boyle E. A. (1988) Cadmium: chemical tracer of deepwater paleoceanography. *Paleoceanography* **3**, 471-489.

Boyle E. A. (1992) Cadmium and δ^{13}C paleochemical ocean distributions during the stage 2 glacial maximum. *Annu. Rev. Earth Planet. Sci.* **20**, 245-287.

Boyle E. A. and Keigwin L. D. (1985) Comparison of Atlantic and Pacific paleochemical records for the last 250,000 years: changes in deep ocean circulation and chemical inventories. *Earth Planet. Sci. Lett.* **76**, 135-150.

Boyle E. A. and Rosenthal Y. (1996) Chemical hydrography of the South Atlantic during the last glacial maximum: Cd vs. δ^{13}C. In *The South Atlantic: Present and Past Circulation* (ed. G. Wefer, W. H. Berger, G. Siedler, and D. J. Webb). Springer-Verlag.

Broecker W. S., Spencer D. W., and Craig H. (1982) *GEOSECS Pacific Expedition* Vol. 3 *Hydrographic Data 1973-1974*. National Science Foundation.

Busenberg E. and Plummer L. N. (1985) Kinetic and thermodynamic factors controlling the distribution of SO_4^{2-} and Na^+ in calcites and selected aragonites. *Geochim. Cosmochim. Acta* **49**, 713-725.

Charles C. D. and Fairbanks R. G. (1990) Glacial to interglacial changes in the isotopic gradients of Southern Ocean surface water. In *Geological History of the Polar Oceans: Arctic versus Antarctic* (ed. U. B. A. J. Thiede). Kluwer Acad.

Curry W. B. and Lohmann G. P. (1983) Reduced advection into Atlantic Ocean deep eastern basins during last glaciation maximum. *Nature* **306**, 577-580.

Duplessy J. C., Shackleton N. J., Fairbanks R. G., Labeyrie L., Oppo D., and Kallel N. (1988) Deepwater source variations during the last climatic cycle and their impact on the global deepwater circulation. *Paleoceanography* **3**, 343-360.

Emiliani C. (1955) Pleistocene temperatures. *J. Geol.* **63**, 538-578.

Epstein S., Buchsbaum R., Lowenstam H. A., and Urey H. C. (1953) Revised carbonate-water isotopic temperature scale. *Geol. Soc. Amer. Bull.* **62**, 417-425.

Erez J. (1994) Calcification mechanisms and trace element distribution in foraminifera shells. Research proposal.

Fairbanks R. G., Sverdlove M., Free R., Wiebe P. H., and Be A. W. H. (1982) Vertical distribution and isotopic fractionation of living planktonic foraminifera in the Panama Basin. *Nature* **298**, 841-844.

Fairbanks R. G., Wiebe P. H., and Be A. W. H. (1979) Vertical distribution and isotopic composition of living planktonic foraminifera in the western North Atlantic. *Science* **207**, 61-63.

Gaillardet J. and Allègre C. J. (1995) Boron isotopic compositions of corals: Seawater or diagenesis record? *Earth Planet. Sci. Lett.* **136**, 665-676.

Hemleben C., Spindler M., and Anderson O. R. (1989) *Modern planktonic foraminifera*. Springer-Verlag.

Lea D. and Boyle E. (1989) Barium content of benthic foraminifera controlled by bottom water composition. *Nature* **338**, 751-753.

Lea D. W. (1995) A trace metal perspective on the evolution of Antarctic Circumpolar Deep Water chemistry. *Paleoceanography* **10**, 733-747.

Mackensen A., Hubberten H.-W., Bickert T., Fischer G., and Futterer D. K. (1993) The $\delta^{13}C$ record in benthic foraminferal tests of *Fontbotia wuellerstorfi* (Schwager) relative to the $\delta^{13}C$ of dissolved inorganic carbon in Southern Ocean deepwater: Implications for glacial ocean circulation models. *Paleoceanography* 8(587-610).

Neftel A., Oeschger H., Schwander J., Stauffer B., and Zumbrunn R. (1982) Ice core sample measurements give atmospheric CO_2 content during the past 40,000 yr. *Nature* **295**, 220-223.

Neftel A., Oeschger H., Staffelbach T., and Stauffer B. (1988) CO_2 record in the Byrd ice core 50,000-5,000 years BP. *Nature* **331**, 609-611.

Pingatore N. E. Jr., Meitzner G., and Love K. M. (1995) Identification of sulfate in natural carbonates by X-ray absorption spectroscopy. *Geochim. Cosmochim. Acta* **59**, 2477-2483.

Reeder R. J., Lamble G. M., Lee J.-F., and Staudt W. J. (1994) Mechanism of SeO_4^{2-} substitution in calcite: An XAFS study. *Geochim. Cosmochim. Acta* **58**, 5639-5646.

Reiss Z. and Hottinger L. (1984) *The Gulf of Aqaba: Ecological micropaleontology.* Springer-Verlag.

Robbins L. L. and Brew K. (1990) Proteins from the organic matrix of core-top and fossil planktonic foraminifera. *Geochim. Cosmochim. Acta* **54**, 2285-2292.

Rosenthal Y. and Boyle E. A. (1993) Factors controlling the fluoride content of planktonic foraminifera: An evaluation of its paleoceanographic applicability. *Geochim. Cosmochim. Acta* **57**, 335-346.

Rosenthal Y., Boyle E. A., and Slowey N. (1997) Temperature control on the incorporation of magnesium, strontium, fluorine, and cadmium into benthic foraminiferal shells from Little Bahama Bank: Prospects for thermocline paleoceanography. *Geochim. Cosmochim. Acta* **61**(17), 3633-3643.

Sanyal A., Bijma J., and Broecker W. S. (1997) Glacial-interglacial changes in pCO_2 of Northwest Africa and Eastern Equatorial Pacific upwelling zones based on boron isotope paleo-pH proxy. *EOS Trans. AGU* **78**(46), F388.

Sanyal A., Hemming N. G., and Hanson G. N. (1996) Changes in pH in the Eastern Equatorial Pacific across stage 5-6 boundary based on boron isotopes in foraminifera. *EOS Trans. AGU* **77**, F297.

Sanyal A., Hemming N. G., Hanson G. N., and Broecker W. S. (1995) Evidence for a higher pH in the glacial ocean from boron isotopes in foraminifera. *Nature* **373**, 234-236.

Shackleton N. J. (1967) Oxygen isotope analyses and Pleistocene temperatures re-assessed. *Nature* **215**, 15-17.

Shackleton N. J. (1977) Tropical rainforest history and the equatorial Pacific carbonate dissolution cycles. In *The Fate of Fossil Fuel CO2 in the Oceans* (ed. N. R. Anderson and A. Malahoff), pp. 401-428. Plenum Press.

Slowey N. and Curry W. B. (1995) Glacial-interglacial differences in circulation and carbon cycling within the upper western North Atlantic. *Paleoceanography* **10**(4), 715-732.

Spivack A. J., You C.-F., and Smith H. J. (1993) Foraminiferal boron isotope ratios as a proxy for surface ocean pH over the past 21 Myr. *Nature* **363**, 149-151.

Staudt W. J., Oswald E. J., and Schoonen M. A. A. (1993) Determination of sodium, chloride, and sulfate in dolomites: a new technique to constrain the composition of dolomitizing fluids. *Chem. Geol.* **107**, 97-109.

Stott L. D. (1992) Higher temperature and lower oceanic pCO_2: A climate enigma at the end of the Paleocene epoch. *Paleoceanography* **7**, 395-404.

Weiner S. and Erez J. (1984) Organic matrix of the shell of the foraminifer, *Heterostegina depressa. J. Foram. Res.* **14**, 206-212.

Appendix

Table A1. Analytical data from Little Bahama Banks benthic foraminifera.

sample	species	# indiv	wt. (mg)	core	depth (m)	[S] (μM)	[Ca] (mM)	S/Ca mmol/mol
AC1	wue	30	1.08	BC79	301	17.63	6.97	2.53
AC2	wue					45.97	7.62	6.03
AC3	wue					50.83	15.85	3.21
AC4	Uvi	33	1.40	BC79	301	35.10	21.83	1.61
AC5	Uvi					19.35	20.14	0.96
AC6	Uvi					10.67	10.16	1.05
AC7	Uvi	22	0.83	BC77	433	9.99	12.84	0.78
AC8	Uvi					10.24	12.76	0.80
AC9	Uvi	23	0.59	BC52	668	11.25	10.71	1.05
AC10	Uvi					4.30	4.71	0.91
AC11	wue	22	1.30	BC60	1312	48.21	21.63	2.23
AC12	wue					20.79	14.61	1.42
AC13	wue					36.22	20.88	1.73
AC14	Uvi	40	1.47	BC48	580	19.44	8.12	2.39
AC15	Uvi					17.07	12.81	1.33
AC16	Uvi					25.38	12.92	1.96
AC17	wue	65-70	1.78	BC48	580	28.97	15.46	1.87
AC18	wue					22.49	14.81	1.52
AC20	Uvi	?	?	BC52	668	21.89	15.64	1.40
AC21	wue	93	3.07	BC52	668	23.19	18.93	1.22
AC22	wue					23.36	17.89	1.31
AC23	wue					19.21	15.16	1.27
AC24	wue					26.13	20.67	1.26
AC25	wue					9.93	7.14	1.39
AC26	wue					15.43	11.46	1.35
AC27	Cib	52	3.11	BC52	668	31.92	20.35	1.57
AC28	Cib					18.49	13.90	1.33
AC29	Cib					24.23	18.04	1.34
AC30	Cib					34.32	23.60	1.45
AC31	Cib					25.87	18.57	1.39
AC32	Cib					31.53	23.43	1.35
AC33	Cib	65-70	3.15	BC60	1312	32.17	25.21	1.28
AC34	Cib					38.06	27.12	1.40
AC35	Cib					23.88	19.18	1.24
AC36	Cib					16.56	11.87	1.40
AC37	Cib					15.81	11.34	1.39
AC38	Cib					13.07	11.24	1.16
AC39	Cib	65-70	3.10	BC54	1043	30.45	25.83	1.18
AC40	Cib					34.54	28.50	1.21
AC41	Cib					19.04	15.98	1.19
AC42	Cib					20.91	16.59	1.26
AC43	Cib					26.78	22.14	1.21
AC44	Cib					24.10	21.31	1.13
AD1	Cib	5	0.47	BC79	301	6.30	3.09	2.04

sample	species	# indiv	wt. (mg)	core	depth (m)	[S] (µM)	[Ca] (mM)	S/Ca mmol/mol
AD2	Cib	7	0.41	BC79	301	29.17	16.32	1.79
AD3	Cib	9	0.63	BC79	301	34.49	18.38	1.88
AD4	Cib	24	1.60	BC79	301	54.12	25.69	2.11
AD5	Cib					42.30	21.77	1.94
AD6	Cib					19.12	8.82	2.17
AD7	Cib	9	0.51	BC77	433	69.22	25.61	2.70
AD8	Cib	10	0.74	BC77	433	54.32	26.63	2.04
AD9	Cib	10	0.37	BC77	433	16.95	7.64	2.22
AD10	Cib	35	1.44	BC77	433	47.56	25.64	1.85
AD11	Cib					23.13	24.41	0.95
AD12	Cib					16.57	8.79	1.88
AD13	Cib	10	0.49	BC61	1585	38.08	25.32	1.50
AD14	Cib	9	0.43	BC61	1585	33.79	21.23	1.59
AD15	Cib	10	0.57	BC61	1585	33.01	22.06	1.50
AD16	Cib	19	1.25	BC61	1585	29.55	17.43	1.70
AD17	Cib					13.96	9.13	1.53
AD18	Cib					21.01	13.27	1.58
AD19	Cib		1.45	BC51	830	17.95	12.72	1.41
AD20	Cib					13.16	15.18	0.87
AD21	Cib					13.54	9.05	1.50
AD22	Cib					10.97	6.92	1.58
AD23	Cib					8.87	6.39	1.39
AD24	Cib					10.28	6.80	1.51

Notes: Species abbreviations as for previous tables.

Table A2. Analytical data for AF run foraminifera.

ID	Species	# indiv.	wt. (mg)	[S] (µM)	[Ca] (mM)	S/Ca (mmol/mol)	Comments
AF1	men	10	1.35	7.39	8.73	0.846	
AF2				23.49	23.35	1.006	
AF3				6.69	7.50	0.892	
AF4	men	12	1.35	20.22	20.55	0.984	
AF5				8.17	9.28	0.880	
AF6				18.23	13.94	1.308	
AF7	sac	20	1.66	25.78	23.01	1.120	
AF8				21.27	18.98	1.121	
AF9				12.13	10.82	1.122	
AF10	sac	20	1.20	21.83	18.39	1.187	
AF11				11.37	10.03	1.134	
AF12				13.63	10.70	1.273	

ID	Species	# indiv.	wt. (mg)	[S] (μM)	[Ca] (mM)	S/Ca (mmol/mol)	Comments
AF13	dut	40	1.31	2.71	6.34	0.428	
AF14				5.38	11.39	0.472	
AF15				8.96	17.34	0.517	
AF16	dut	35	1.20	6.20	9.99	0.621	
AF17				5.24	8.91	0.589	
AF18				5.94	9.88	0.601	
AF19	Uvi	50	0.59	3.93	7.64	0.515	
AF20				3.91	7.86	0.498	
AF21	Uvi	40	0.60	6.18	20.55	0.301	
AF22				6.96	26.33	0.264	
AF23	umb	19	0.30	5.46	12.96	0.421	
AF24	umb	20	0.34	8.43	19.41	0.434	
AF25	wue	35	0.35	4.60	6.64	0.693	
AF26	wue	30	1.20	9.33	18.97	0.492	
AF27				6.50	12.29	0.529	
AF28				7.58	15.03	0.504	
AF29	dut	30	1.77	23.75	19.38	1.226	
AF30				19.53	17.24	1.133	
AF31				13.58	11.07	1.227	
AF32	dut	50	1.59	17.29	20.18	0.857	
AF33				11.18	14.41	0.776	
AF34				26.52	15.70	1.689	
AF35	Uvi	11	0.77	3.68	7.86	0.468	
AF36				7.84	17.57	0.446	
AF37	Uvi	20	1.12	10.34	21.83	0.474	
AF38				9.75	22.28	0.438	
AF39	Cib	6	1.07	23.48	26.82	0.875	
AF40				15.41	16.73	0.921	
AF41	Cib	12	1.04	33.00	33.80	0.976	
AF42				27.43	29.67	0.924	
AF43	men	7	0.82	4.65	7.46	0.624	
AF44				2.70	4.24	0.637	
AF45	men	9	1.03	6.25	11.57	0.540	
AF46				11.79	19.83	0.595	
AF47	sac	4	-	20.78	7.14	2.911	pH = 7.81
AF48	sac	4	0.11	16.57	9.98	1.659	pH = 8.41
AF49	siph	7	0.27	28.00	18.38	1.523	pH = 8.62
AF50	sac	3	0.10	21.76	15.30	1.422	pH = 8.60
AF51	sac	11	0.23	46.29	18.35	2.523	pH = 8.20
AF52	Cib	0-27%	14.81	198.37	150.49	1.318	sequential
AF53		27-62%		283.36	193.93	1.461	dissolution
AF54		62-100%		296.66	212.74	1.394	experiment

Notes: Species abbreviations as for previous tables, except men for *G. menardii*. # indiv. column for samples AF52-AF54 denotes the percentage of the bulk sample dissolved for that analysis. Balance did not give a reading above 0.01 mg for sample AF47.